JAERI - M
90-130

COMPARISON OF FACILITY CHARACTERISTICS BETWEEN SCTF CORE-I AND CORE-II

August 1990

Hiromichi ADACHI*, Takamichi IWAMURA, Makoto SOBAJIMA
Akira OHNUKI, Yutaka ABE and Yoshio MURAO

日本原子力研究所
Japan Atomic Energy Research Institute

JAERI-Mレポートは，日本原子力研究所が不定期に公刊している研究報告書です。
入手の問合わせは，日本原子力研究所技術情報部情報資料課（〒319-11茨城県那珂郡東海村）あて，お申しこしください。なお，このほかに財団法人原子力弘済会資料センター（〒319-11 茨城県那珂郡東海村日本原子力研究所内）で複写による実費頒布をおこなっております。

JAERI-M reports are issued irregularly.
Inquiries about availability of the reports should be addressed to Information Division, Department of Technical Information, Japan Atomic Energy Research Institute, Tokai-mura, Naka-gun, Ibaraki-ken 319-11, Japan.

編集兼発行　日本原子力研究所
印　　刷　㈱原子力資料サービス

JAERI-M 90-130

Comparison of Facility Characteristics between SCTF Core-I and Core-II

Hiromichi ADACHI*, Takamichi IWAMURA, Makoto SOBAJIMA+
Akira OHNUKI, Yutaka ABE and Yoshio MURAO

Department of Reactor Engineering
Tokai Research Establishment
Japan Atomic Energy Research Institute
Tokai-mura, Naka-gun, Ibaraki-ken

(Received July 13, 1990)

The Slab Core Test Facility (SCTF) was constructed to investigate two-dimensional thermal-hydraulics in the core and fluid behavior of carryover water out of the core including its feed-back effect to the core behavior mainly during the reflood phase of a large break loss-of-coolant accident (LOCA) of a pressurized water reactor (PWR).

Since three simulated cores are used in the SCTF Test Program and the design of these three cores are slightly different one by one, repeatability test is required to justify a direct comparison of data obtained with different cores.

In the present report, data of Test S2-13 (Run 618) obtained with SCTF Core-II were compared with those of Test S1-05 (Run 511) obtained with the Core-I, which were performed under the forced-flooding condition. Thermal-hydraulic behaviors in these two tests showed quite similar characteristics of both system behavior and two-dimensional core behaviors. Therefore, the test data obtained from the two cores can be compared directly with each other. After the turnaround of clad temperatures, however, some differences were found in upper plenum water accumulation and resultant two-dimensional core cooling behaviors such as quench front propagation from bottom to top of the core.

+ Department of Fuel Safety Research
* Yamagata University

Keywords: Reactor Safety, ECCS, Loss-of-coolant Accident, Reflood, Thermal-hydraulics, Heat Transfer, Two-phase Flow, Quench, SCTF

JAERI－M 90－130

平板炉心試験装置第１次および第２次模擬炉心の装置特性の比較

日本原子力研究所東海研究所原子炉工学部
安達　公道*・岩村　公道・傍島　真+
大貫　晃・阿部　豊・村尾　良夫

（ 1990 年７月13日受理）

平板炉心試験装置（ＳＣＴＦ）は，加圧水型原子炉（ＰＷＲ）の大口径破断による冷却材喪失事故（ＬＯＣＡ）時の，主として再冠水過程における，炉心内の２次元的な熱水力学的挙動，及び炉心からキャリーオーバされた水の炉心挙動へのフィードバック作用を含めた挙動を解明することを目的として建設された。

ＳＣＴＦ試験計画では３体の模擬炉心を使用する予定であり，それぞれの炉心の設計が少しづつ異なるので，異なる炉心を用いて得た試験データを直接比較して良いかどうかを再現性試験によって明らかにしておく必要がある。

本報では，共に強制冠水条件下で行われた，第２次炉心使用の試験Ｓ２－13（Run 618）と第１次炉心使用の試験Ｓ１－05（Run 511）とのデータの比較を行った。システムの熱水力学的挙動においても，炉心の２次元挙動においても，これらの２つの試験はきわめて類似のものであった。このことから，両装置から得た試験データを直接比較して良いと考えられる。ただし，被覆管温度が最高値に達した後の時間帯において，上部プレナムの蓄水挙動や，炉心下部から上方へのクエンチフロントの進行状況等の２次元的な炉心冷却挙動に有意な違いが見られた。

東海研究所：〒319－11 茨城県那珂郡東海村白方字白根２－４
＋燃料安全工学部
＊山形大学

Contents

目　　次

1. Introduction

The Slab Core Test Facility (SCTF) Test Program is a part of the Large Scale Reflood Test Program[1] of the Japan Atomic Energy Research Institute (JAERI) together with the Cylindrical Core Test Facility (CCTF) Test Program. The purpose of the Large Scale Reflood Test Program are to clarify the thermal hydraulic behavior in the core and the primary cooling system of a pressurized water reactor (PWR) during the last part of blowdown, refill and reflood phases of a postulated loss-of-coolant accident (LOCA) and to demonstrate experimentally the effectiveness of the emergency core cooling system (ECCS). In the CCTF Test Program, overall simulation of the system behavior is the primary concern. On the other hand, in the SCTF Test Program, the major objectives are to clarify the following items:

(1) Two-dimensional thermal-hydraulics in a wide core induced by radial power/temperature distribution in the core, non-uniform water accumulation above the core, geometrical relationship to the hot leg, local effect due to flow blockage, etc..

(2) Behavior of carryover water from the core, i.e., entrainment/deentrainment, pool formation, fall back of water to the core, carryover of water to the hot leg, water back-flow from the hot leg, etc..

The SCTF Test Program is a part of the coordinated research program called the 2D/3D Program among the United states (US), the Federal Republic of Germany (FRG) and Japan. Coupling tests with the Upper Plenum Test Facility (UPTF) tests of the FRG are planned to be performed in the SCTF Core-III test series to investigate fluid behaviors in the core, upper plenum, downcomer, and primary loops and the resultant core cooling behavior under the common proper interfacial two-phase flow condition between the core and the upper plenum.

To meet these objectives, the SCTF pressure vessel is designed and fabricated to simulate a radial slab with full height, full radius and one bundle width extracted from an 1,100 MWe PWR core. The relation between the SCTF pressure vessel and the PWR pressure vessel is illustrated in Fig. 1.1.

In the SCTF Test Program, three simulated cores are used and the design of these three cores are slightly different one by one. Therefore, a repeatability test is required to verify the wide applicability of the test results and to make reasonable comparison between the test data from

the different cores.

In the present report, data of Test S2-13 (Run 618) were compared to those of Test S1-05 (Run 511)[2]. Both tests were performed under the forced-feed flooding condition to realize as close test conditions to each other as possible. Only major difference between the two tests was the core designs, i.e., Core-I in Test S1-05 and Core-II in Test S2-13. The other design differences were minor.

A brief description on the design[3] of the SCTF is given in Appendix A for reference. Selected test data from the Test S2-13 are also given in Appendix B. Those for Test S1-05 are introduced in reference (2).

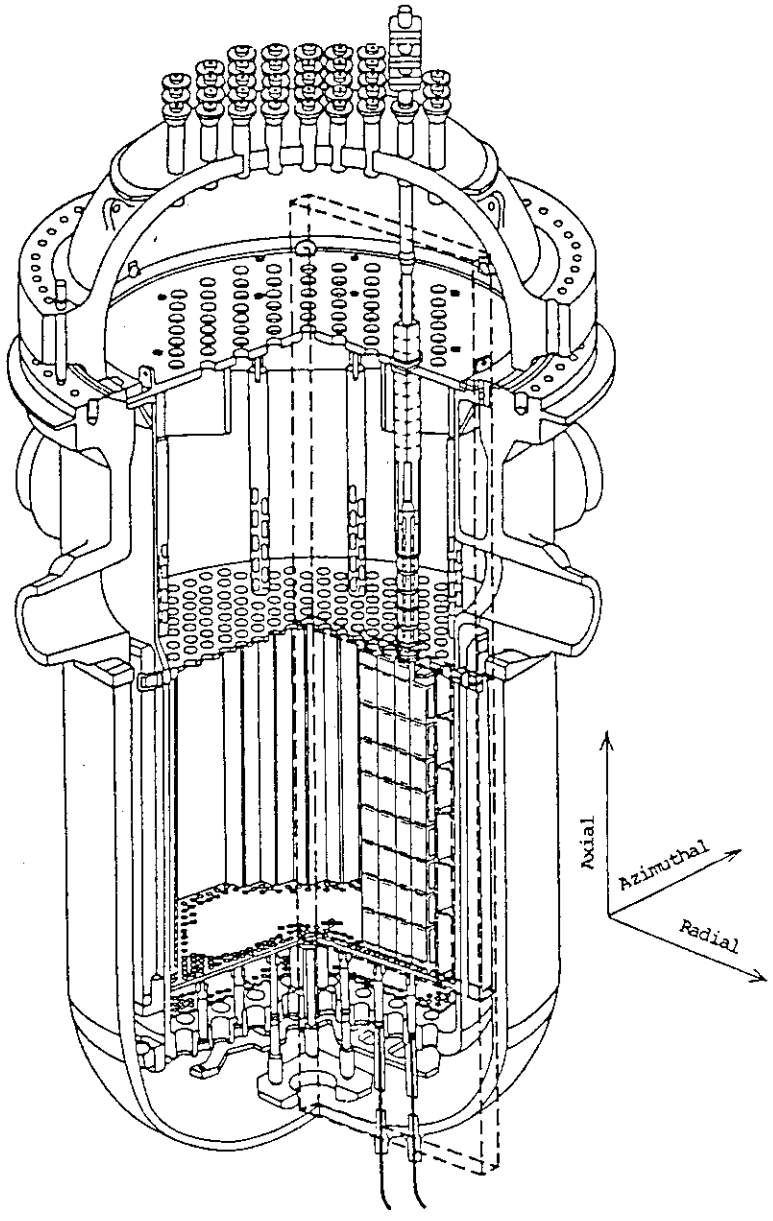

Fig. 1.1 Simulated Part of PWR Pressure Vessel with SCTF

2. Difference of Core Design

Design of the SCTF Core-I and Core-II are basically the same but there are two important different points.

The one is that the Core-I has blockage sleeves shown in Fig. 2.1 at the mid-elevation of all heater rods of Bundles 3 and 4 to simulate a flow blockage but the Core-II does not have them. In connection with this, the Core-I has closing plates and flow interceptors on the both sides of all eight bundles facing the side walls at the elevation of the blockage section. Detail of these structures is illustrated in Fig. 2.2. The Core-II does not have such structures.

The second different point between the Core-I and Core-II is the structure of side wall. In the Core-I, inner surface of the core barrel and upper plenum barrel are covered with a number of honeycomb type thermal insulator panels made of Inconel 625 of which surface plate thickness is 0.8 mm as shown in Fig. 2.3. Therefore, inner surface of the side wall is not smooth but has gaps between each of two thermal insulator panels, and in addition, it can be easily quenched because of the small heat capacity of the surface plate. In the Core-II, wall plate made of Inconel 625 is attached to the inner surface of the honeycomb thermal insulator panels to smooth the inner surface of the side wall as shown in Fig. 2.4. Thickness of the wall plate is 6 mm and it gives proper heat capacity to the side wall surface. The nominal gap between the rod bundle and the thermal insulator of the Core-I is 10.9 mm and that between the rod bundle and the wall plate of the Core-II is 7.4 mm. As a result, the effective core flow area based on the measured level-volume relationship is estimated to be 0.35 m^2 for the Core-I and 0.32 m^2 for the Core-II.

There are some minor design changes between the Core-I and the Core-II. One of them is the electrical insulator material between the heater element and the clad. In the Core-I, MgO was used throughout the core heated part. On the other hand, BN was used for the middle 1/3 length in the Core-II.

There is an entrance hole at the bottom of the core baffle region of the Core-I as shown in Fig.A-6. The flow area of the entrance hole is 2.53×10^4 mm^2. In the Core-II, the entrance hole is closed. Due to this design change, the water mass accumulation in the core baffle region is evaluated more accurately in the Core-II because of the smaller pressure loss at the baffle plates. However, this change does not affect so much the

overall fluid behavior because enough amount of water still can flow into the core baffle region through the gap between the partition plate separating the core and core baffle region and the core barrel groove in the Core-II.

Flow resistance of the primary loops is slightly changed in Test S2-13 from Test S1-05. The reason is that the contribution of carryover water flow rate in the hot leg to the loop pressure drop in the reference case is slightly modified to be more realistic. The estimated K-factors of each loop for Test S1-05 and Test S2-13 are as shown in Table 2.1.

Table 2.1 Loop K-factors in Tests S1-05 and S2-13

	Test S1-05		Test S2-13	
	K	Note	K	Note
hot leg	1.94 (1.94)		1.94 (1.94)	
intact cold leg piping	3.61 (4.57)		3.61 (4.57)	
intact cold leg pipe orifice	5.97 (7.56)	orifice dia. = 191.1 mm	8.95 (11.3)	orifice dia. = 179.9 mm
pump simulator orifice	16.3 (149)	orifice dia. = 173.7 mm	16.3 (149)	orifice dia. = 173.7 mm
broken cold leg (S/W) piping	4.08 (46.5)		4.08 (46.5)	
broken cold leg (S/W) pipe orifice	18.2 (13.7)	orifice dia. = 87.7 mm	20.4 (15.3)	orifice dia. = 86.4 mm
broken cold leg (PV) piping	3.61 (41.1)		3.61 (41.1)	
broken cold leg (PV) pipe orifice	0 (0)	no orifice	0 (0)	no orifice
S/W separator	0.43		0.43	
intact loop total K	28.3		31.2	
broken loop total K	28.3		30.0	

* K-value is defined based on the hot leg flow area.
( ) shows K-value defined based on the local pipe flow area.

** Hot leg steam quality is assumed to be 0.95 in Test S1-05 and 0.90 in Test S2-13 for estimation of K-value required.

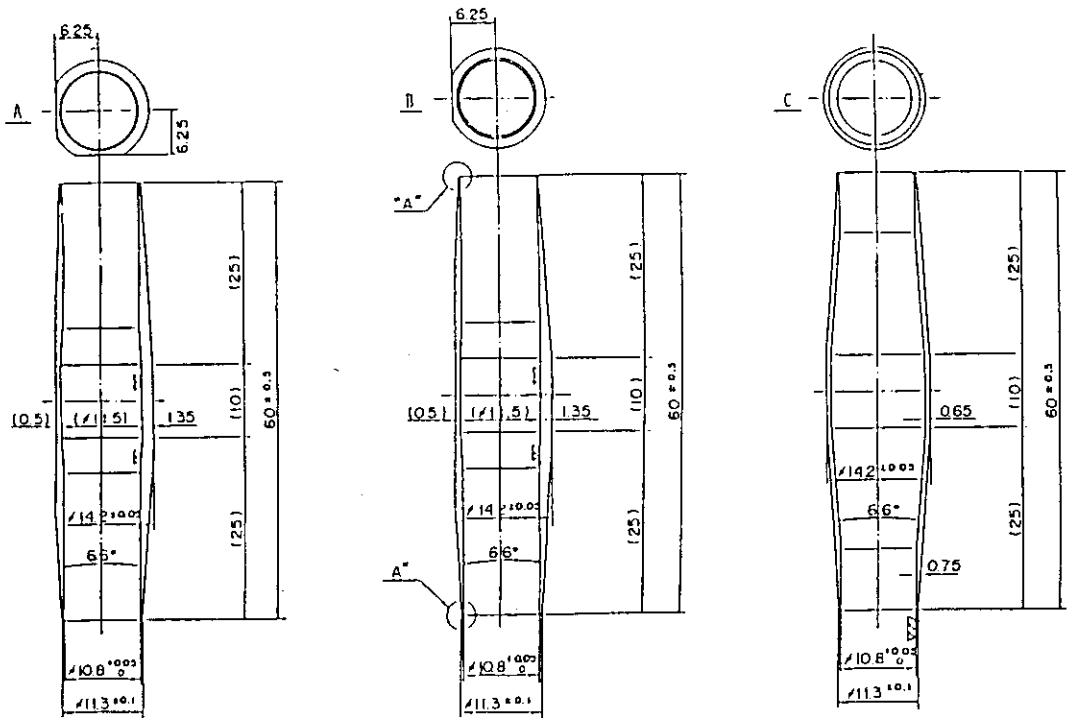

Fig. 2.1 Blockage Sleeves of SCTF Core-I

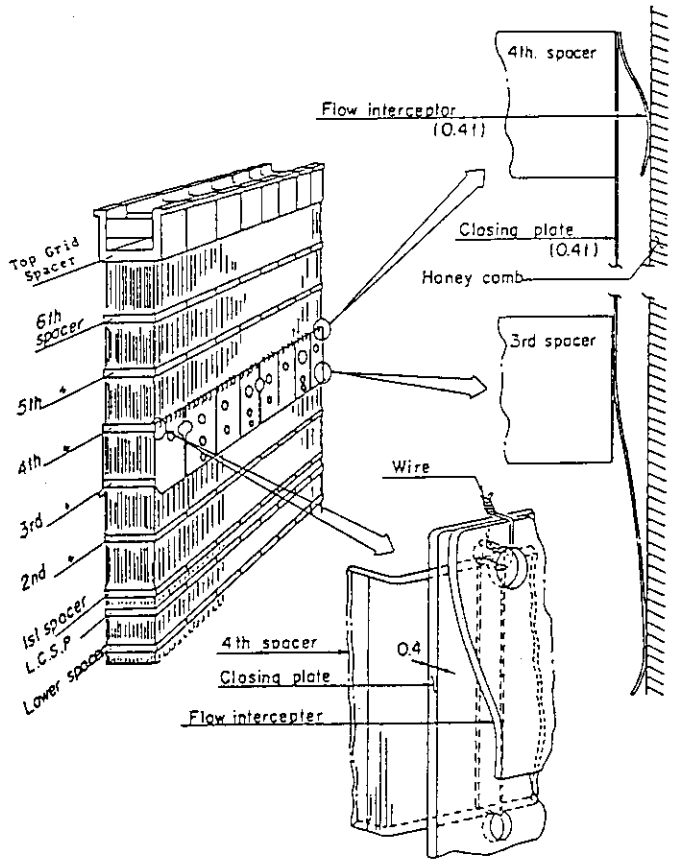

Fig. 2.2 Closing Plates and Flow Interceptors of SCTF Core-I Attached to the Blocked Section

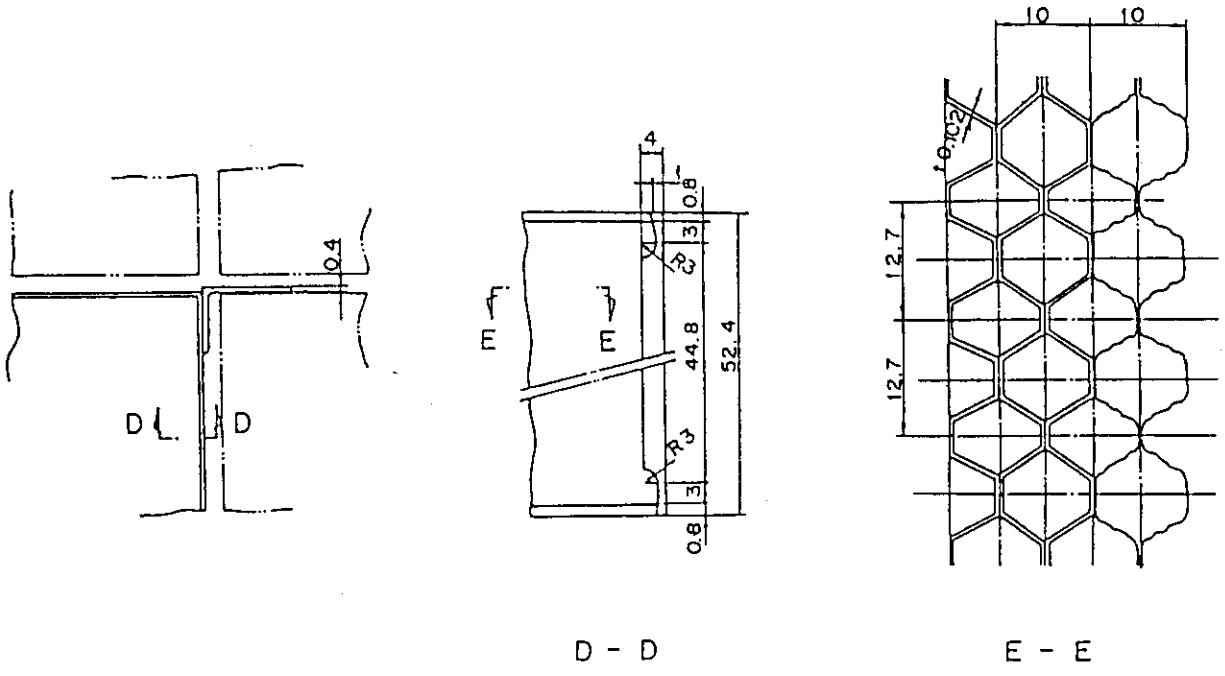

Fig. 2.3 Honeycomb Thermal Insulator of SCTF Core-I

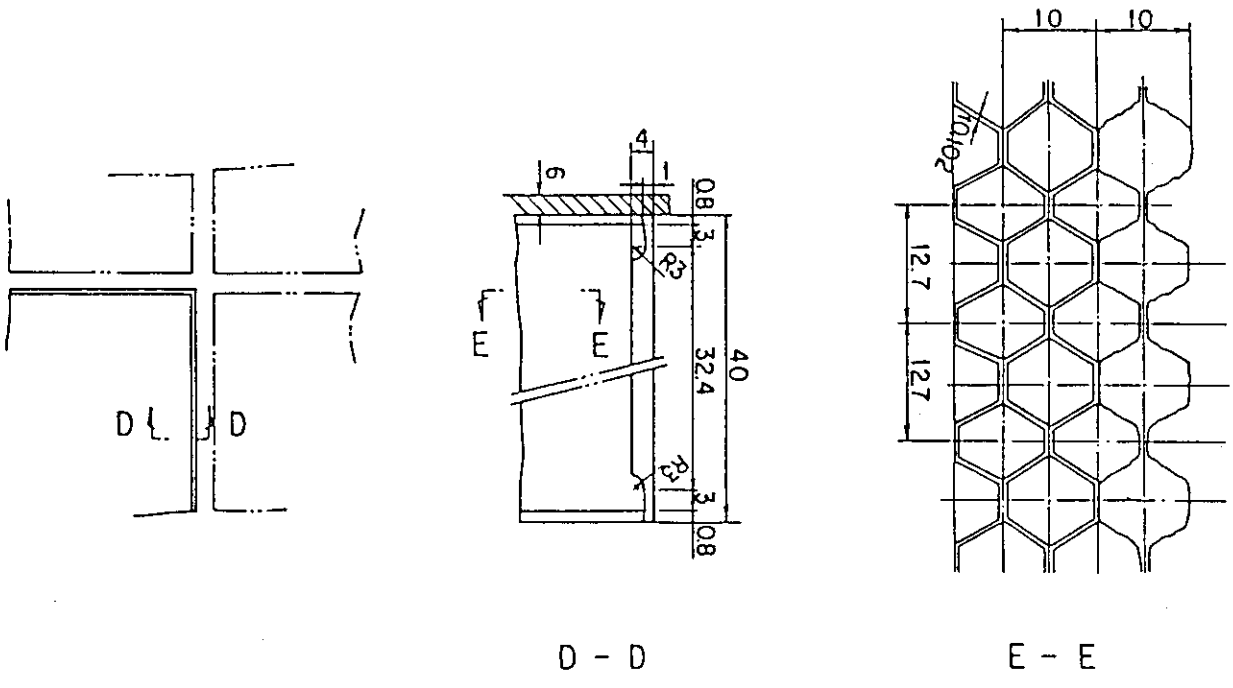

Fig. 2.4 Honeycomb Thermal Insulator and Wall Plate of SCTF Core-II

3. Test Conditions and Chronology of Events

Tables 3.1 and 3.2 show the comparison of test conditions and chronology of major events in Tests S1-05 and S2-13, respectively.

Test conditions for these two tests were almost the same as each other but there were small differences which should be taken into account in detailed comparison between the two tests.

Figures 3.1(a) and 3.1(b) show the power decay curves for Bundles 2, 4, 6 and 8 for Tests S1-05 and S2-13, respectively. The curves for the two tests were slightly different because, in Test S2-13, the decay curve of Test S1-05 with delayed neutron effect was replaced with the close curve without delayed neutron effect.

Figure 3.2 shows the comparison of core inlet water flow rate between the two tests. The injection rate of emergency core cooling (ECC) water in Test S2-13 was not exactly equal to Test S1-05, especially in the beginning stage of the test. The overshoot and undershoot of core inlet flow rate in the beginning stage of Test S2-13 were caused probably by remained gas in the injection piping system though we have carefully degassed the piping. Core inlet flow during low pressure coolant injection (LPCI) period was almost the same between the two tests.

Figure 3.3 shows the comparison of core inlet water temperature between the two tests. In spite of constant ECC water temperature throughout the whole transients of the two tests, core inlet water temperatures did not behave similarly. This is maybe due to different fluid mixing in the lower plenum during the beginning stage of the test caused by the different core inlet flow transients during the accumulator (Acc) injection period.

Figure 3.4 shows the comparison of system pressure measured at the center of the core between Tests S1-05 and S2-13. Initial overshoot of system pressure was slightly larger in Test S2-13 than in Test S1-05 and also higher system pressure was detected in the later portion of transient in Test S2-13.

Figure 3.5 shows the comparison of back pressure measured at the containment tank-II. Test S2-13 showed higher back pressure especially in the early stage of the transient.

Chronology of major events given in Table 3.2 shows more rapid core cooling down in Test S2-13 than in Test S1-05. There are various differences of order and timing of each event. However, some variables show so gentle peaks that uncertainty of timing of the maximum point is very

large. Therefore, it is not necessary to compare those chronologies so severely.

Table 3.1 Test Conditions in Tests S1-05 and S2-13

	TEST S1-05	TEST S2-13
TEST TYPE	FORCED FLOODING	FORCED FLOODING
INITIAL PRESS.(CORE CENTER)	0.20 MPa	0.20 MPa
MAX.CONTAINMENT PRESS.	0.217 MPa	0.221 MPa
MAX.CORE TEMP.(AT BOCREC*)	957 K	959 K
POWER HOLDING TIME AFTER ECC INITIATION	5 SEC	5 SEC
POWER DECAY CURVE	ANS+ACTINIDES+D.N. FROM 30 SEC(REAC.TIME)	(ANS+ACTINIDES)X1.02 FROM 20 SEC(REAC.TIME)
MAX.ACC INJ.RATE	25 KG/SEC	38 KG/SEC
LPCI INJ.RATE	6.2 KG/SEC	6.2 KG/SEC
MAX.CORE INLET SUBCOOLING	14.6 K	10.3 K

Table 3.2 Chronologies of Events in Tests S1-05 and S2-13

	TEST S1-05	TEST S2-13
CORE POWER "ON"	- 101 SEC	- 92 SEC
ECC INJ.INITIATION	- 6	- 4
CORE POWER DECAY INITIATION	- 1	1
BEGINNING OF REFLOOD	0	0
MAX.CORE PRESS.	17 (0.257 MPa)	24 (0.262 MPa)
MAX.CONTAINMENT-II PRESS.	20 (0.217 MPa)	18 (0.221 MPa)
MAX.CORE TEMP.	64 (1014 K)	52 (986 K)
MAX.CORE INLET SUBCOOLING	~199 (14.6 K)	60 (10.3 K)
WHOLE CORE QUENCH	333	319

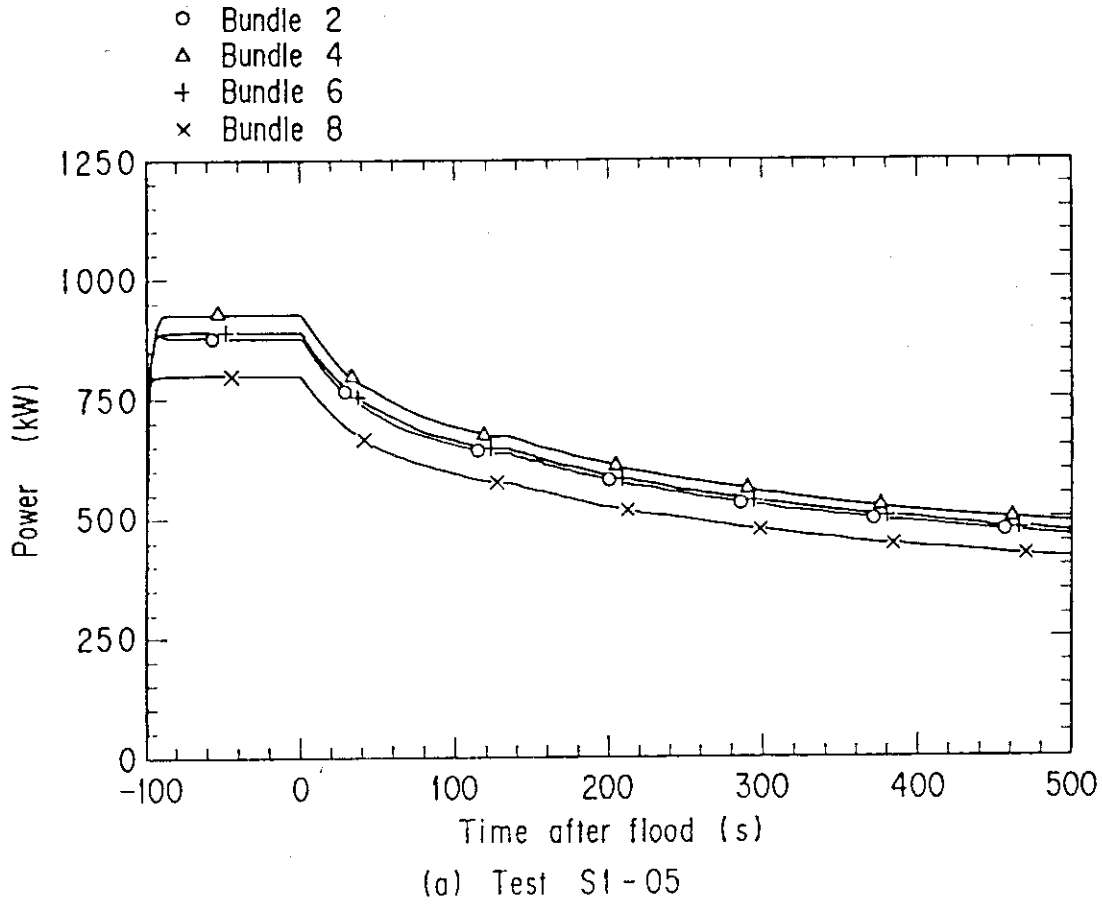

(a) Test S1-05

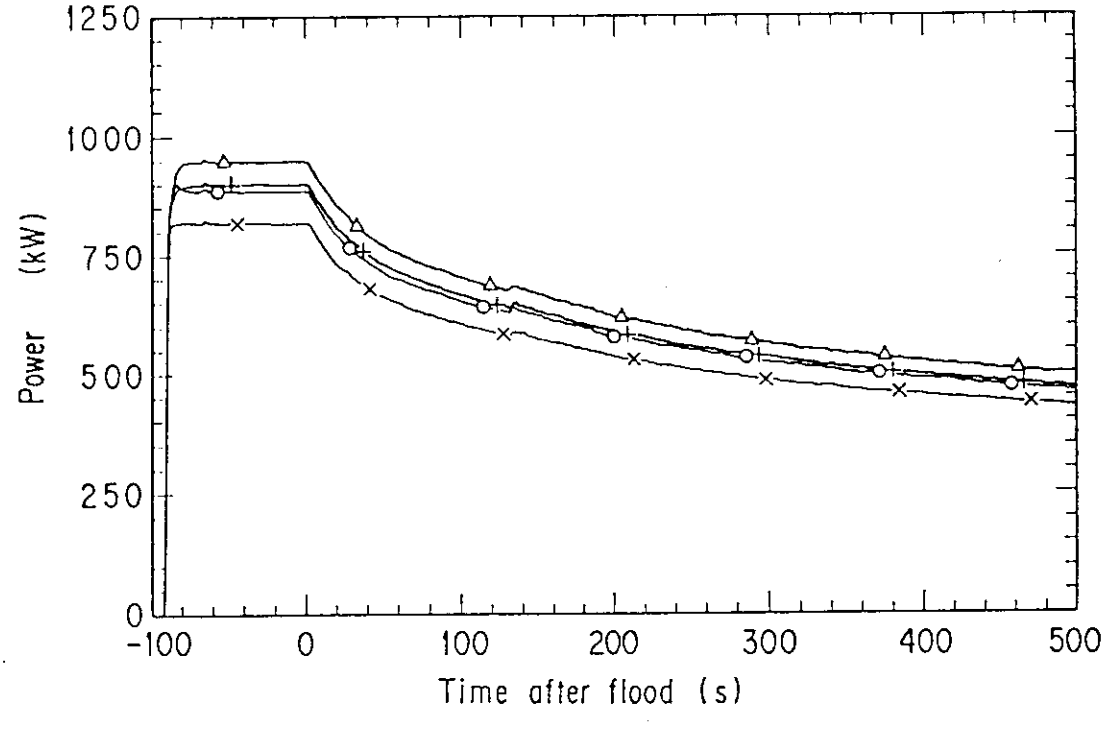

(b) Test S2-13

Fig. 3.1 Power Decay Curves in Tests S1-05 and S2-13

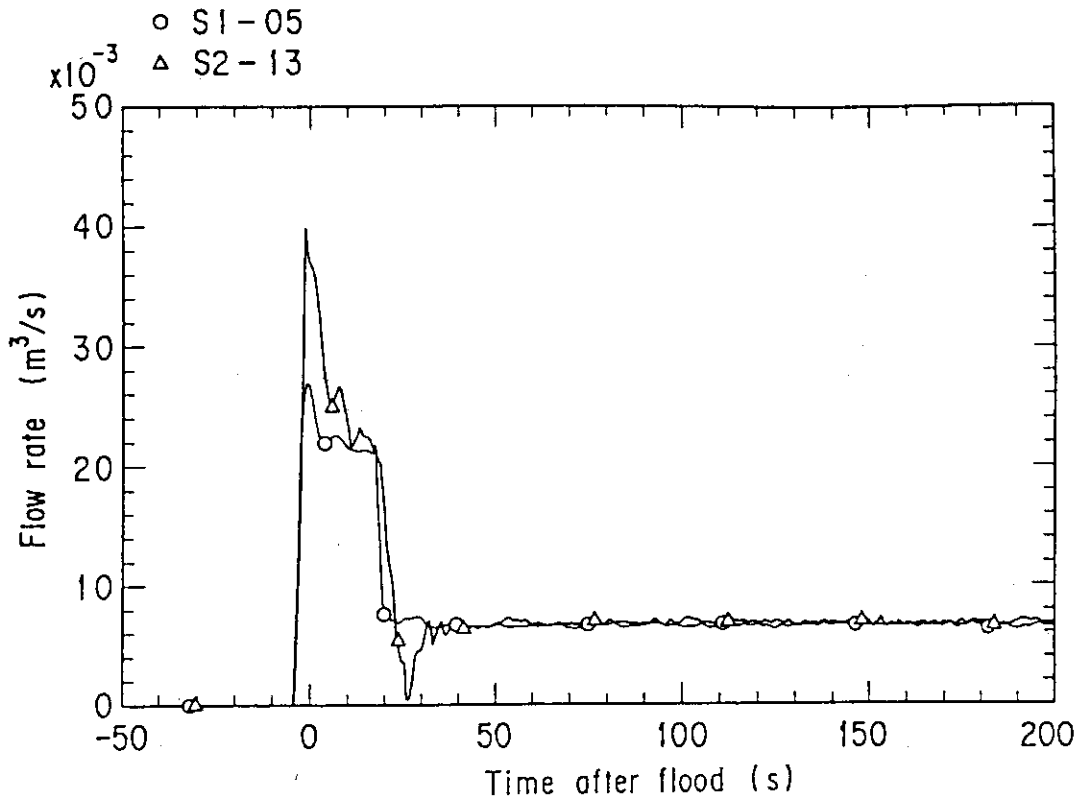

Fig. 3.2 Core Inlet Flow Rates in Tests S1-05 and S2-13

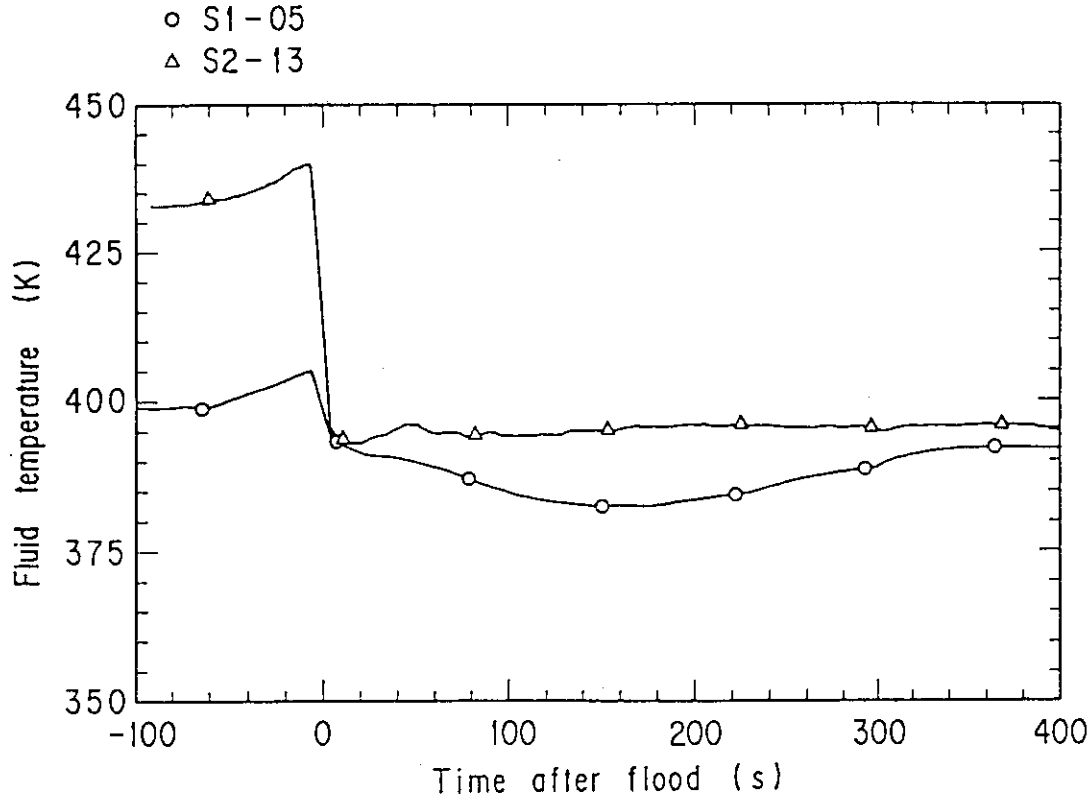

Fig. 3.3 Core Inlet Water Temperatures in Tests S1-05 and S2-13

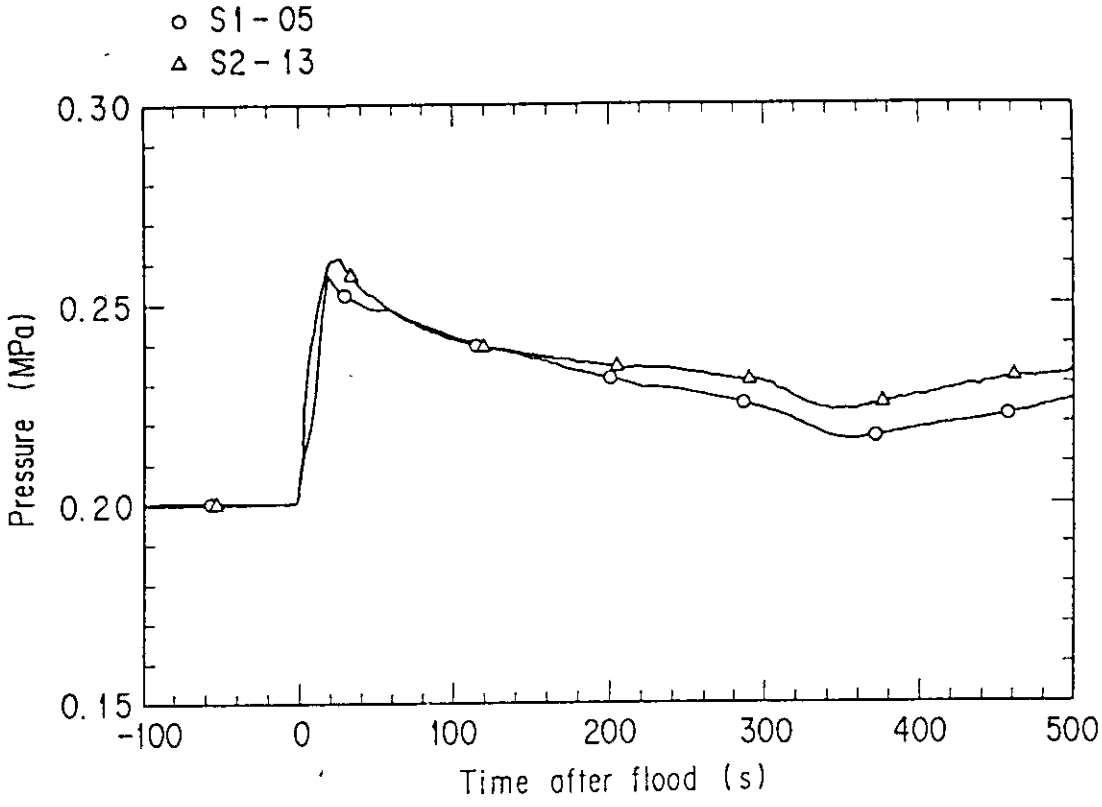

Fig. 3.4 Core Center Pressures in Tests S1-05 and S2-13

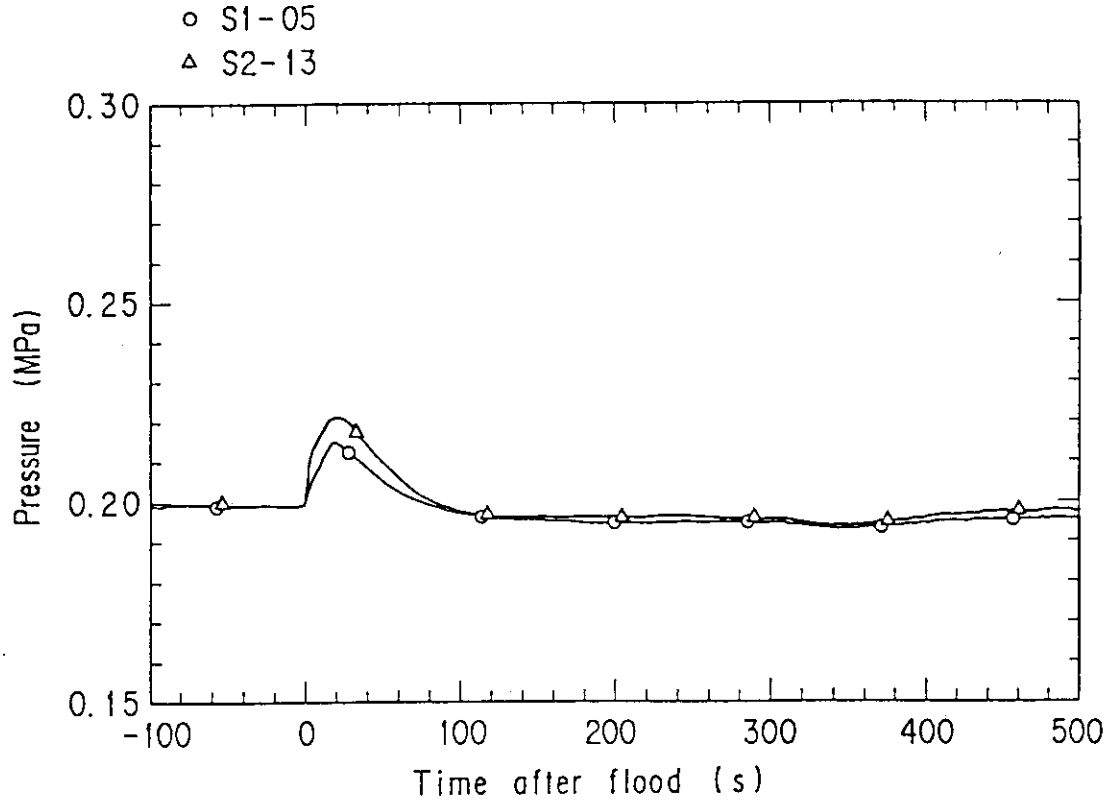

Fig. 3.5 Containment-II Pressures in Tests S1-05 and S2-13

4. Test Results

4.1 Hydraulic Behaviors

Figure 4.1 shows a comparison of vertical pressure differences across the core full height measured in Bundle 4. Test S2-13 shows slightly lower differential pressure from 100 to 300 s after the beginning of reflood (BOCREC: Bottom of Core Recovery). However, it can be said that almost the same core water accumulations are observed in the two tests until the whole core quench (333 s for Test S1-05 and 319 s for Test S2-13).

In spite of the quite similar transients of vertical differential pressure across core full height, vertical distribution of void fraction (estimated from section differential pressure data, neglecting fricitional and accelerational pressure drops) was clearly different between the two tests. In Test S2-13, void fraction in the lower part of the core was higher and that in the upper part of core was lower in comparison with Test S1-05 as shown in Figures 4.2(a) and 4.2(b). This was maybe caused by the initially higher core inlet flow rate and the higher core inlet water temperature, resulting in the earlier water distribution in the upper part of the core and the more significant swelling of two-phase mixture in the lower part of the core.

Figures 4.3(a) and 4.3(b) show the comparison of upper plenum collapsed water level between the two tests. Test S2-13 showed much more rapid water accumulation than Test S1-05, especially until the whole core quench. The reason why such a large difference appeared in the upper plenum water accumulation behaviors is not clear. One of the possible reasons is the change of honeycomb thermal insulator design, i.e., since SCTF Core-II upper plenum side wall has the wall plate, the side wall surface is smooth. Therefore re-entrainment which occured in the Core-I tests at the gaps between each of two honeycomb thermal insulator panels is almost eliminated in the Core-II tests. It results in larger net de-entrainment and more rapid water accumulation in the upper plenum.

The most important fact related to the upper plenum water accumulation behavior is that the larger amount of the accumulated water results in the steeper radial distribution of the amount of accumulated water. For example, difference of collapsed water level between Bundles 8 and 2 at 200 s in Fig. 4.3(b) roughly corresponds to that at 380 s in Fig. 4.3(a). This means radial distribution of the amount of the accumulated water became steep much more rapidly in Test S2-13 than in Test S1-05.

This fact resulted in a higher pressure in the designated peripheral side (Bundle 8 side) than the designated central side (Bundle 1 side) at the upper boundary of the core and caused various related phenomena. For example, Fig. 4.4 indicates that the horizontal differential pressures beteen Bundles 1 and 8 became negative from positive in the earlier time in Test S2-13 than in Test S1-05.

Figures 4.5(a) and 4.5(b) indicate that the comparison of differential pressure across the tie-plate beteen the two tests. In both cases, decrease of the pressure drop across tie-plate above Bundle 8 and the increase of those above the other bundles can be seen. However, in Test S2-13, such behavior began to appear significantly from very eary time of the transient, on the other hand, in Test S1-05 it began to appear from about 200 s after the beginning of reflood. These facts suggest that flow circulation involving the core and upper plenum regions and resultant water fall back into the peripheral bundles were more significant in Test S2-13 than in Test S1-05.

Figures 4.6(a) through 4.6(f) show isobar lines in the core at the various time in Test S2-13. The isobar lines in the upper part of the core became inclined from 150 s after the beginning of reflood. This fact suggests that steam flow in the upper part of the core had a tendency to converage to the designated central region of the core and resultant small steam flow rate at the outlet of the designated peripheral region of the core caused the large water fall back into the peripheral bundles. Similar isobar lines could not be obtained for Test S1-05, however, Figs. 4.3 through 4.5 suggest that development of inclined isobar lines in the upper part of core delayed much in Test S1-05 in comparison with Test S2-13.

Figures 4.7 through 4.11 show the comparisons of steam flow rates at the various locations of the test facility between Tests S1-05 and S2-13. Because of the differences of system pressure and loop K-factors, there were small differences of these steam flow rates, but roughly speaking, they showed good agreements between the two tests. The reason of the large zero offsets in Figs. 4.7 and 4.8 is the square root conversion of the measured differential pressure into the flow rate, therefore, the error at higher flow rate is negligible.

4.2 Thermal Behaviors

Figures 4.12(a) and 4.12(b) show the comparison of quench time for the same measuring points between Test S1-05 and S2-13. The number of measuring points which indicate exceptionally long quench time was more in Test S2-13 than in Test S1-05, however, average quench for each elevation at and below 2,330 mm was slightly shorter in Test S2-13 than in Test S1-05. This is maybe due to the slightly higher system pressure transient, and more rapid water accumulation in the upper core during the early stage of transient due to the higher injection rate and the smaller subcooling. Difference in electrical insulator material of heater rods also can be a candidate of the cause of earlier quench in Test S2-13. At and above 2,760 mm, the quench time has a so wide scattering that general trend can not be pointed out.

Similar comparison for quench temperature is given in Figs. 4.13(a) and 4.13(b). It can be concluded that the quench temperatures in these two tests were statistically the same to each other, though scattering of the data was very wide.

The comparison of turnaround temperature between Tests S1-05 and S2-13 shown in Figs. 4.14(a) and 4.14(b) indicates a little lower turnaround temperature in the latter than in the former, espacially in the middle and upper part of the core.

In spite of these small differences between Tests S1-05 and S2-13, it can be concluded that the overall thermal behaviors in these two tests were almost the same as each other.

Figures 4.15(a) through 4.15(f) show the relationship between heat transfer coefficient and distance from the approarching quench front at various elevation in Test S2-13. Data bands shown by the vertical lines at every 0.25 m interval are for Test S1-05. The absolute value of heat transfer coefficient, difference of the maximum and the minimum heat transfer coefficient at each distance from the quench front and the bundle order in the heat transfer coefficient were almost the same for these tests. Therefore, heat transfer behaviors of the two tests almost the same to each other.

Detailed examination on thermal behavior of the core pointed out a more significant delay of quench propagation in the designated peripheral side of the core in Test S2-13. However, it is not so important item from the view point of reactor safety. Because, it is the phenomenon a long time after the appearance of the peak clad temperature (PCT).

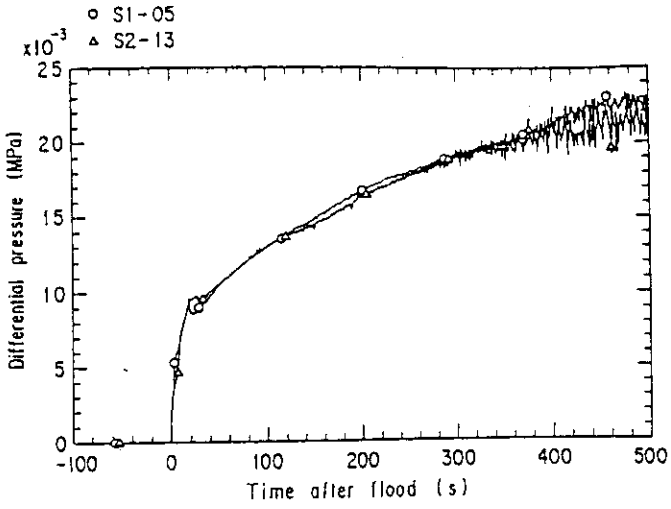

Fig. 4.1 Vertical Differential Pressures across Core Full Height in Tests S1-05 and S2-13

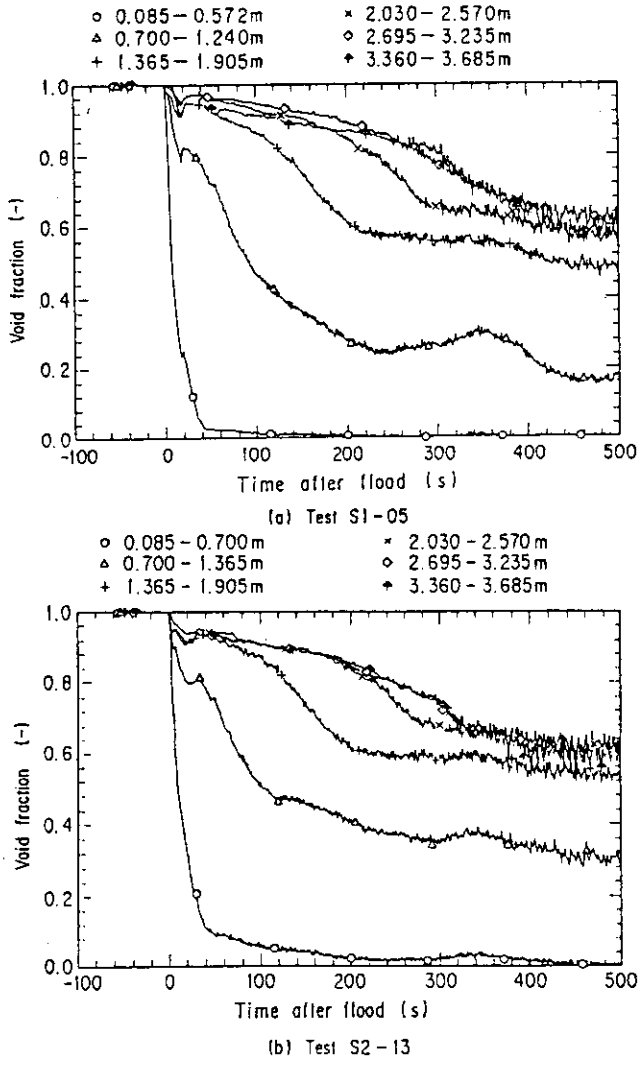

Fig. 4.2 Vertical Distributions of Void Fraction in Tests S1-05 and S2-13

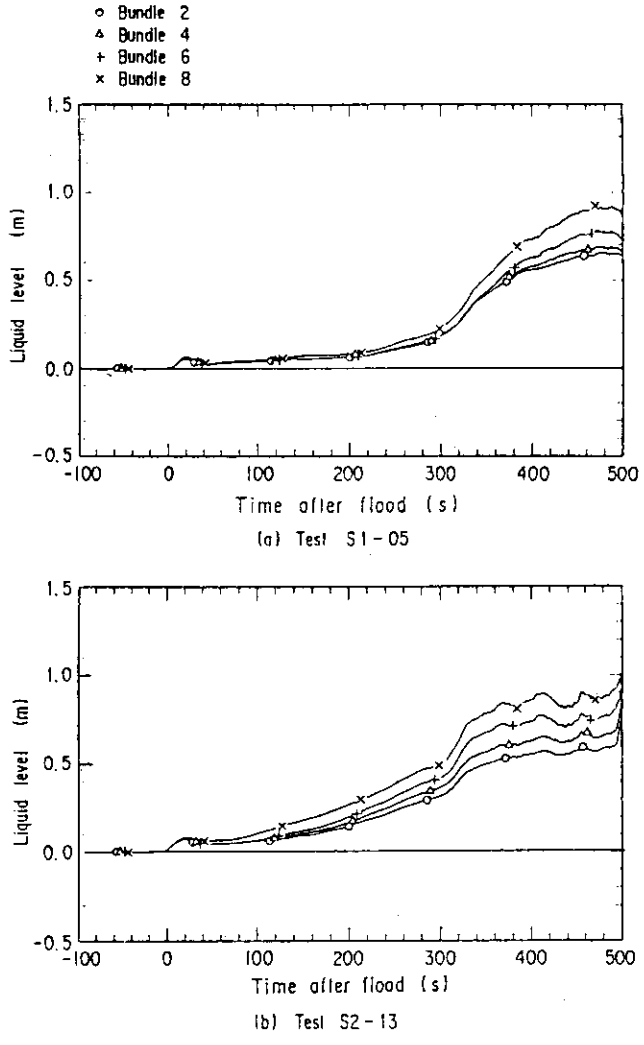

Fig. 4.3 Collapsed Water Levels in Upper Plenum in Tests S1-05 and S2-13

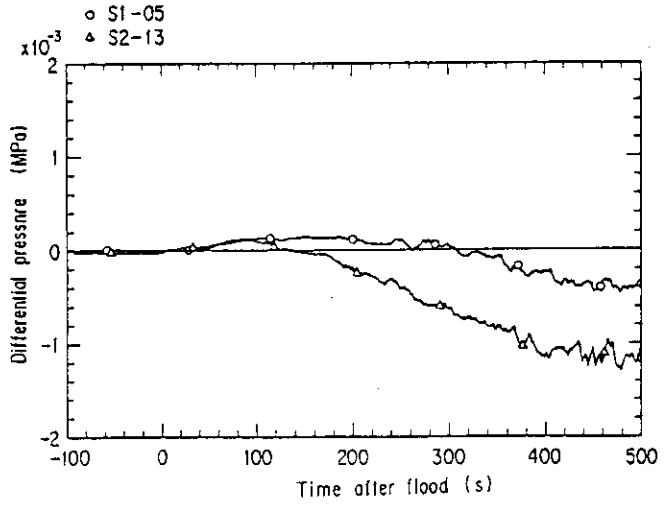

Fig. 4.4 Horizontal Differential Pressures between Bundles 1 and 8 at elevation 1.905 m in Tests S1-05 and S2-13

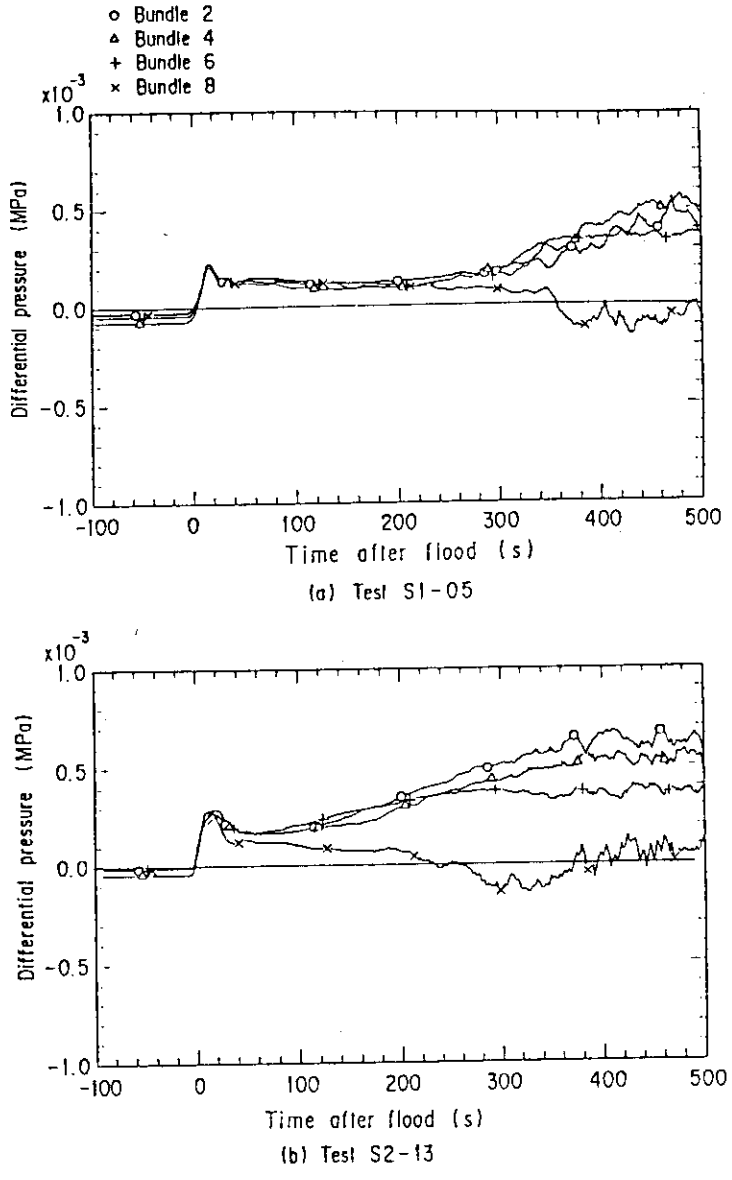

Fig. 4.5 Differential Pressures across tie plates in Tests S1-05 and S2-13

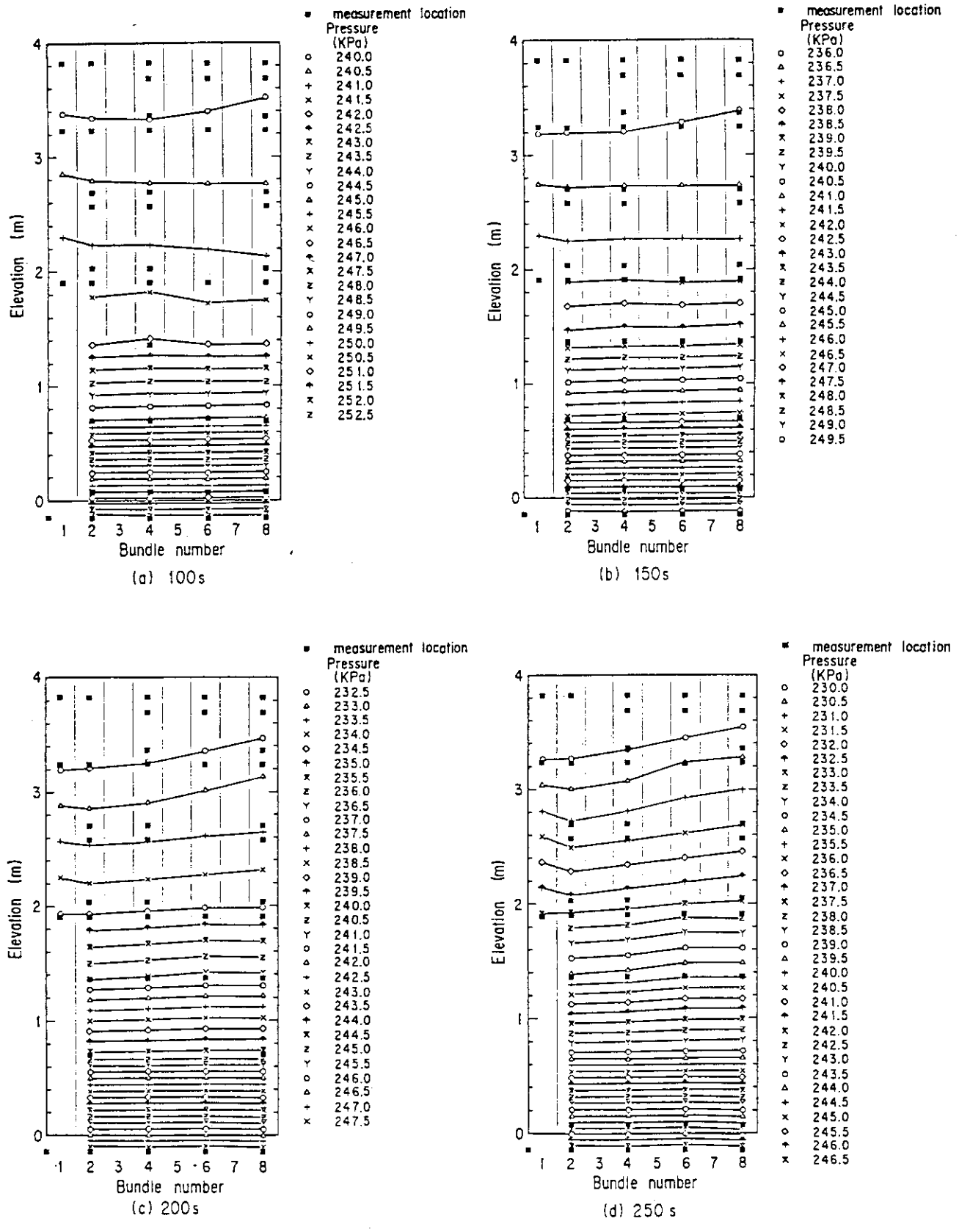

Fig. 4.6 Isobar Lines in Core in Test S2-13

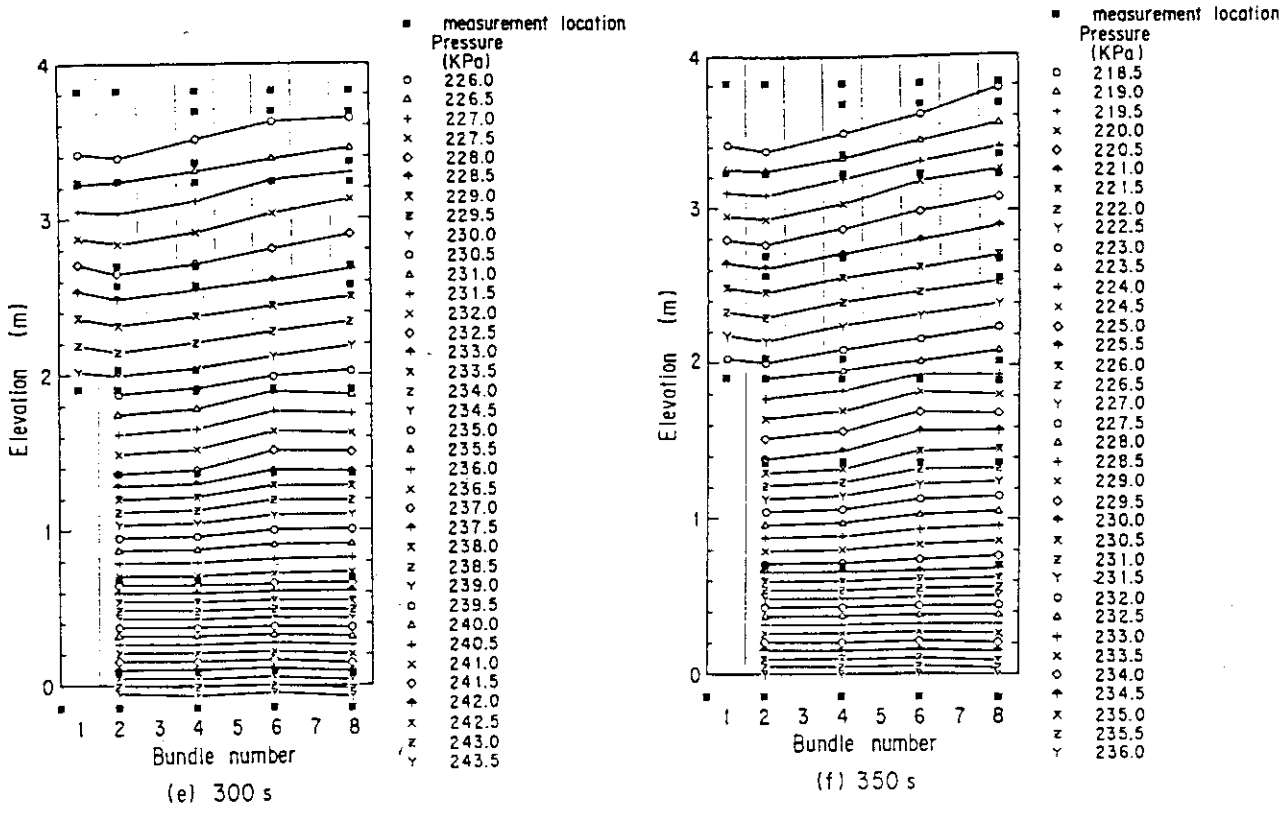
measurement location
Pressure (KPa)
226.0
226.5
227.0
227.5
228.0
228.5
229.0
229.5
230.0
230.5
231.0
231.5
232.0
232.5
233.0
233.5
234.0
234.5
235.0
235.5
236.0
236.5
237.0
237.5
238.0
238.5
239.0
239.5
240.0
240.5
241.0
241.5
242.0
242.5
243.0
243.5
Elevation (m)
Bundle number
(e) 300 s
measurement location
Pressure (KPa)
218.5
219.0
219.5
220.0
220.5
221.0
221.5
222.0
222.5
223.0
223.5
224.0
224.5
225.0
225.5
226.0
226.5
227.0
227.5
228.0
228.5
229.0
229.5
230.0
230.5
231.0
231.5
232.0
232.5
233.0
233.5
234.0
234.5
235.0
235.5
236.0
Elevation (m)
Bundle number
(f) 350 s

Fig. 4.6 (cont.)

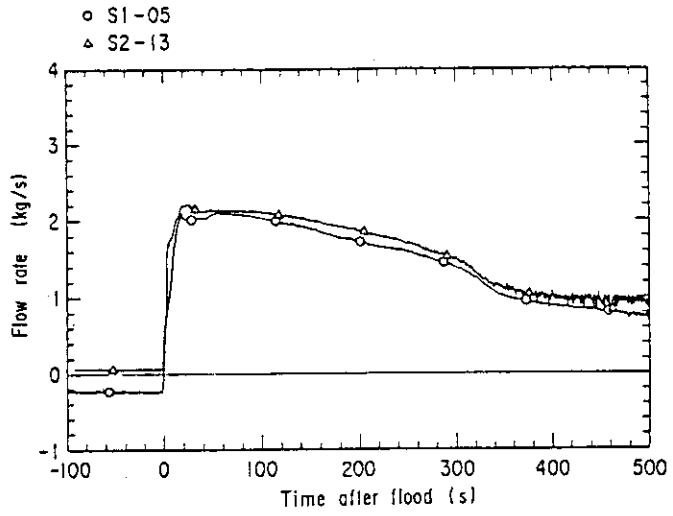

Fig. 4.7 Steam Mass Flow Rates in Intact Cold Leg in Tests S1-05 and S2-13

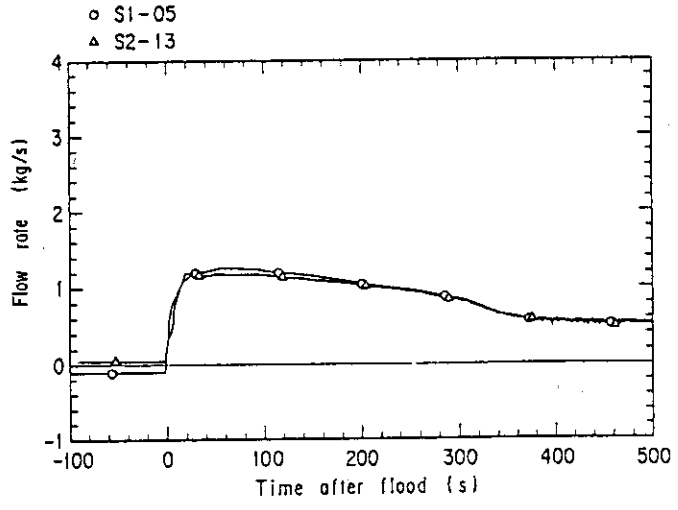

Fig. 4.8 Steam Mass Flow Rates in Broken Cold Leg Steam-Water Separator Side in Tests S1-05 and S2-13

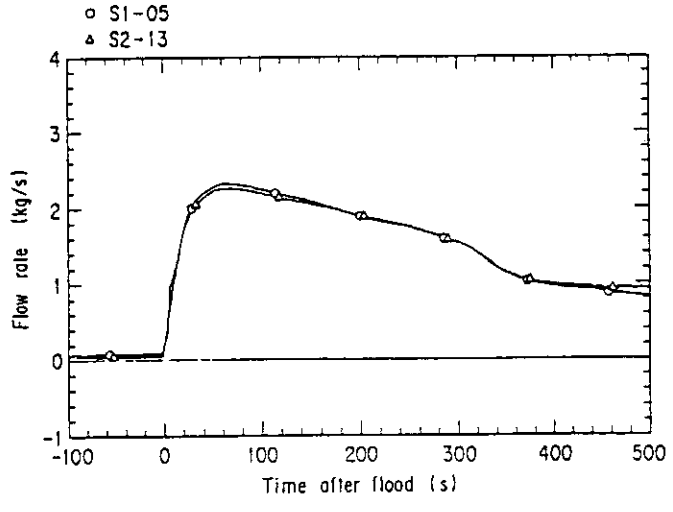

Fig. 4.9 Steam Mass Flow Rates from Containment-I to Containment-II in Tests S1-05 and S2-13

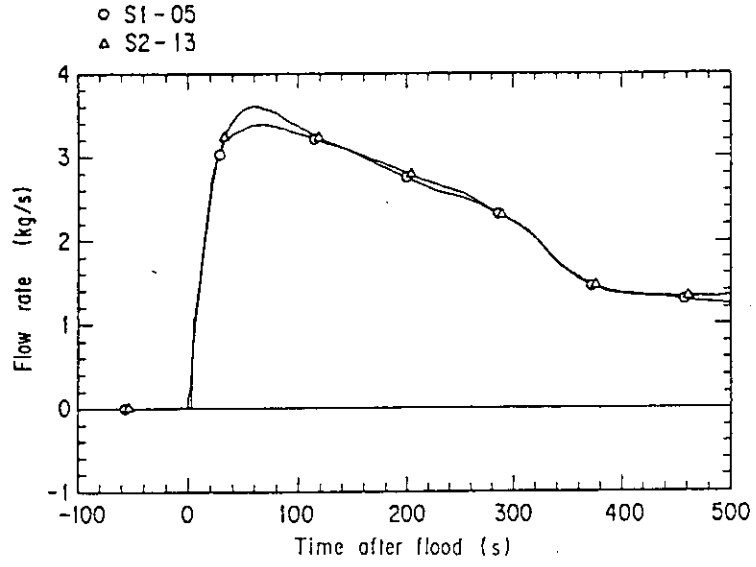

Fig. 4.10 Steam Mass Flow Rates from Containment-II to the Atmosphere in Tests S1-05 and S2-13

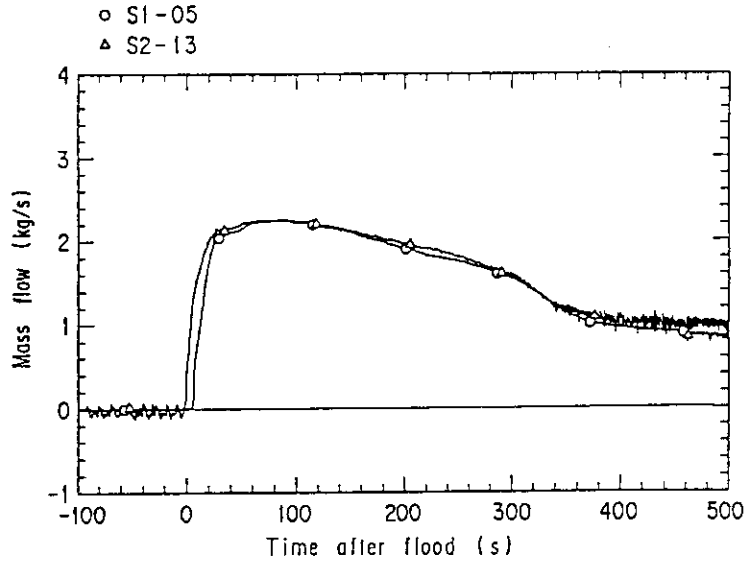

Fig. 4.11 Steam Mass Flow Rates in Broken Cold Leg Pressure Vessel Side in Tests S1-05 and S2-13 (Spool piece data)

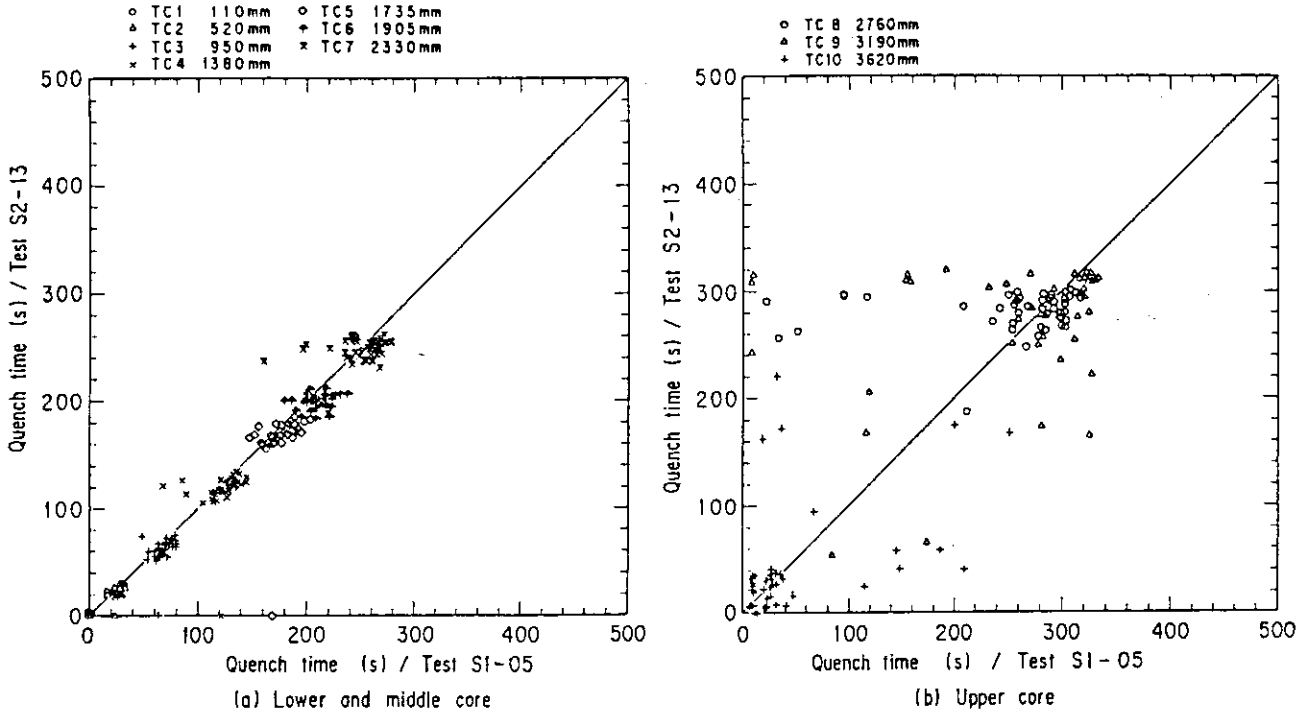

Fig. 4.12 Comparison of Quench Time between Tests S1-05 and S2-13

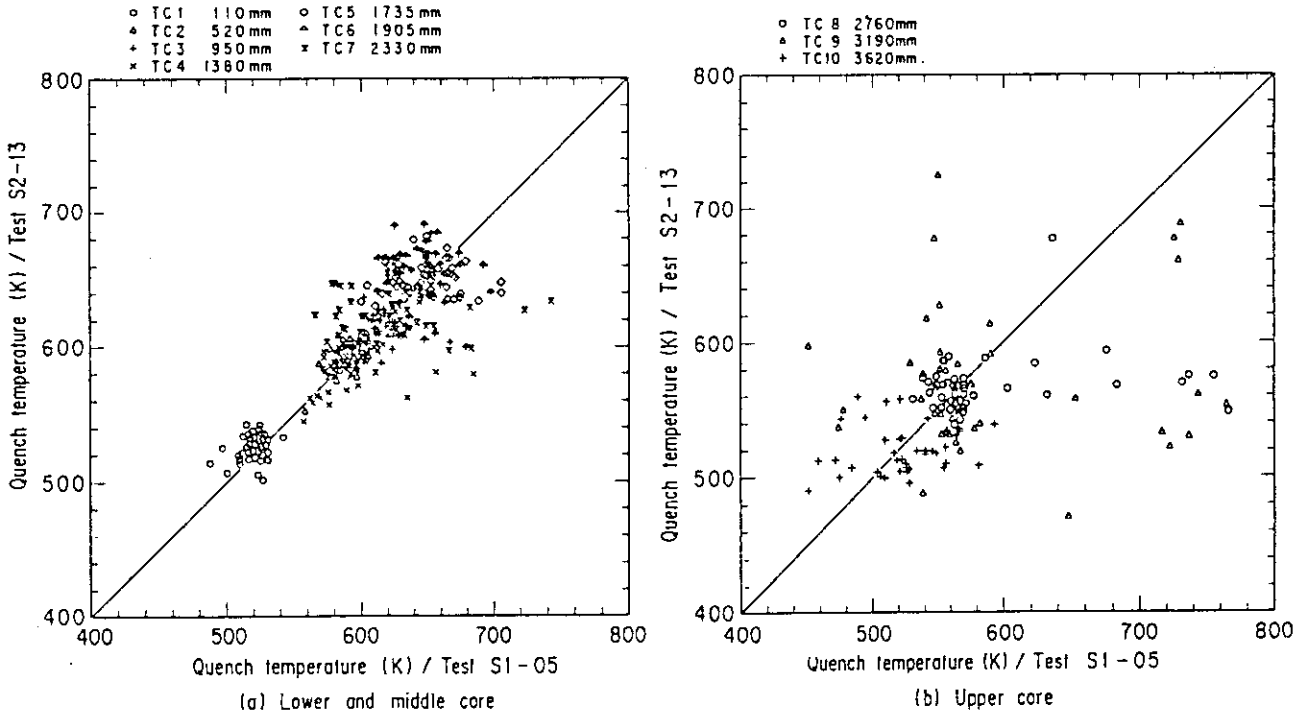

Fig. 4.13 Comparison of Quench Temperature between Tests S1-05 and S2-13

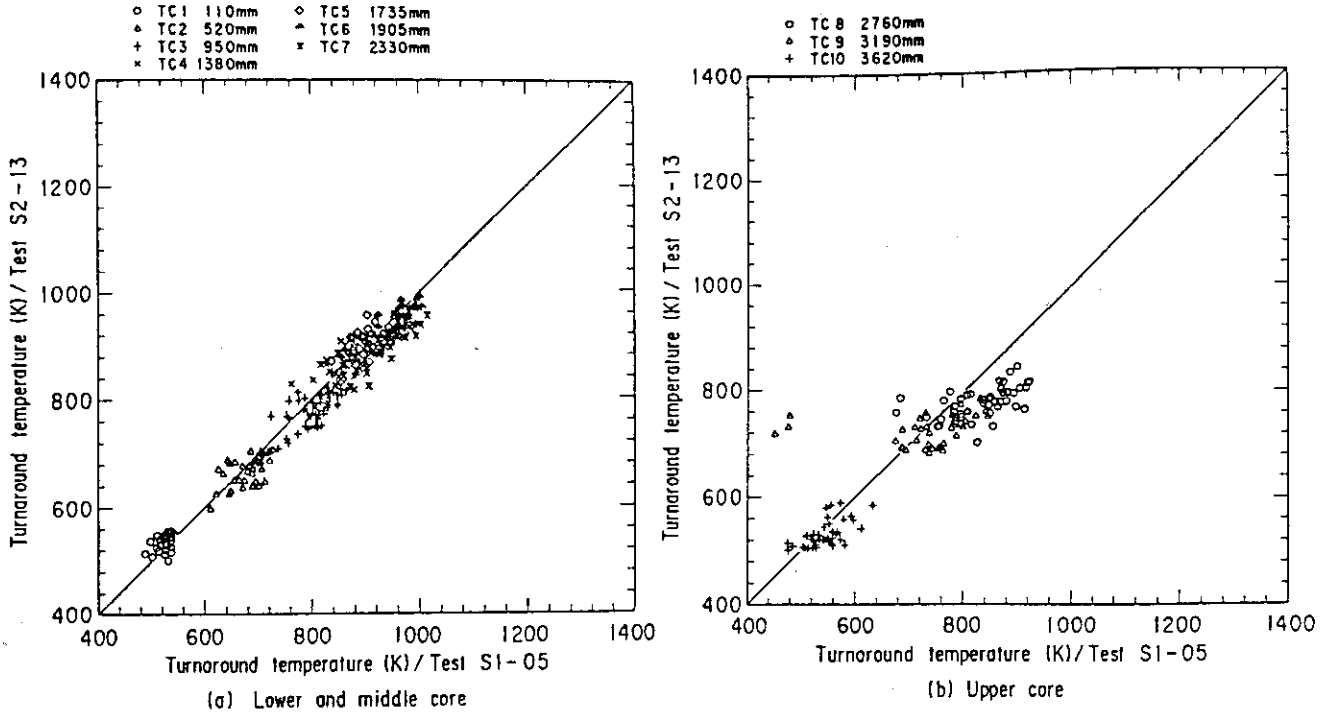

Fig. 4.14 Comparison of Turnaround Temperature between Tests S1-05 and S2-13

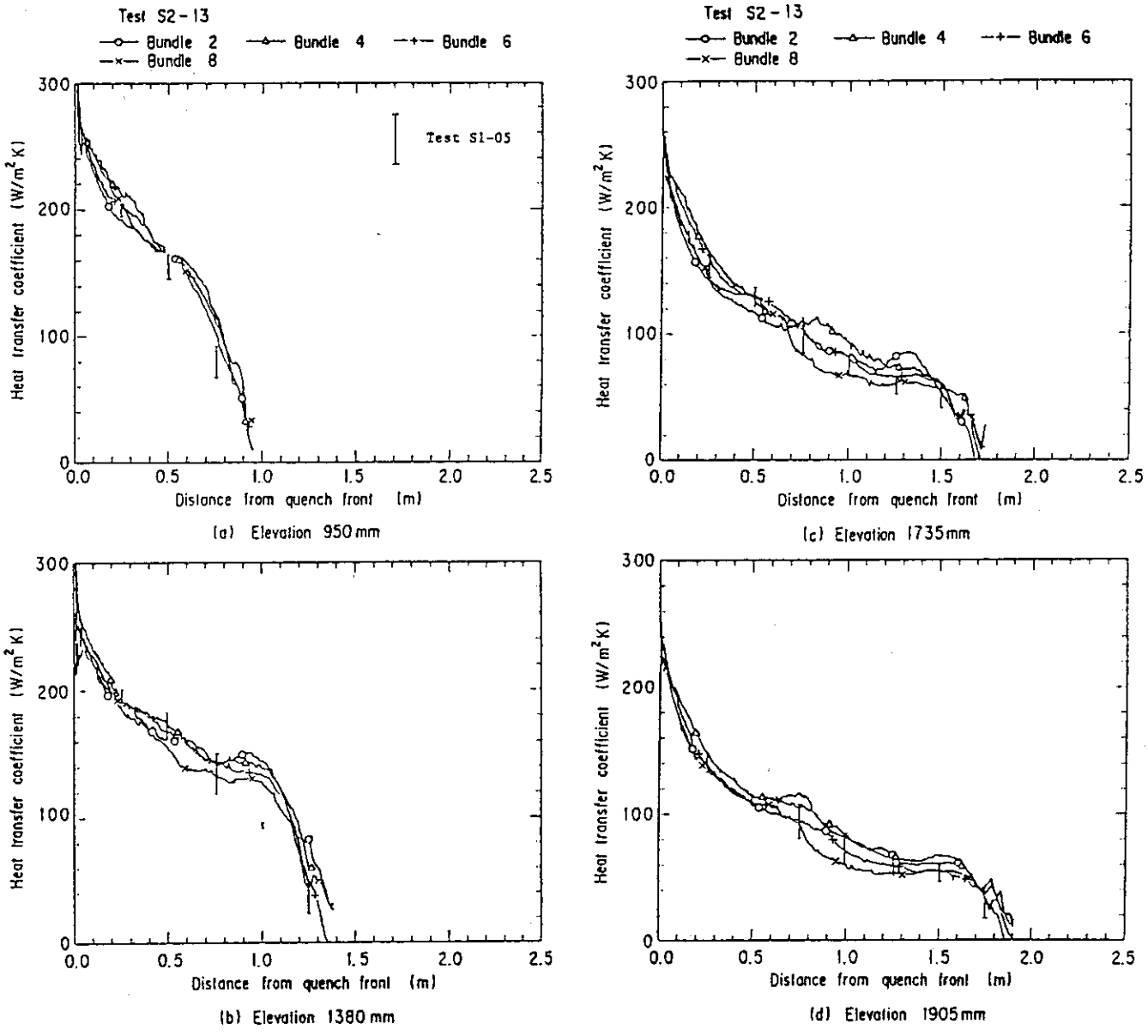

Fig. 4.15 Comparison of Bundle Dependent Characteristic of Heat Transfer Coefficient with Respect to Distance from Approaching Quench Front between Tests S1-05 and S2-13

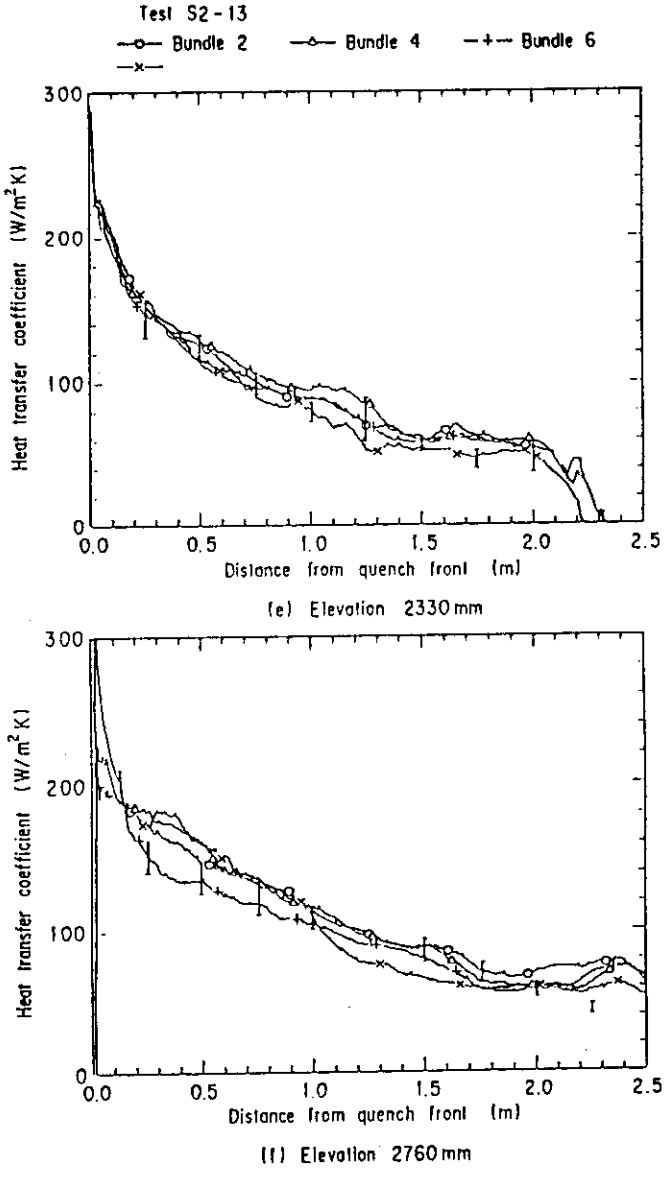
Test S2-13
Bundle 2
Bundle 4
Bundle 6
Heat transfer coefficient (W/m²K)
300
200
100
0
0.0
0.5
1.0
1.5
2.0
2.5
Distance from quench front (m)
(e) Elevation 2330mm
Heat transfer coefficient (W/m²K)
300
200
100
0
0.0
0.5
1.0
1.5
2.0
2.5
Distance from quench front (m)
(f) Elevation 2760mm

Fig. 4.15 (cont.)

5. Conclusions

Based on the test data introduced in chapter 4 for the two forced-feed reflooding tests by using the SCTF Core-I and the Core-II performed under almost the same test conditions, the following conclusions were obtained:

(1) Difference of core design between the SCTF Core-I and the Core-II gave an only little effect on thermal-hydraulic behavior in the core including two-dimensional behavior.

(2) Therefore, we can reasonably compare the test data from the Core-I and the Core-II tests regardless of the different core design except the phenomena described in the items (3).

(3) A clear effect of the core design change was seen only in the different upper plenum water accumulation behaviors and the resultant different two-dimensional fluid behaviors especially in the later portion of transient. Slope of the bottom-up quench front in the designated peripheral side of the core was also affected a little.

Acknowledgement

The authors are much indebted to Mr. T. Okubo, Mr. T. Iguchi, Dr. H. Akimoto and Mr. T. Hojo, for their useful discussions.

References

(1) K. Hirano and Y. Murao: Large Scale Reflood Test, J. At. Energy Soc. Japan, Vol. 22, No. 10, pp. 681 `@688 (1980).

(2) A. Ohnuki, et al.: Effect of Core Inlet Water Mass Flow Rate on Reflooding Phenomena in the Forced Feed SCTF Core-I Tests, JAERI-M 88-166 (1988).

(3) H. Adachi, et al.: Design of Slab Core test Facility (SCTF) in Large Scale Reflood Test Program, Part 1: Core-I, JAERI-M 83-080 (1983).

5. Conclusions

Based on the test data introduced in chapter 4 for the two forced-feed reflooding tests by using the SCTF Core-I and the Core-II performed under almost the same test conditions, the following conclusions were obtained:

(1) Difference of core design between the SCTF Core-I and the Core-II gave an only little effect on thermal-hydraulic behavior in the core including two-dimensional behavior.

(2) Therefore, we can reasonably compare the test data from the Core-I and the Core-II tests regardless of the different core design except the phenomena described in the items (3).

(3) A clear effect of the core design change was seen only in the different upper plenum water accumulation behaviors and the resultant different two-dimensional fluid behaviors especially in the later portion of transient. Slope of the bottom-up quench front in the designated peripheral side of the core was also affected a little.

Acknowledgement

The authors are much indebted to Mr. T. Okubo, Mr. T. Iguchi, Dr. H. Akimoto and Mr. T. Hojo, for their useful discussions.

References

(1) K. Hirano and Y. Murao: Large Scale Reflood Test, J. At. Energy Soc. Japan, Vol. 22, No. 10, pp. 681 `@688 (1980).

(2) A. Ohnuki, et al.: Effect of Core Inlet Water Mass Flow Rate on Reflooding Phenomena in the Forced Feed SCTF Core-I Tests, JAERI-M 88-166 (1988).

(3) H. Adachi, et al.: Design of Slab Core test Facility (SCTF) in Large Scale Reflood Test Program, Part 1: Core-I, JAERI-M 83-080 (1983).

5. Conclusions

Based on the test data introduced in chapter 4 for the two forced-feed reflooding tests by using the SCTF Core-I and the Core-II performed under almost the same test conditions, the following conclusions were obtained:

(1) Difference of core design between the SCTF Core-I and the Core-II gave an only little effect on thermal-hydraulic behavior in the core including two-dimensional behavior.

(2) Therefore, we can reasonably compare the test data from the Core-I and the Core-II tests regardless of the different core design except the phenomena described in the items (3).

(3) A clear effect of the core design change was seen only in the different upper plenum water accumulation behaviors and the resultant different two-dimensional fluid behaviors especially in the later portion of transient. Slope of the bottom-up quench front in the designated peripheral side of the core was also affected a little.

Acknowledgement

The authors are much indebted to Mr. T. Okubo, Mr. T. Iguchi, Dr. H. Akimoto and Mr. T. Hojo, for their useful discussions.

References

(1) K. Hirano and Y. Murao: Large Scale Reflood Test, J. At. Energy Soc. Japan, Vol. 22, No. 10, pp. 681 `@688 (1980).

(2) A. Ohnuki, et al.: Effect of Core Inlet Water Mass Flow Rate on Reflooding Phenomena in the Forced Feed SCTF Core-I Tests, JAERI-M 88-166 (1988).

(3) H. Adachi, et al.: Design of Slab Core test Facility (SCTF) in Large Scale Reflood Test Program, Part 1: Core-I, JAERI-M 83-080 (1983).

Appendix A

Slab Core Test Facility (SCTF)
Core-I and Core-II

A.1 Test Facility

The Slab Core Test Facility was designed under the following design phylosophy and design criteria:

a. Design Philosophy

(1) The facility should provide the capability to study the two-dimensional, thermal-hydraulic behavior in the core and in the pressure vessel especially due to the radial power distribution during the end of blowdown, refill and reflood phases of a simulated LOCA for a pressurized water reactor.

(2) To properly simulate the core heat transfer and hydrodynamics, a special emphasis is put on the proper simulation of the components in the pressure vessel. As the components in the pressure vessels are provided a simulated core, downcomer, core baffle region, lower plenum, upper plenum and upper head. On the other hand, simplified primary coolant loops are provided. As the primary coolant loops are provided a hot leg, an intact cold leg, broken cold legs and a steam-water separator. The object of the steam-water separator is to measure the flow rate of carryover water coming out of the upper plenum.

b. Design Criteria

(1) The reference reactor for simulation in the SCTF is the Trojan reactor in the United States which is a four loop 3,300 MWt PWR. The Ooi reactor in Japan is also referred which is of the similar type to the Trojan reactor.

(2) A full scale radial and axial section of a pressurized water reactor is provided as a simulated core of the SCTF with single bundle width.

(3) The simulated core consists of 8 bundles arranged in a row. Each bundle has electrically heated rods simulating fuel rods and non-heated rod with 16 × 16 array.

(4) The flow area and fluid volume of components are scaled down based on the core flow area scaling.

(5) To properly simulate the flow behavior of carryover water and entrainment, the elevations of hot leg and cold legs are designed to be the same as the PWRs as much as possible.

(6) The honeycomb structure is used as the side walls which accomodate the slab core, upper plenum and the upper part of lower plenum, so as to minimize the effect of walls on the disturbance of the

core heat transfer and hydrodynamics. In Core-II, wall plates are attached to the inner surface of the honeycomb structure pannels to smoothen the side wall surface.

(7) To investigate the effect of flow resistance in the primary loops are provided the orifices of which dimension is changeable.

(8) The maximum allowable temperature of the simulated fuel rods is 1273 K and the maximum allowable pressure of the facility is 0.6 MPa.

(9) The facility is equipped with a hot leg equivalent to four actual hot legs connecting the upper plenum to the steam-water separator, an intact cold leg equivalent to three actual cold legs connecting the steam-water separator to the downcomer and two broken cold legs, one is for the steam-water separator side and the other for the pressure vessel side.

(10) The emergency core cooling system (ECCS) consists of an accumulator system (Acc.), a low pressure coolant injection system (LPCI) and a combined injection system.

(11) ECC water injection ports are the cold leg, hot leg, upper plenum, downcomer, lower plenum and above the upper core support plate. These portions are to be chosen according to the object of the test.

(12) For better simulation of lower plenum flow resistance, simulated fuel rods do not penetrate through the bottom plate of the lower plenum but terminate below the bottom of the core.

(13) For measurements in the pressure vessel including core measurements, the feature of the slab geometry of the pressure vesse is utilized as much as possible. Design and arrangement of the instruments are done so as to be able to carry out installation, calibration and removal of the instruments.

(14) View windows are provided where flow pattern recognition is important. The locations are, the core, the interface between the core and the upper plenum, hot leg, pressure vessel side broken cold leg and the downcomer.

(15) The blocked bundle test is carried out in Core-I in order to investigate the effect of the ballooned fuel rods and the unblocked normal bundle test for the Core-II.

(16) Simulated types of break are cold leg break and hot leg break.

(17) The components and systems such as the containment tanks and ECC water supply system of the CCTF are shared with the SCTF to the maximum extent.

The overall schematic diagram of the SCTF is shown in Fig. A-1. The principal dimensions of the facility is shown in Table A-1, and the comparison of dimensions between the SCTF and the referred PWR is shown in Fig. A-2.

A.1.1 Pressure Vessel and Internals

The pressure vessel is of slab geometry as shown in Fig. A-3. The height of the components in the pressure vessel is almost the same as the reference reactor's, and the flow area and the fluid volume of each component are scaled down based on the nominal core flow area scaling, 1/21.

The core consists of 8 bundles in a row and each bundles include simulated fuel rods and non-heated rods with 16 × 16 array. The core arrangement for the SCTF Core-I and Core-II is shown in Figs. A-4 and A-5. As shown in these figures, the Core-I has two blockage bundles, Bundles 3 and 4, of which all heater rods have blockage sleeves at their mid-plane to simulate flow blockage, on the other hand, in the Core-II there are no blockage sleeves. Relating to this, the Core-I has closing plates and flow interceptors on the both sides of all eight bundles facing the side walls at the elevation including the blockage section, on the other hand, the Core-II does not have them. The core is enveloped in the Core-I by the honeycomb thermal insulator which is attached on the barrel, on the other hand, in the Core-II the wall plates with 6 mm thickness are attached to the inner surface of the honeycomb pannels to smoothen the inner surface of the side walls.

The downcomer is located at one end of the pressure vessel which corresponds to the periphery of the actual reactor. The downcomer can be isolated at the bottom from the lower plenum with a partition plate for performing forced-feed reflooding tests. The core baffle region is, on the other hand, located between the core and the downcomer. The core baffle region for the SCTF Core-I is shown in Fig. A-6. Bottom flow path of 110 mm × 230 mm size is closed in the Core-II. In both cases, contact lines of the vertical partition plate between the core and core baffle region and the core barrel groove is not sealed.

For better understanding, the cross section of the pressure vessel at the elevation of midplane of the core is shown in Fig. A-7.

The design of upper plenum internals is based on that of the new Westinghouse 17 × 17 array fuel assemblies. The internals consist of control rod guide tubes, support columns, orifice plates and open holes and those arrangements is shown in Fig. A-8. The radius of each internal is scaled down by factor 8/15 from that of an actual reactor. Flow resistance baffles are inserted into the guide tubes. The elevation and the configuration of baffles plates are shown in Fig. A-9 and A-10.

The height of the hot leg and cold legs are designed as close to the actual PWR as possible. However, in order to avoid the interference of the nozzles in the downcomer, the height of nozzles for the broken cold leg and the intact cold leg are shifted down compared to that of the hot leg as shown in Fig. A-3.

A.1.2 Heater Rod Assembly

The heater rod assembly for the SCTF Core-I consists of 8 bundles arranged in a row. These bundles are composed of 6 normal unblocked bundles which are located at the 1st, 2nd and 5th to 8th bundles and 2 blocked bundles which are 3rd and 4th bundles as shown in Fig. A-4. Each bundle has 234 electrically heated rods and 22 non-heated rods. The dimensions of the heater rods are based on a Westinghouse 15 × 15 fuel rod bundle, and the heated length and the outer diameter of each heater rod are 3.66 m and 10.7 mm, respectively. A heater rod consists of a nichrome heater element, magnesium oxide (MgO) and Nichrofer-7216 sheath (equivalent to Inconel 600). The sheath wall thickness is about 1.0 mm and is thicker than the actual fuel cladding because of the requirements for thermocouple installation. The heater element is a helical coil and has a 17 step chopped cosine axial power profile as shown in Fig. A-11. The peaking factor is 1.4.

In the Core-II, there are no blocked bundles as described before, and in addition, 1/3 of the heated part of the simulated fuel rods has boron nitrate (BN) insulator between the heater element and the cladding, instead of MgO. Cladding material for the Core-II is Inconel 600, instead of Nichrofer-7216, but these two materials are equivalent.

Non-heated rods are either stainless steel pipes or solid rods of 13.8 mm O.D. The heater rods and non-heated rods are fixed at the top

of the core allowing the rods to move downward when the thermal expansion occurs. In Fig. A-12 the axial position where blockage sleeves for simulating the balooned fuel rod are equipped in the Core-I is shown. The blockage sleeves consist of three types of sleeve, one is used for the rods at the corner adjacent to the next blocked bundle, another for the rods adjacent to the side walls and the third for the rods except for the periphery of the blocked bundle. These are named A, B and C respectively in the Fig. A-13.

For better simulation for flow resistance in the lower plenum the simulated rods do not penetrate through the bottom plate of the lower plenum as shown in Fig. A-12.

A.1.3 Primary Loops and ECCS

Primary loops consist of a hot leg equivalent to the four actual hot legs, a steam-water separator for measuring the flow rate of carry over water, an intact cold leg equivalent to the three actual intact loops, a broken cold leg on the pressure vessel side and a broken cold leg on the steam-water separator side. These two broken cold legs are connected to two containment tanks through break valves, respectively. The arrangement of the primary loops is shown in Fig. A-14. The flow area of each loop is scaled down based on the core flow area scaling. It should be emphasized that the cross section of the hot leg is a elongated circle to realize the proper flow pattern in the hot leg. The steam-water separator has a steam generator inlet plenum simulator to realize the proper flow characteristics of carryover water. The cross section of the hot leg and the configuration of the steam generator inlet plenum simulator are shown in Fig. A-15.

A pump simulator and a loop seal part are provided for the intact cold leg. The arrangement of the intact cold leg is shown in Fig. A-16. The pump simulator consists of the casing and duct simulators and an orifice plate as shown in Fig. A-17. The loop resistance is adjusted with the orifice plate.

In principle, ECCS consists of an accumulator and a low pressure injection system. The injection port is located as already described in the design criteria. Besides, a combined injection system is provided to inject water into the upper plenum through top and/or side nozzles just above the upper core support plate (UCSP). This system also can inject water into the other ECC injection ports. In addition, UCSP

water extraction system is provided at the opposite side of the UCSP injection system.

A.1.4 Containment Tanks and Auxiliary System

Two containment tanks are provided to the SCTF. The containment tank-I is connected with the downcomer through the pressure vessel side broken cold leg and the containment tank-II is connected with the steam-water separator through the steam-water separator side broken cold leg. Especially in the containment tank-I, carryover water from the downcomer is measured by phase separation. These containment tanks and auxiliary system such as a pressurizer for injecting water from the Acc. tank, etc. are shared with the CCTF.

A.2 Instrumentation

The instrumentation in the SCTF has been provided both by JAERI and USNRC. The JAERI-provided instrumentation includes the measurement of temperatures, pressures, differential pressures, liquid levels, flow velocities, and heating powers. USNRC has provided film probes, impedance probes, string probes, liquid level detectors (LLDs), fluid distribution grids (FDGs), turbine meters, drag disks, γ-densitometers, spool pieces and video optical probes. The measurement items of the JAERI- and USNRC- provided instruments are listed in Tables A-2 and A-3, respectively. Location of each instrument is shown in Figs. A-18 through A-31.

Table A-1 Principal Dimensions of Test Facility

1. Core Dimension	
(1) Quantity of Bundle	8 Bundles
(2) Bundle Array	1×8
(3) Bundle Pitch	230 mm
(4) Rod Array in a Bundle	16×16
(5) Rod Pitch in a Bundle	14.3 mm
(6) Quantity of Heater Rod in a Bundle	234 rods
(7) Quantity of Non-Heated Rod in a Bundle	22 rods
(8) Total Quantity of Heater Rods	234×8=1872 rods
(9) Total Quantity of Non-Heated Rods	22×8=176 rods
(10) Effective Heated Length of Heater Rod	3660 mm
(11) Diameter of Heater Rod	10.7 mm
(12) Diameter of Non-Heateed Rod	13.8 mm
2. Flow Area & Fluid Volume	
(1) Core Flow Area* (nominal)	0.259 m²
(2) Core Fluid Volume	0.92 m³
(3) Baffle Region Flow Area	0.10 m²
(4) Baffle Region Fluid Volume	0.36 m³
(5) Downcomer Flow Area	0.121 m²
(6) Upper Annulus Flow Area	0.158 m²
(7) Upper Plenum Horizontal Flow Area	0.525 m²
(8) Upper Plenum Fluid Volume	1.16 m³
(9) Upper Head Fluid Volume	0.86 m³
(10) Lower Plenum Fluid Volume	1.305 m³
(11) Steam Generator Inlet Plenum Simulator Flow Area	0.626 m²
(12) Steam Generator Inlet Plenum Simulator Fluid Volume	0.931 m³
(13) Steam Water Separator Fluid Volume	5.3 m³
(14) Flow Area at the Top Plate of Steam Generator Inlet Plenum Simulator	0.195 m²
(15) Hot Leg Flow Area	0.0826 m²
(16) Intact Cold Leg Flow Area (Diameter = 297.9 mm)	0.0697 m²
(17) Broken Cold Leg Flow Area (Diameter = 151.0 mm)	0.0179 m²

* Effective core flow area based on the measured level-volume relationship including gap between core barrel and pressure vessel wall and various penetration holes is :

0.35 m² for Core I

0.32 m² for Core II

Table A-1 (cont.)

(18) Containment Tank I Fluid Volume	30 m^3
(19) Containment Tank II Fluid Volume	50 m^3

3. Elevation & Height

(1) Top Surface of Upper Core Support Plate (UCSP)	0 mm
(2) Bottom Surface of UCSP	-76 mm
(3) Top of the Effective Heated Length of Heater Rod	-393 mm
(4) Bottom of the Skirt in the Lower Plenum	-5270 mm
(5) Bottom of Intact Cold Leg	+724 mm
(6) Bottom of Hot Leg	+1050 mm
(7) Top of Upper Plenum	+2200 mm
(8) Bottom of Steam Generator Inlet Plenum Simulator	+1933 mm
(9) Genterline of Loop Seal Bottom	-2281 mm
(10) Bottom Surface of End Box	-185.1 mm
(11) Top of the Upper Annulus	+2234 mm
(12) Height of Steam Generator Inlet Plenum Simulator	1595 mm
(13) Height of Loop Seal	3140 mm
(14) Inner Height of Hot Leg Pipe	737 mm
(15) Bottom of Lower Plenum	-5770 mm
(16) Top of Upper Head	+2887 mm

Table A-2 Measurement Items of SCTF
(JAERI-provided instruments)

LOCATION	ITEM	PROBE	QUANTITY CORE-I/II
1. CORE			
center	pressure	DP cell	1/1
short range of core	diff. press.	DP cell	22/22
half length of core	diff. press.	DP cell	16/16
full length of core	diff. press.	DP cell	8/8
across spacers	diff. press.	DP cell	7/7
across end box	diff. press.	DP cell	8/8
across 3 assemblies	diff. press.	DP cell	0/5
across 4 assemblies	diff. press.	DP cell	3/3
across 5 assemblies	diff. press.	DP cell	0/4
across 8 assemblies	diff. press.	DP cell	3/0
below and above end box	steam velocity	Pitot-tube	3/0
sub-channel	steam velocity	Pitot-tube	13/2
below end box hole	fluid temp.	T/C	16/16
above end box hole	fluid temp.	T/C	16/16
core baffle	fluid temp.	T/C	6/6
non-heating rods	fluid temp.	T/C	96/144
	steam temp.	SSP	16/28
	clad temp.	T/C	108/48
heater rods	clad temp.	T/C	640/642
side walls	wall temp.	T/C	36/36
core baffle	wall temp.	T/C	6/6
core baffle	liquid level	DP cell	1/0
short range of core baffle	liquid level	DP cell	6/6
heater rod bundles	power		8/8
			sum(1039)/ (1032)
2. UPPER PLENUM			
center	pressure	DP cell	1/1
across end box tie plate	diff. press.	DP cell	8/8
core outlet-hot leg inlet	diff. press.	DP cell	4/2
upper part of upper plenum	diff. press.	DP cell	0/2
periphery of UCSP hole	fluid temp.	T/C	8/8

Table A-2 (cont.)

LOCATION	ITEM	PROBE	QUANTITY CORE-I/II
center of UCSP hole	fluid temp.	T/C	8/8
250mm & 1000mm above UCSP	fluid temp.	T/C	8/8
surface of UCSP	fluid temp.	T/C	8/8
above UCSP hole	steam temp.	SSP	8/8
surface of structure	wall temp.	T/C	15/15
side walls	wall temp.	T/C	8/8
above end box tie plate	liquid level	DP cell	8/8
above UCSP	liquid level	DP cell	9/9
above UCSP (v.)	steam velocity	Pitot-tube	2/0
inter-structures (h.)	steam velocity	Pitot-tube	2/0
			sum(97)/(93)
3. LOWER PLENUM			
below bottom spacer	pressure	DP cell	1/1
lower plenum - upper plenum	diff. press.	DP cell	1/1
core inlet	fluid temp.	T/C	8/8
inlet from downcomer	fluid temp.	T/C	2/2
side & bottom walls	wall temp.	T/C	4/4
below bottom spacer	lqiuid level	DP cell	1/1
			sum(17)/(17)
4. DOWNCOMER			
upper position	pressure	DP cell	1/1
horizontal direction	diff. press.	DP cell	1/1
four levels	fluid temp.	T/C	8/8
side wall	wall temp.	T/C	2/2
inner wall	wall temp.	T/C	2/2
below cold leg level	liquid level	DP cell	1/1
above cold leg level	liquid level	DP cell	1/1
below core inlet level	liquid level	DP cell	1/1
bottom	momentum flux	Drag disk	2/2
			sum(19)/(19)

Table A-2 (cont.)

LOCATION	ITEM	PROBE	QUANTITY CORE-I/II
5. HOT LEG			
full length	diff. press.	DP cell	1/1
multiple points	fluid temp.	T/C	3/3
	steam temp.	SSP	3/3
	wall temp.	T/C	1/1
	liquid level	DP cell	2/2
			sum(10)/(10)
6. S/W SEPARATOR SIDE BROKEN COLD LEG			
across resistance simulator	diff. press.	DP cell	1/1
S/W separator to containment tank II	flow rate	Venturi	1/1
multiple points	fluid temp.	T/C	1/1
	steam temp.	SSP	1/1
	wall temp.	T/C	1/1
			sum(5)/(5)
7. INTACT COLD LEG			
full length	diff. press.	DP cell	1/1
across resistance simulator	diff. press.	DP cell	1/1
across pump simulator	diff. press.	DP cell	1/1
	flow rate	Venturi	1/1
near resistance simulator	fluid temp.	T/C	1/1
pump simulator	fluid temp.	T/C	3/3
	wall temp.	T/C	1/1
			sum(9)/(9)
8. PV SIDE BROKEN COLD-LEG			
	pressure	DP cell	1/1
full length	diff. press.	DP cell	1/1
across resistance simulator	diff. press.	DP cell	1/1

Table A-2 (cont.)

LOCATION	ITEM	PROBE	QUANTITY CORE-I/II
multiple points	fluid temp.	T/C	4/4
	wall temp.	T/C	2/2
	liquid level	DP cell	2/2
			sum(11)/(11)
9. VENT LINE			
across the length	diff. press.	DP cell	1/1
			sum(1)/(1)
10. S/W SEPARATOR			
	pressure	DP cell	1/1
between inlet and outlet	diff. press.	DP cell	1/1
SG plenum simulator	diff. press.	DP cell	1/1
SG plenum simulator	fluid temp.	T/C	2/2
top and bottom	fluid temp.	T/C	2/2
wall	wall temp.	T/C	2/2
full height	liquid level	DP cell	1/1
liquid extraction	flow rate	DP cell	1/1
			sum(11)/(11)
11. CONTAINMENT TANK-I			
	pressure	DP cell	1/1
downcomer-CT-I	diff. press.	DP cell	1/1
CT-I-CT-II	diff. press.	DP cell	1/1
	flow rate	DP cell	1/1
full height	liquid level	DP cell	1/1
		float	1/1
top, middle & bottom	fluid temp.	T/C	3/3
wall	wall temp.	T/C	1/1
			sum(10)/(10)
12. CONTAINMENT TANK-II			
	pressure	DP cell	1/1
upper plenum-CT-II	diff. press.	DP cell	1/1
separator-CT-II	diff. press.	DP cell	1/1
steam blow line	flow rate	DP cell	1/1

Table A-2 (cont.)

LOCATION	ITEM	PROBE	QUANTITY CORE-I/II
full height	liquid level	DP cell	1/1
top, middle & bottom	fluid temp.	T/C	3/3
			sum(8)/(8)
13. ECC INJECTION SYSTEM			
downcomer/lower plenum/ hot leg	flow rate	E-M flow meter	1/1
intact cold leg	flow rate	E-M flow meter	1/1
broken cold leg	flow rate	E-M flow meter	1/1
LPCI	flow rate	E-M flow meter	1/1
primary line flom combined inj. system	flow rate	E-M flow meter	0/1
just above UCSP	flow rate	E-M flow meter	0/4
top of upper plenum	flow rate	E-M flow meter	0/4
ECC heater	fluid temp.	T/C	1/2
hot leg inj. port	fluid temp.	T/C	0/1
intact cold leg inj. port	fluid temp.	T/C	0/1
broken cold leg inj. port	fluid temp.	T/C	0/1
downcomer inj. port	fluid temp.	T/C	0/1
lower plenum inj. port	fluid temp.	T/C	0/1
combined injection to primary line	fluid temp.	T/C	0/1
just above UCSP	fluid temp.	T/C	0/4
top of upper plenum	fluid temp.	T/C	0/4
			sum(5)/(29)
14. UCSP WATER EXTRACTION SYSTEM			
extraction line	flow rate	DP cell + E-M flow meter	4/4
steam line	flow rate	DP cell	4/4
extraction line	fluid temp.	T/C	5/4
steam line	fluid temp.	T/C	1/0
extraction line	liquid level	DP cell	4/4
			sum(18)/(16)

Table A-2 (cont.)

LOCATION	ITEM	PROBE	QUANTITY CORE-I/II
15. SATURATED WATER TANK			
	fluid temp.	T/C	1/1
	liquid level	DP cell	1/1
			sum(2)/(2)
16. NITROGEN GAS SYSTEM			
	flow rate	DP cell	1/1
injection port	fluid temp.	T/C	1/1
			sum(2)/(2)

Total 1264/1275

Table A-3 Measurement Items of SCTF
(USNRC-provided instruments)

LOCATION	ITEM	PROBE	QUANTITY CORE-I/II
1. CORE			
non-heated rods	liquid level	LLD	80/80
non-heated rods	film thickness and velocity	film probe	6/6
non-heated rods	void fraction and droplet velocity	flag probe	8/4
side walls	film thickness and velocity	film probe	8/8
sub-channel	fluid density	γ-densitometer	10/10
end box	fluid density	γ-densitometer	5/5
end box	flow pattern	video optical probe	1/1
2. UPPER PLENUM			
full height	liquid level	FDG	64/64
structure surface	film thickness and velocity	film probe	6/0
side walls	film thickness and velocity	film probe	6/6
inter structure	void fraction	prong probe	8/8
above UCSP hole	velocity	turbine	8/8
inter structure	velocity	turbine	4/4
inter structure	fluid density	γ-densitometer	4/4
hot leg inlet	flow pattern	video optical probe	1/1
3. LOWER PLENUM			
core inlet	velocity	turbine	4/4
bottom	reference conductivity	reference probe	1/1
4. DOWNCOMER			
full height	liquid level	FDG	42/42
two levels	velocity	drag disk	3/3
two levels	void fraction	string probe	3/3

Table A-3 (cont.)

LOCATION	ITEM	PROBE	QUANTITY CORE-I/II
5. HOT LEG	mass flow rate fluid density void fraction	spool piece	1/1
6. PV SIDE BROKEN COLD-LEG	mass flow rate fluid density void fraction	spool piece	1/1
7. VENT LINE	mass flow rate void fraction	spool piece	1/1

sum(275)/(265)

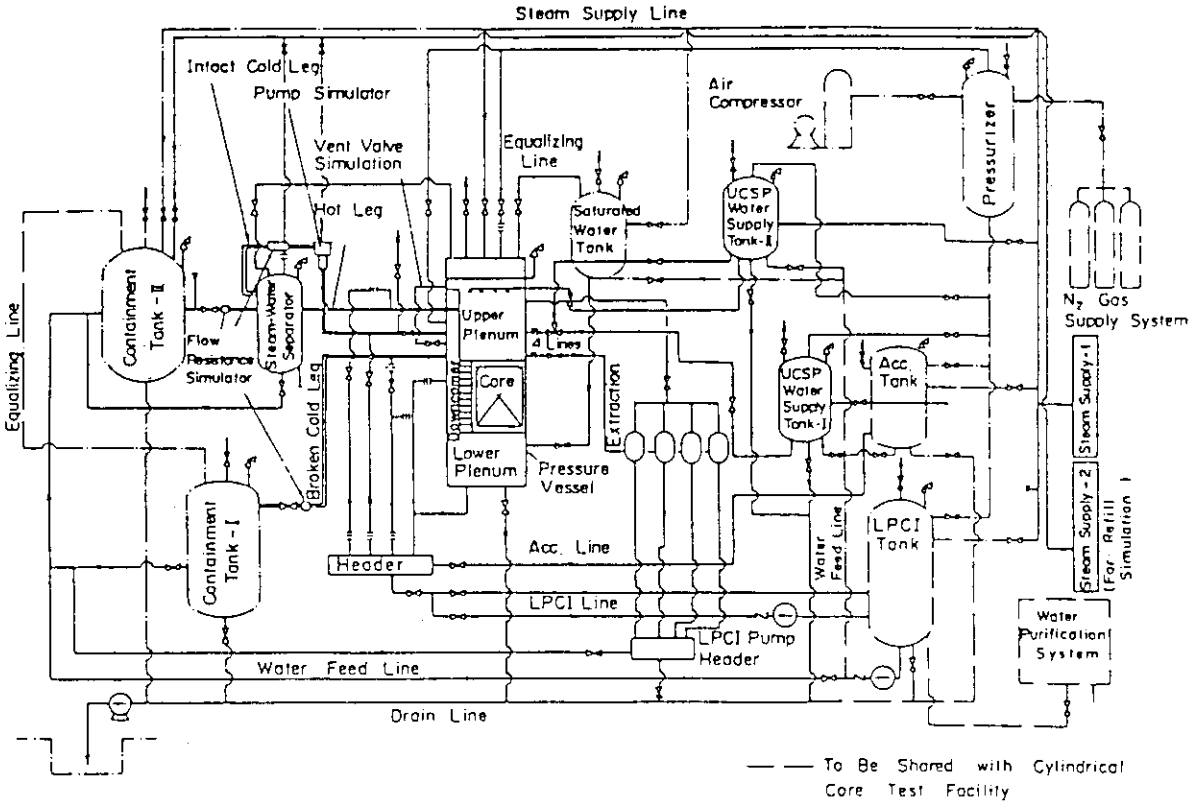

Fig. A-1 Schematic Diagram of Slab Core Test Facility

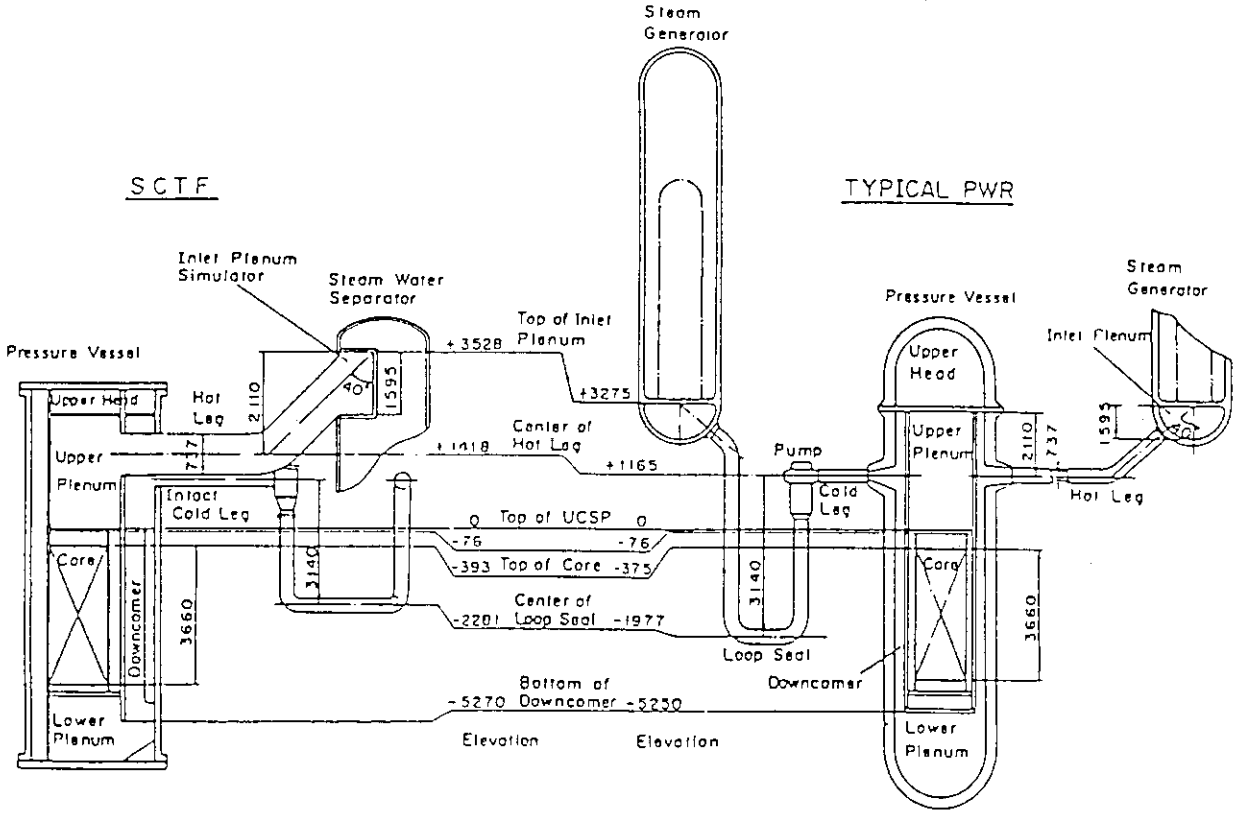

Fig. A-2 Comparison of Dimensions between SCTF and a Reference PWR

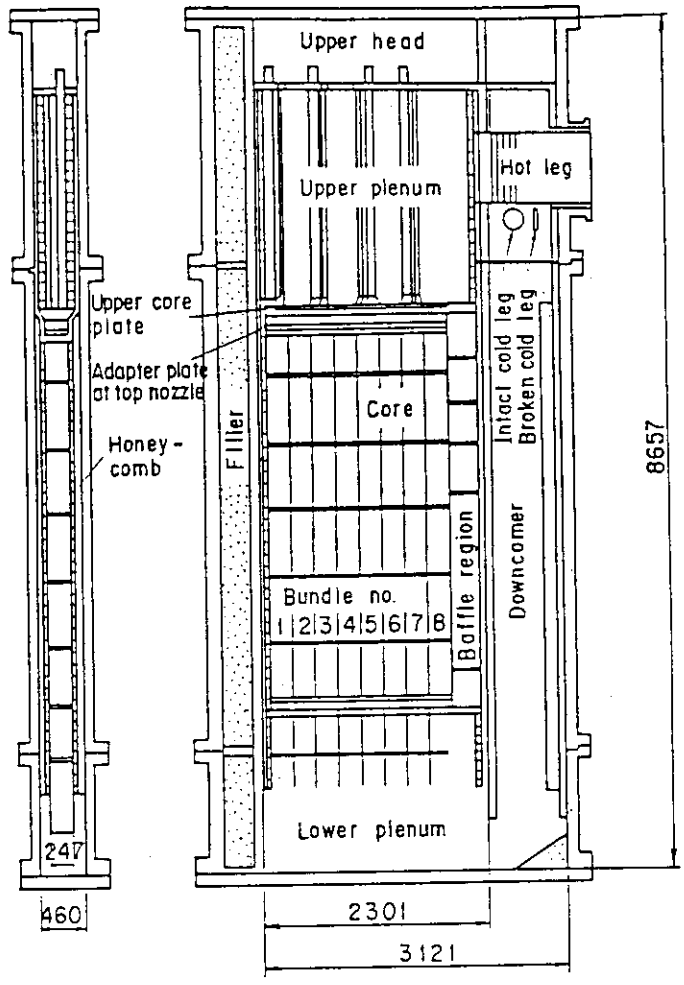

Fig. A-3 Vertical Cross Section of the Pressure Vessel

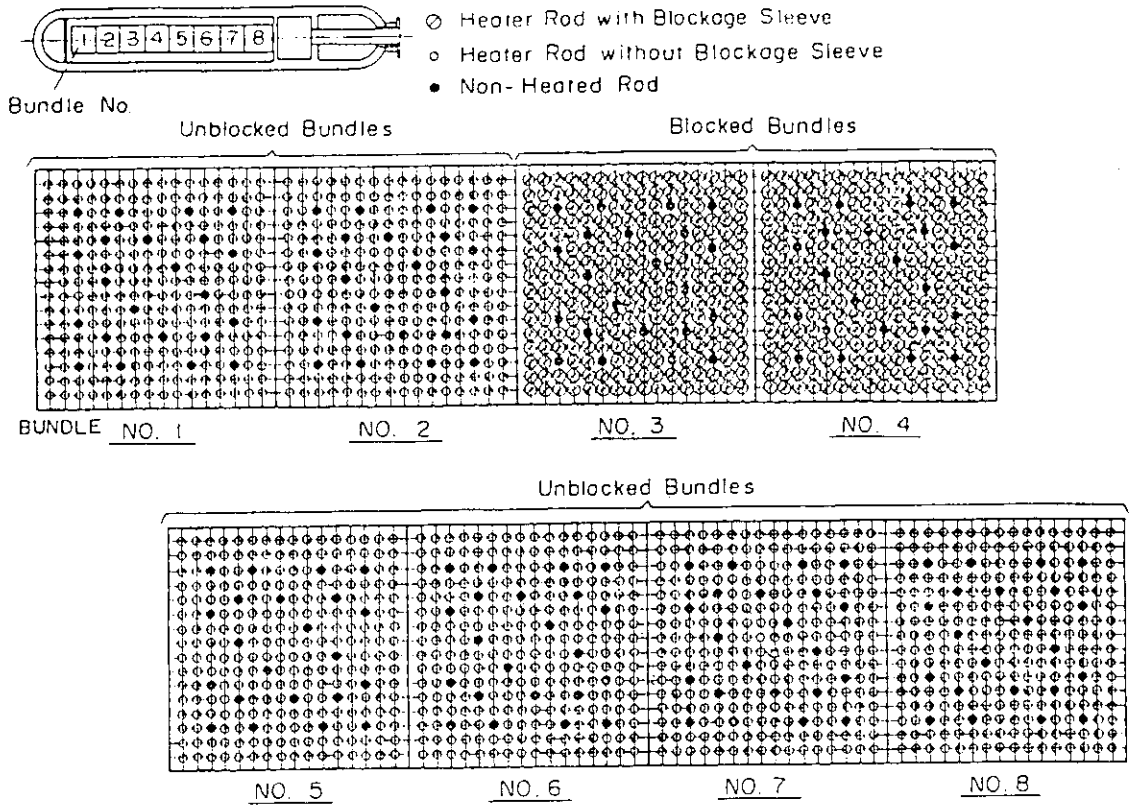

Fig. A-4 Arrangement of Heater Rod Bundles for Core-I

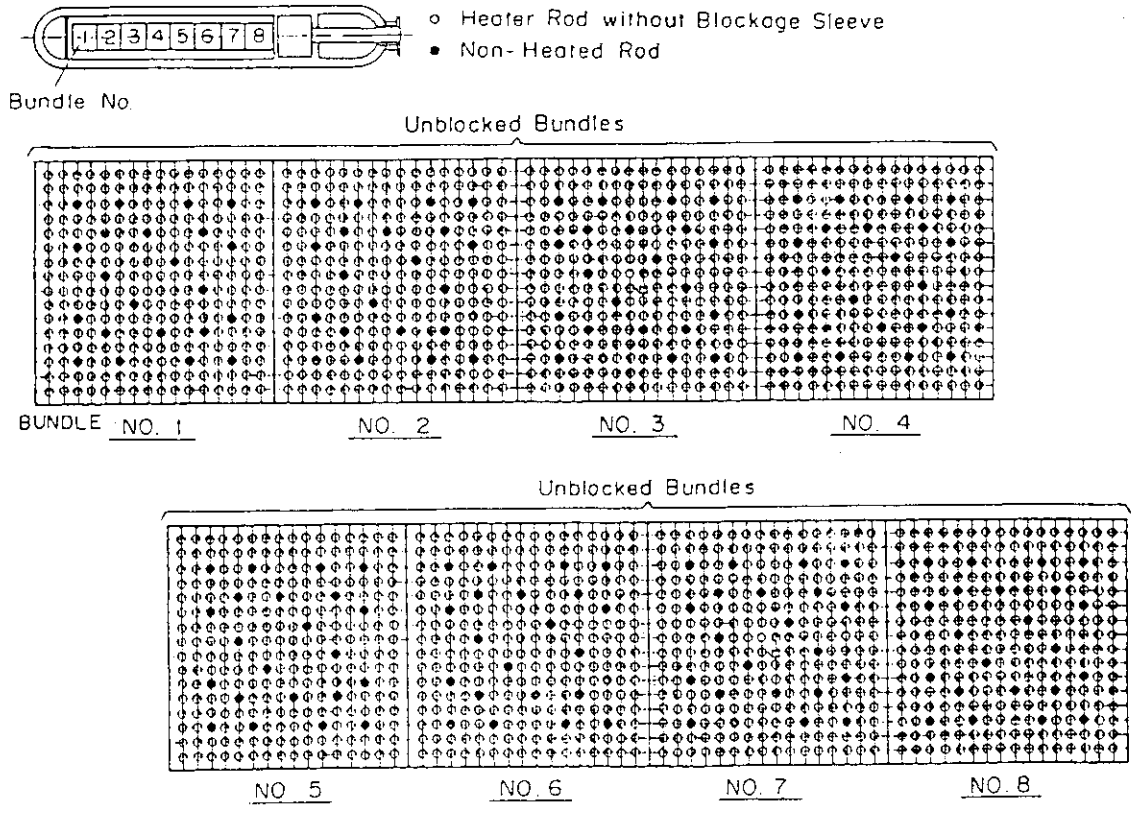

Fig. A-5 Arrangement of Heater Rod Bundles for Core-II

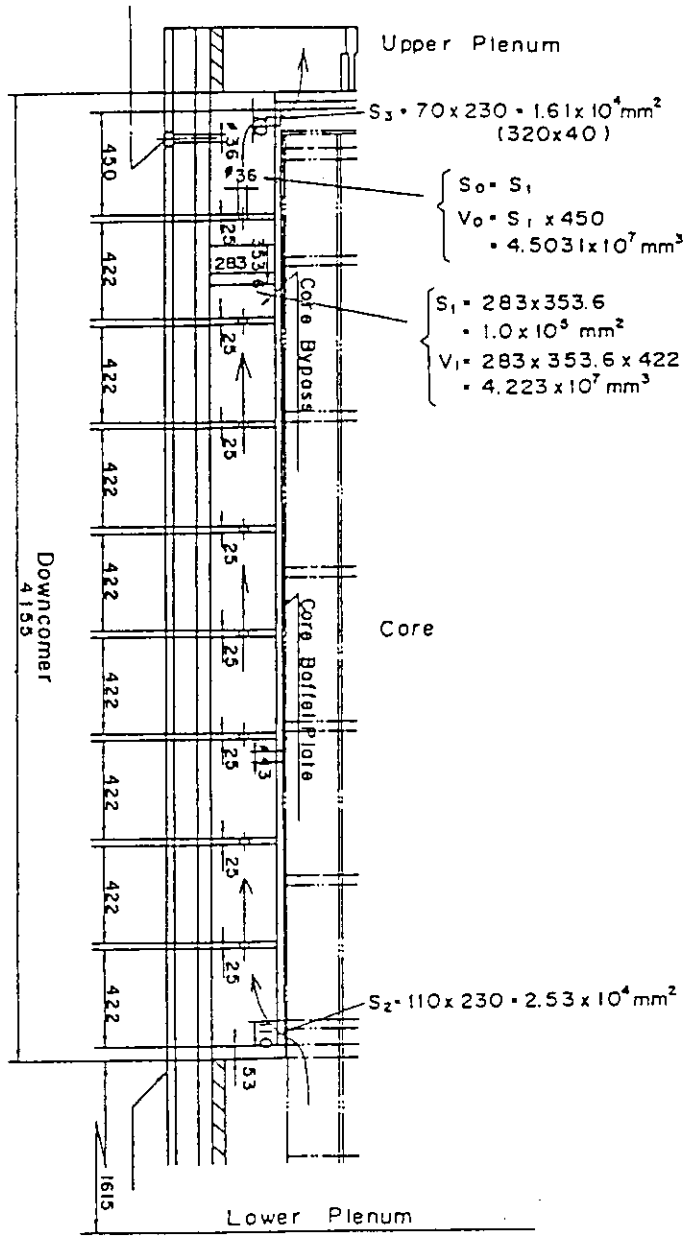

Fig. A-6 Dimension of Core Baffle Region for Core-I

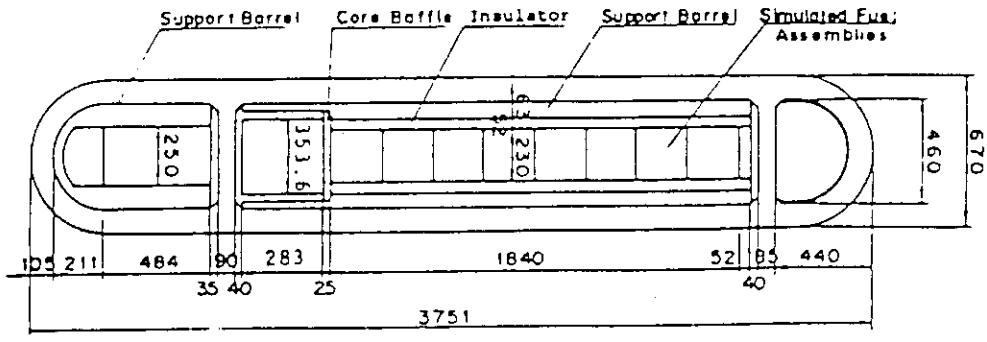

Fig. A-7 Horizontal Cross Section of the Pressure Vessel (1)

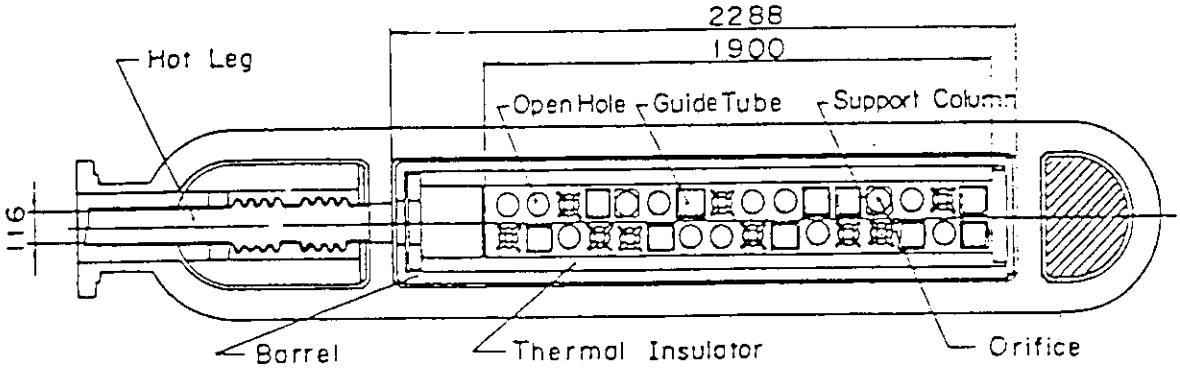

Upper Plenum Cross Section

Fig. A-8 Horizontal Cross Section of the Pressure Vessel (2)

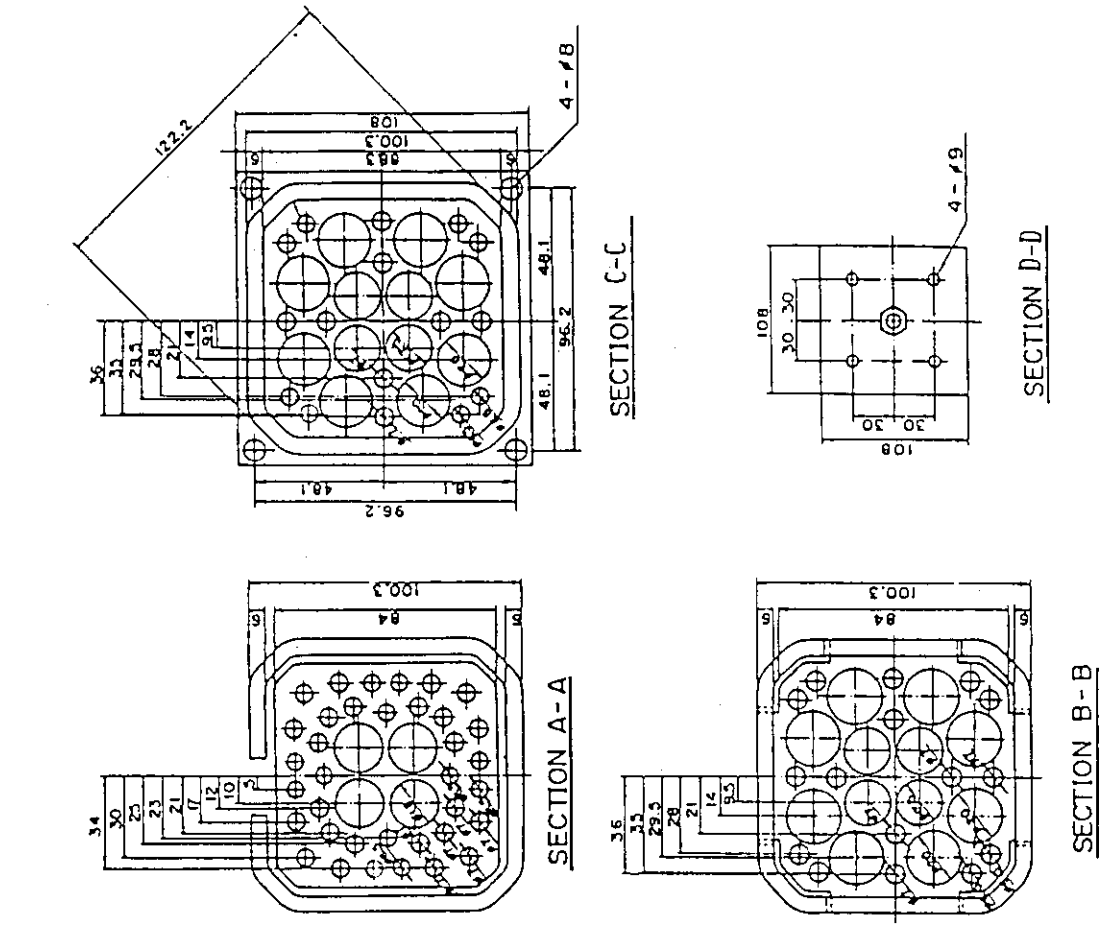

Fig. A-10 Dimension of Guide Tube (2)

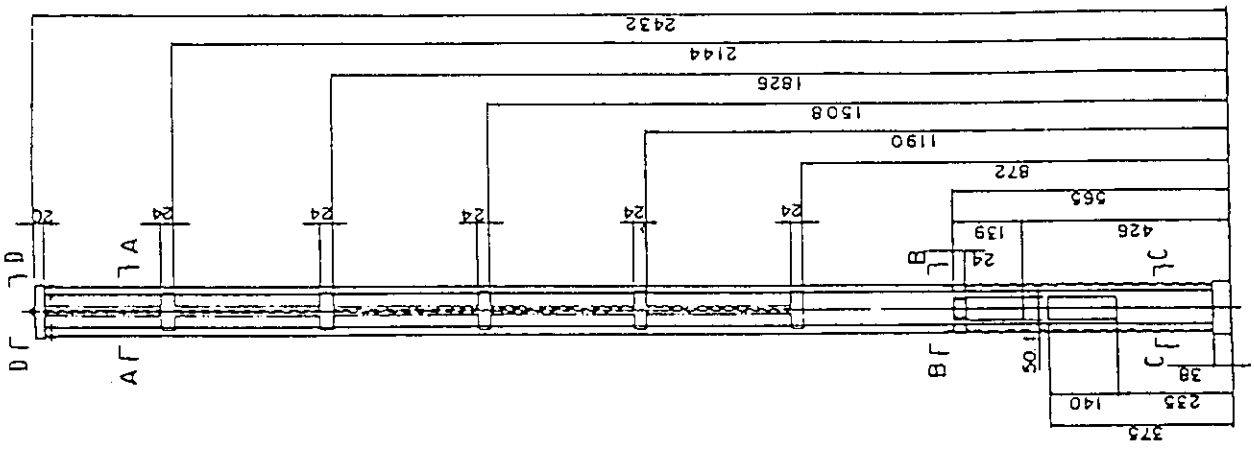

Fig. A-9 Dimension of Guide Tube (1)

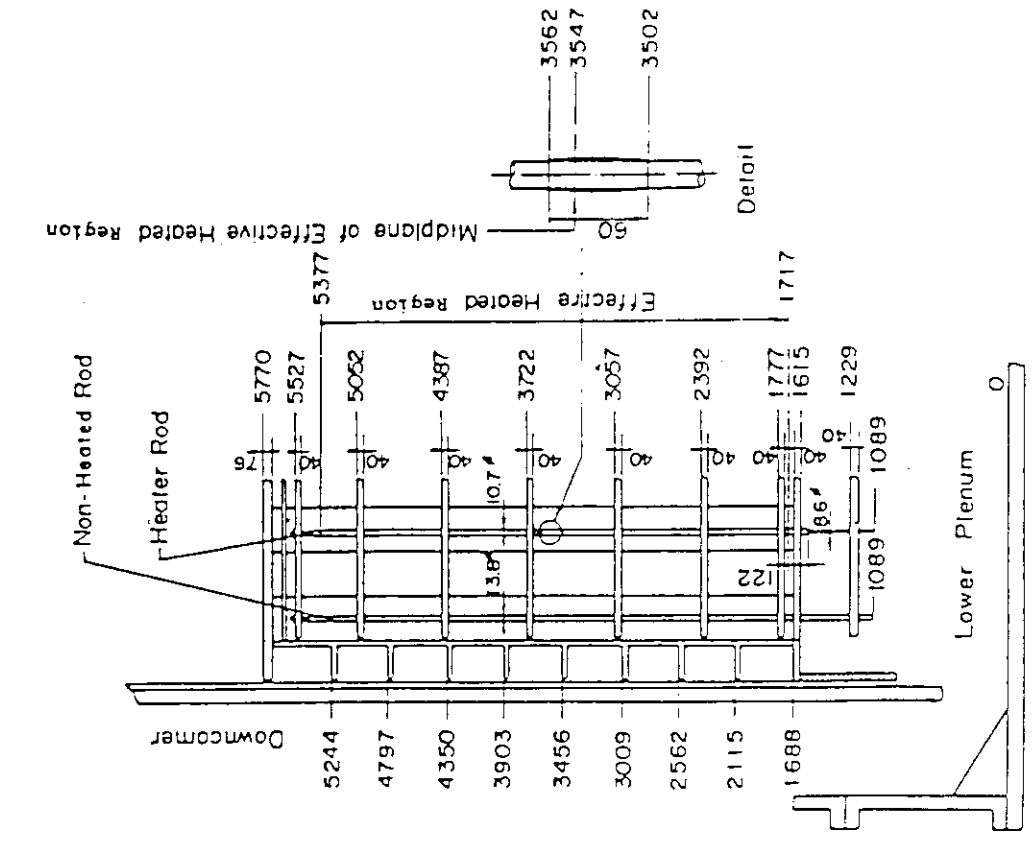

Fig. A-12 Relative Elevation and Dimension of the Core in SCTF

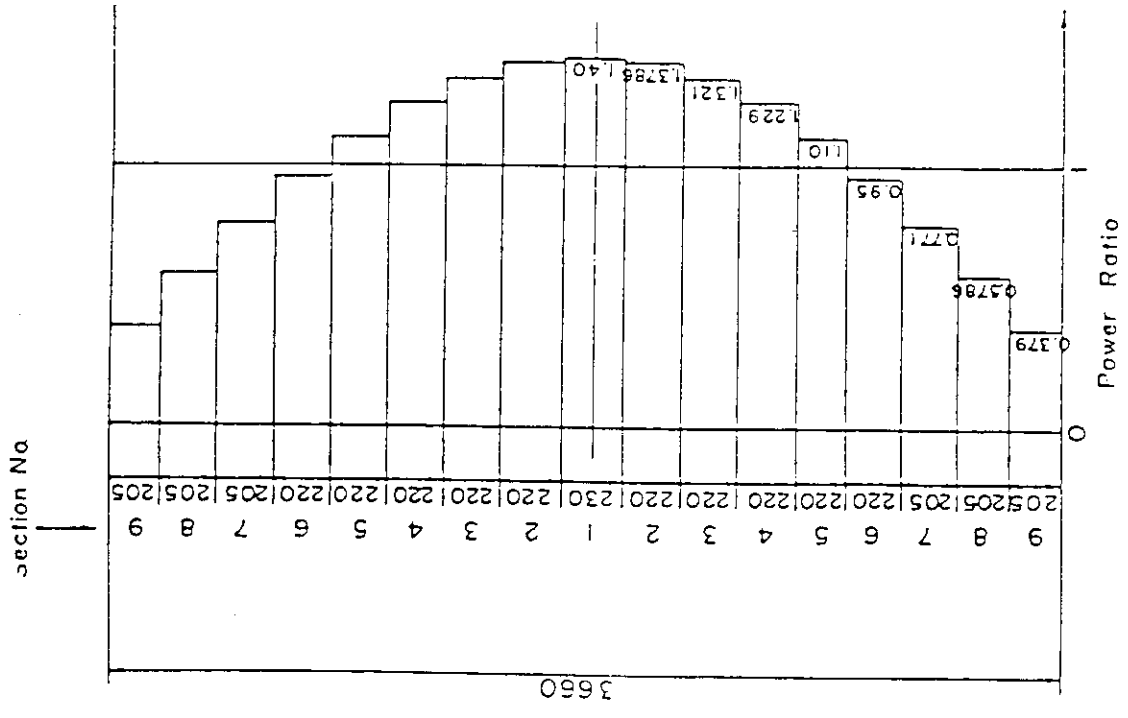

Fig. A-11 Axial Power Distribution of Heater Rod

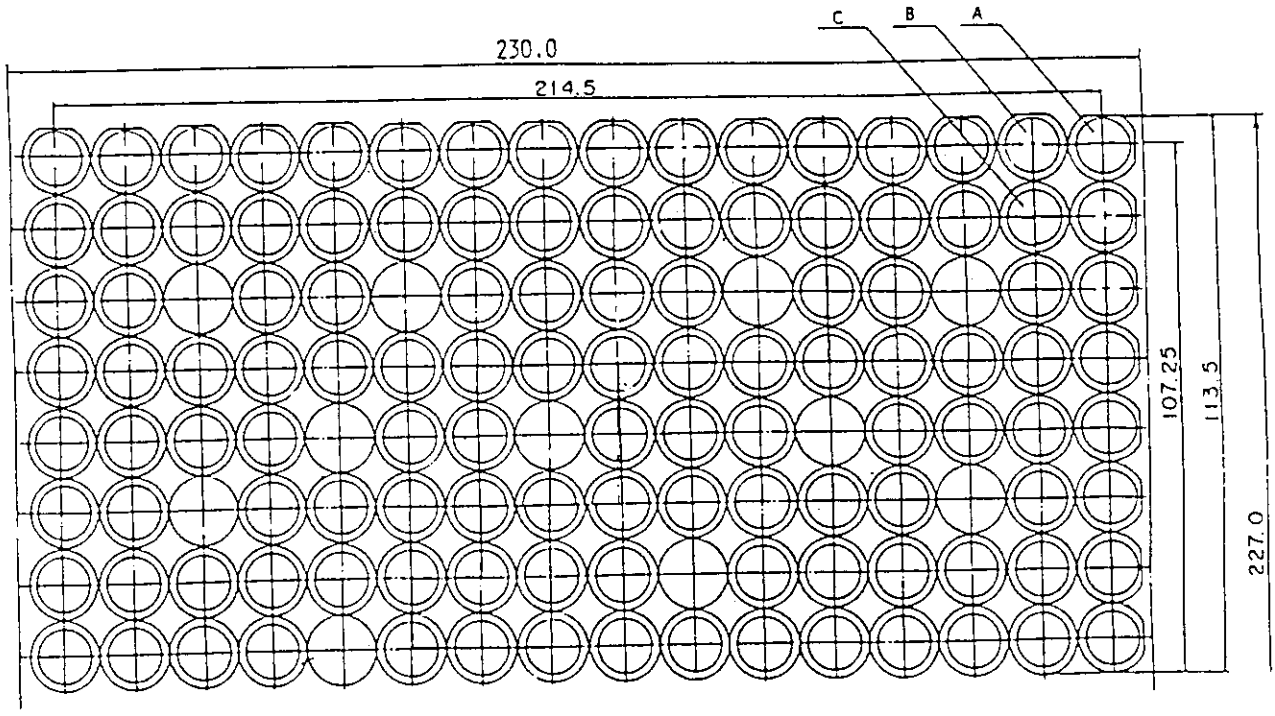

Fig. A-13 Arrangement of the Heater Rods with Three Kinds of Blackage Sleeve for Core-I

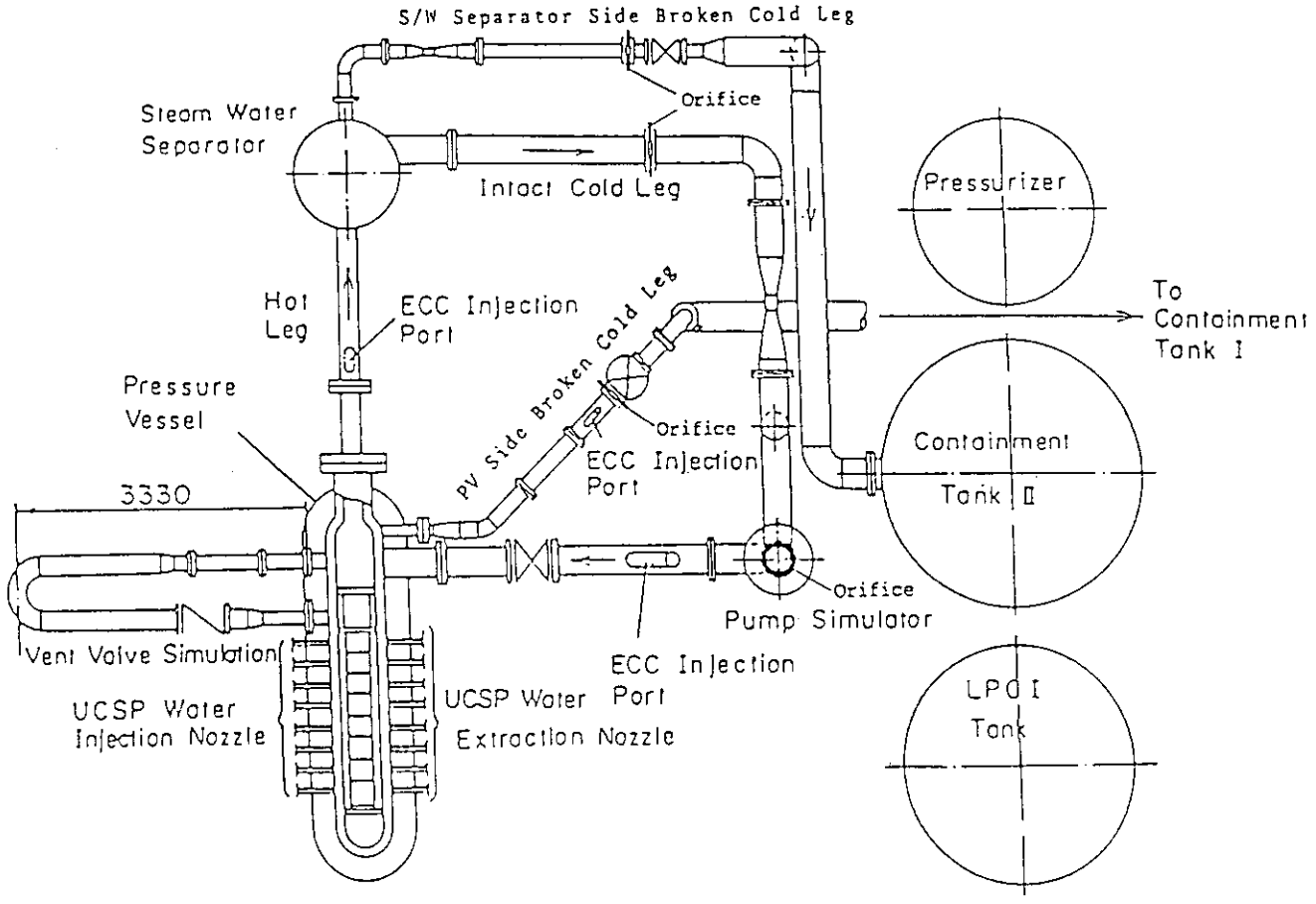

Fig. A-14 Overview of the Arrangement of the SCTF

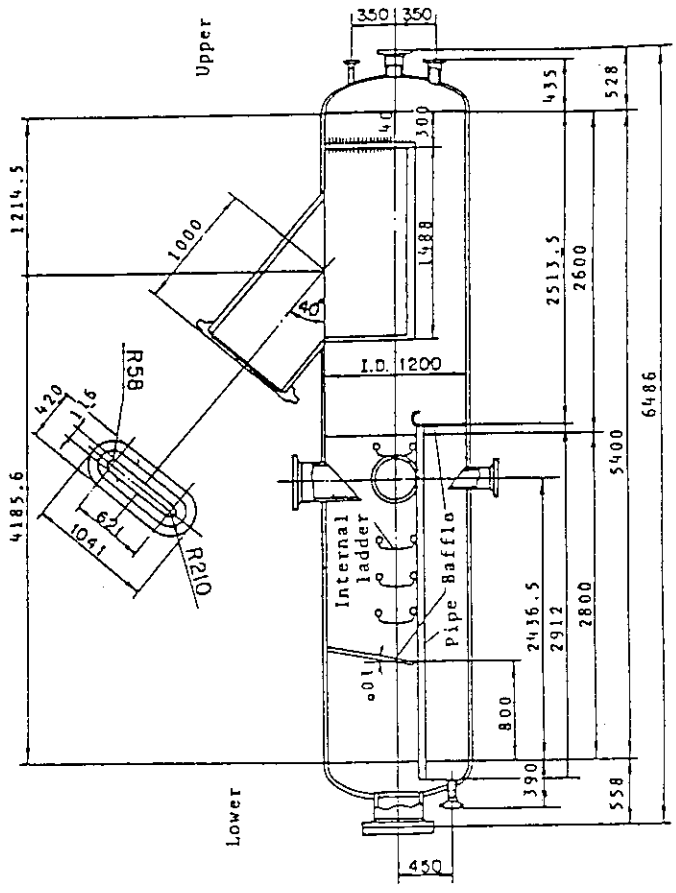

Fig. A-15 Steam-Water Separator

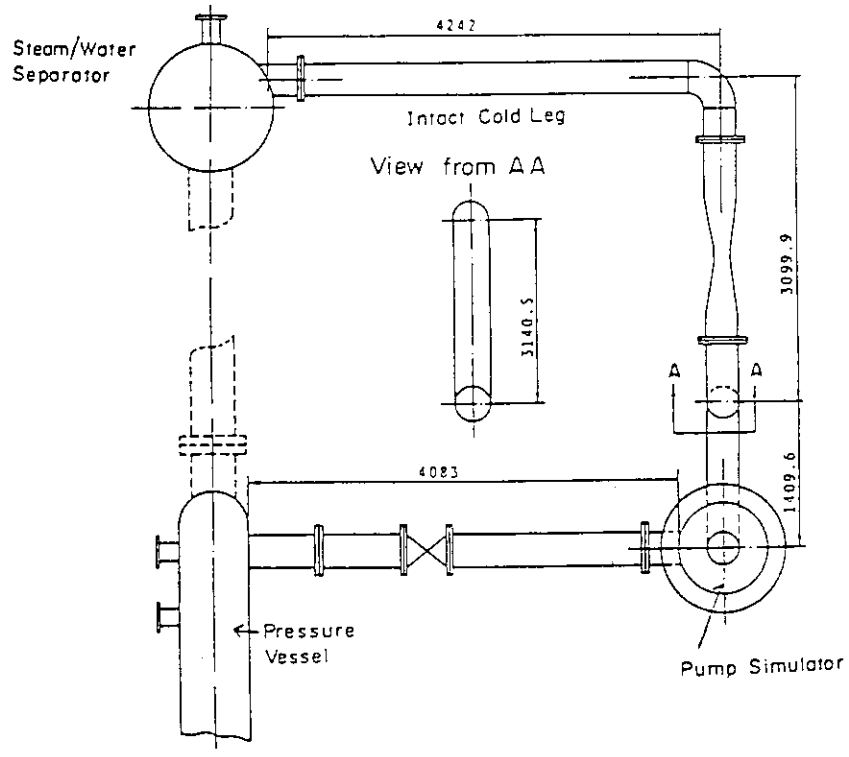

Fig. A-16 Arrangement of Intact Cold Leg

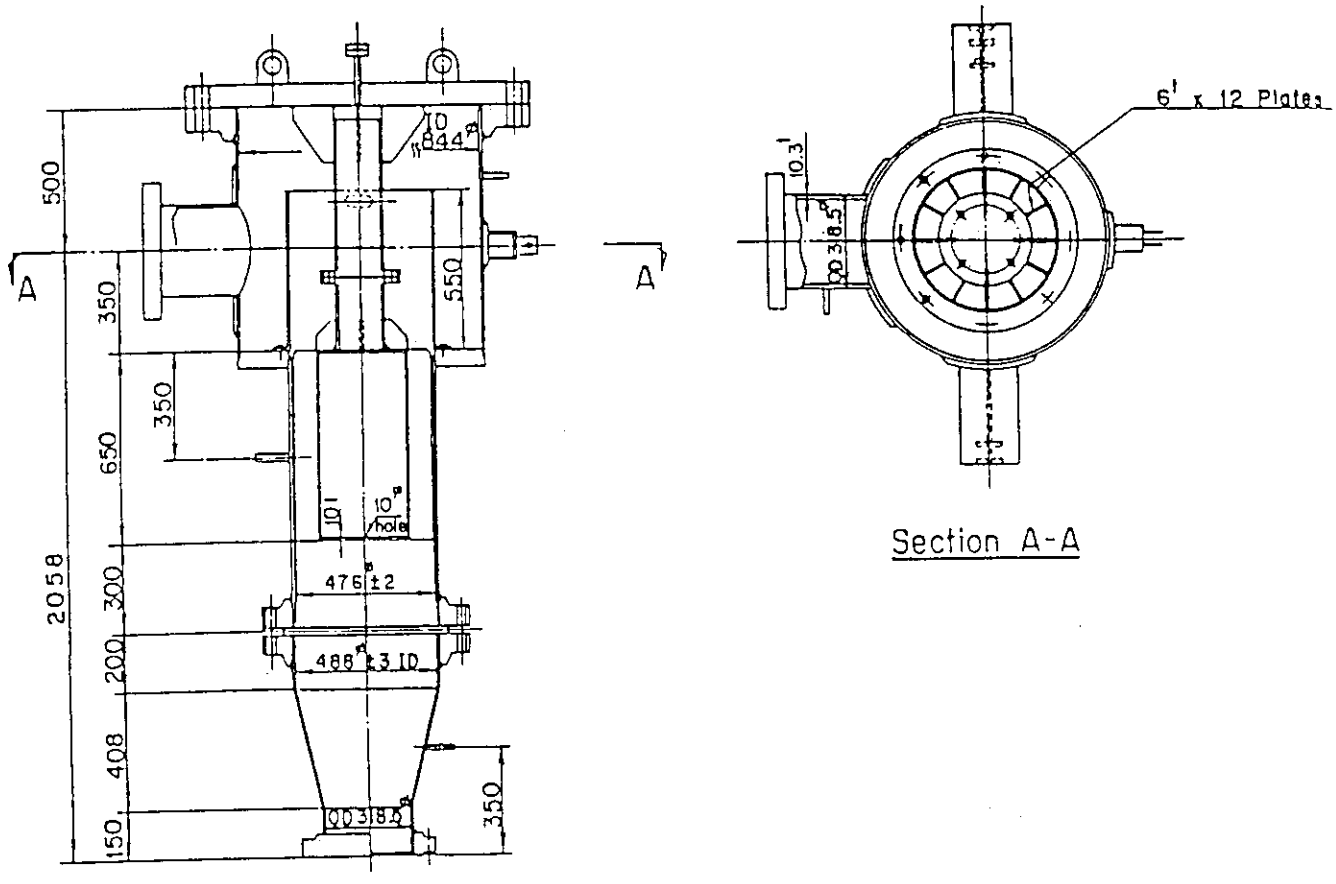

Fig. A-17 Configuration and Dimension of Pump Simulator

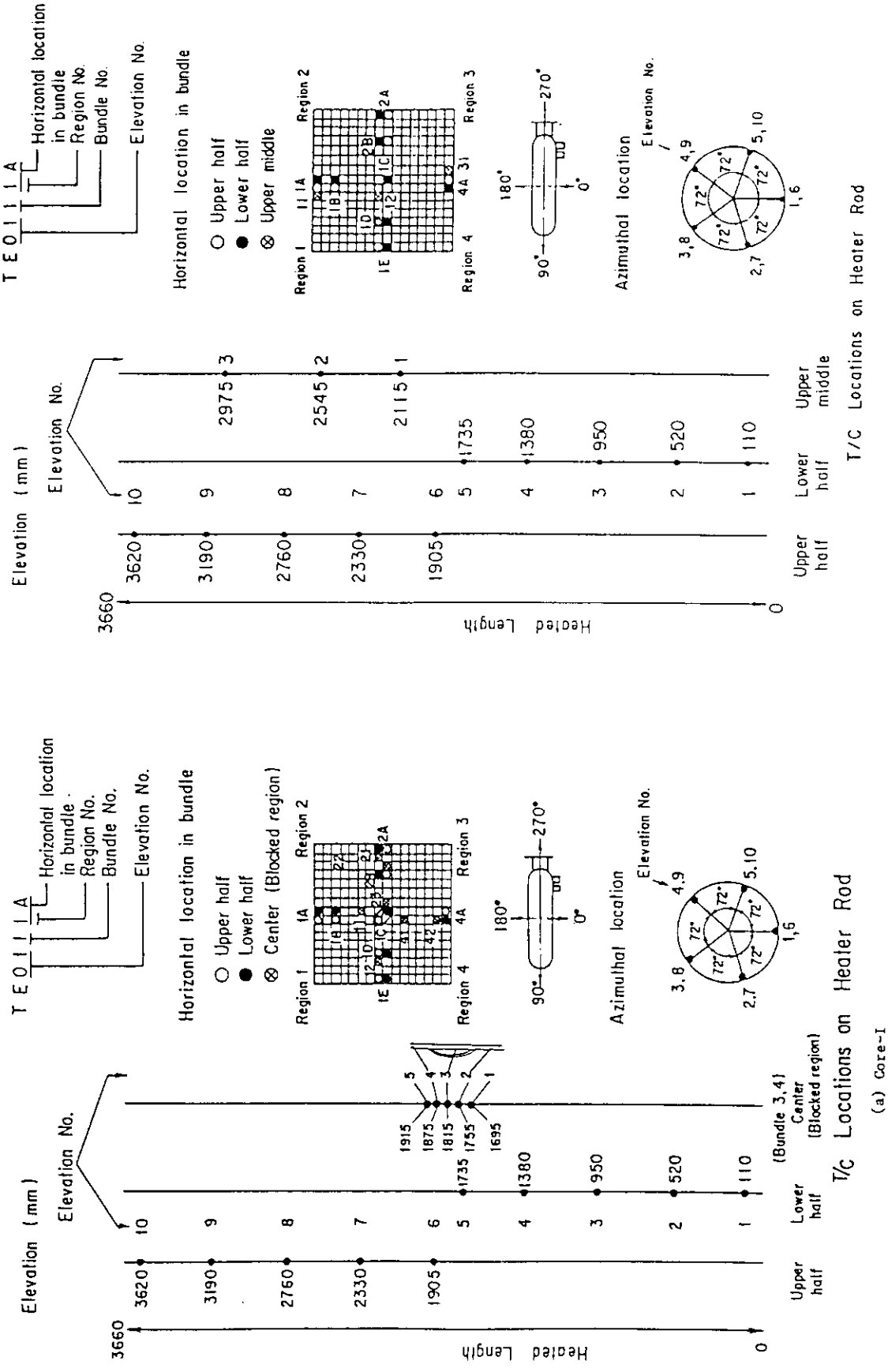

Fig. A-18 Thermocouple Locations of Heater Rod Surface Temperature Measurements

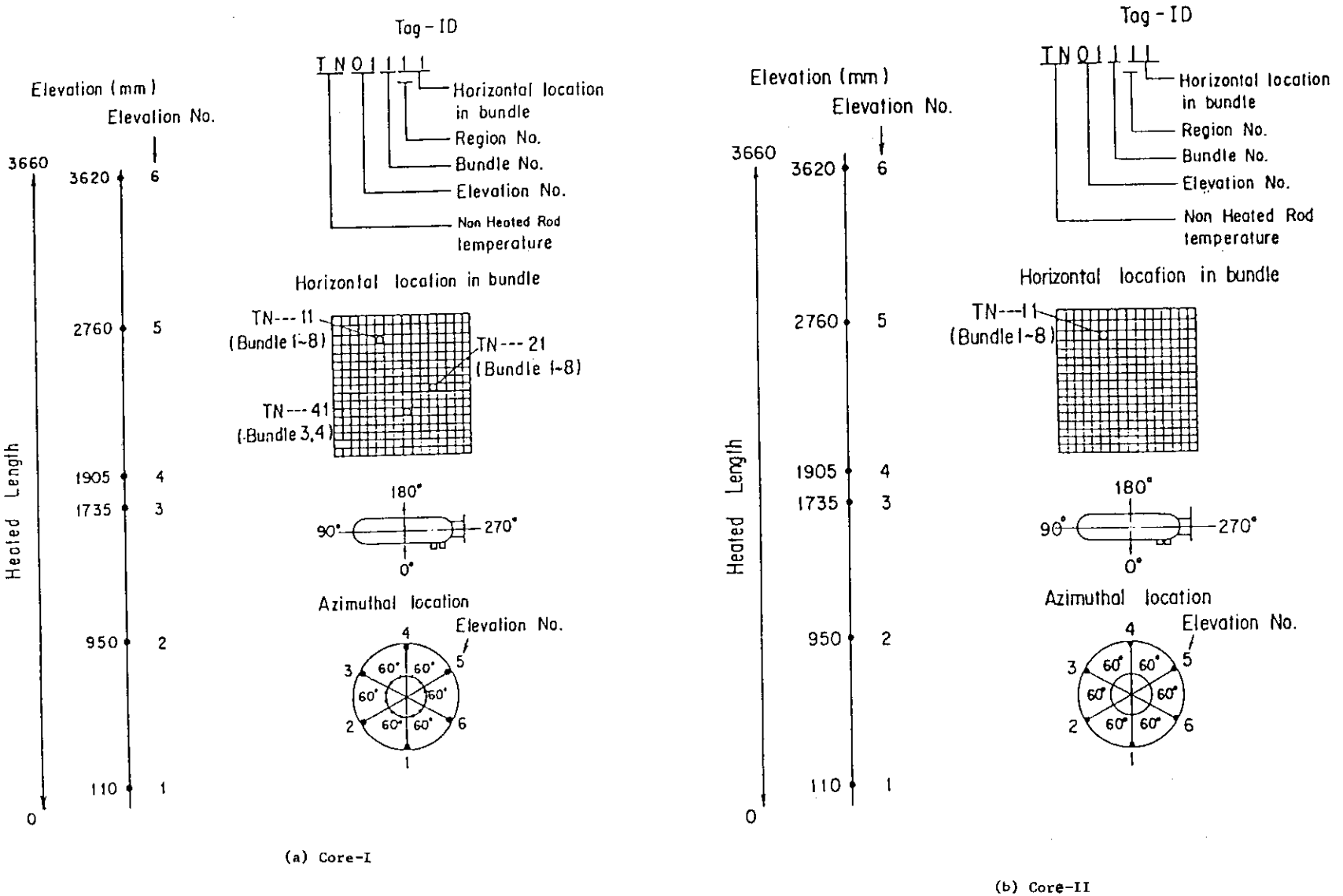

Fig. A-19 Thermocouple Locations of Non-Heated Rod Surface Temperature Measurements

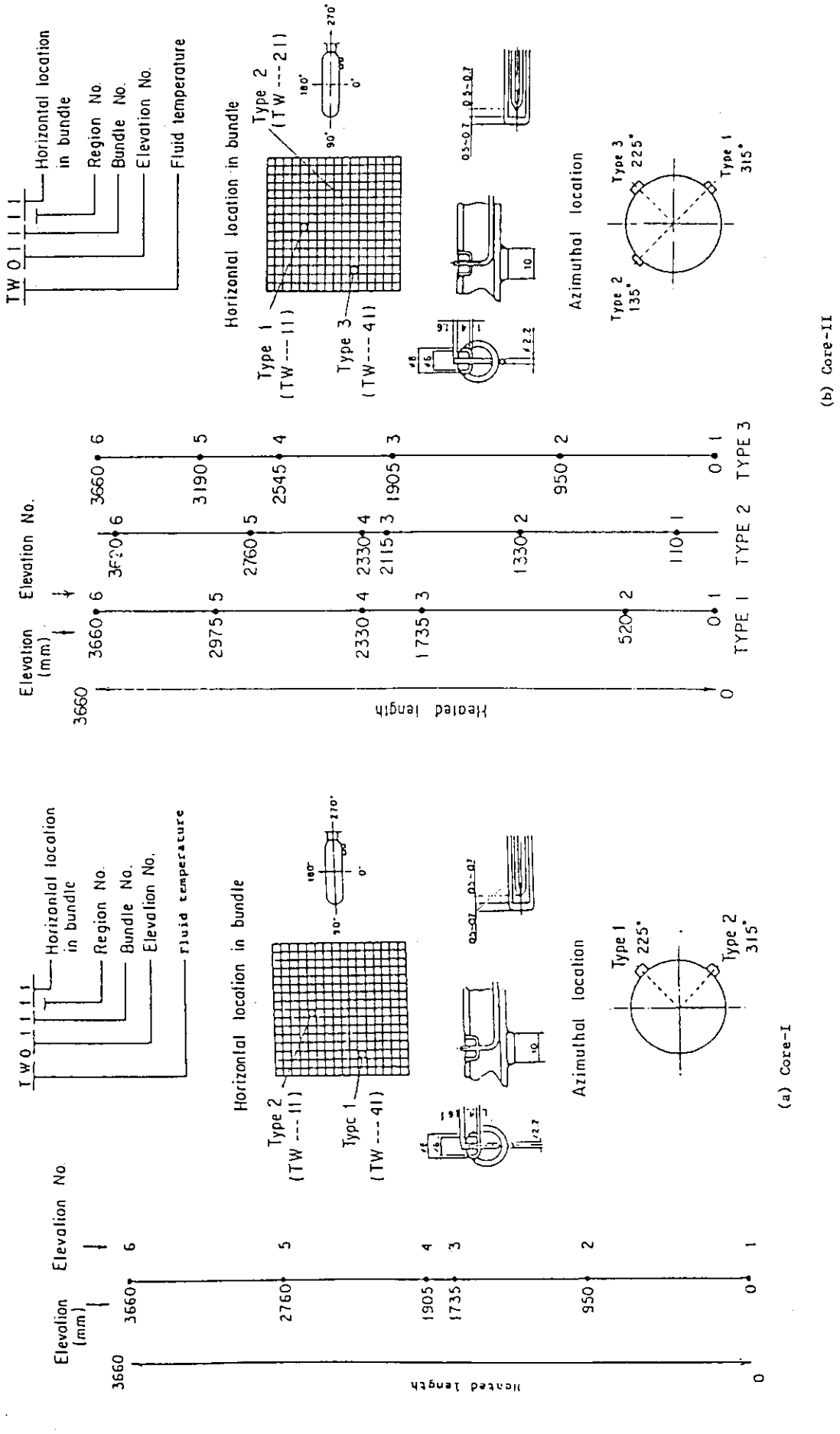

Fig. A-20 Thermocouple Locations of Fluid Temperature Measurements in Core

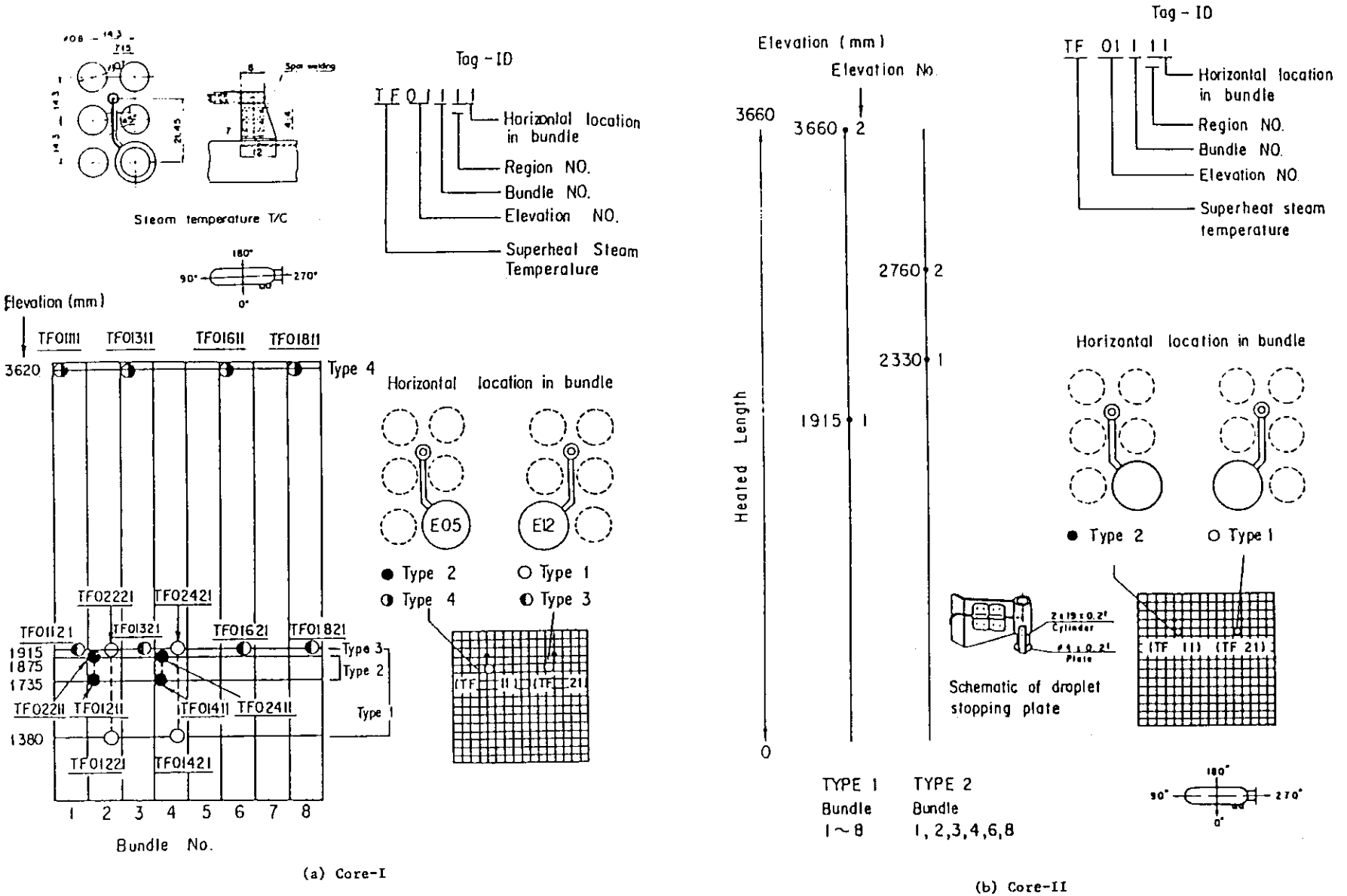

Fig. A-21 Thermocouple Locations of Steam Temperature Measurements in Core

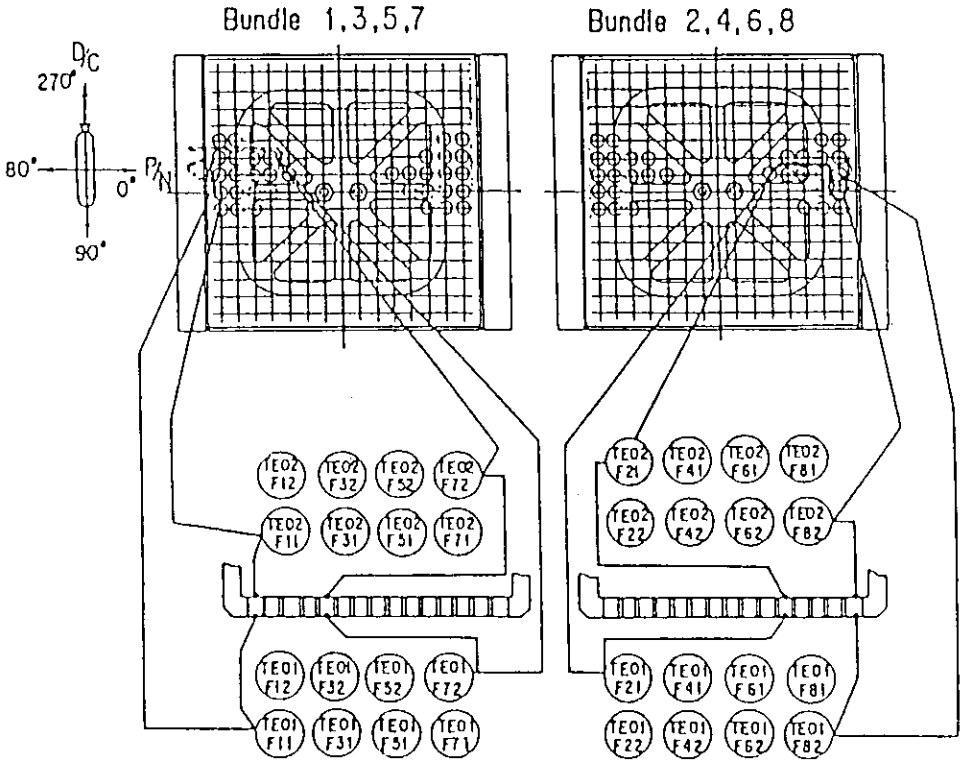

Fig. A-22 Thermocouple Locations of Fluid Temperature Measurements Just above and below End Box Tie Plate

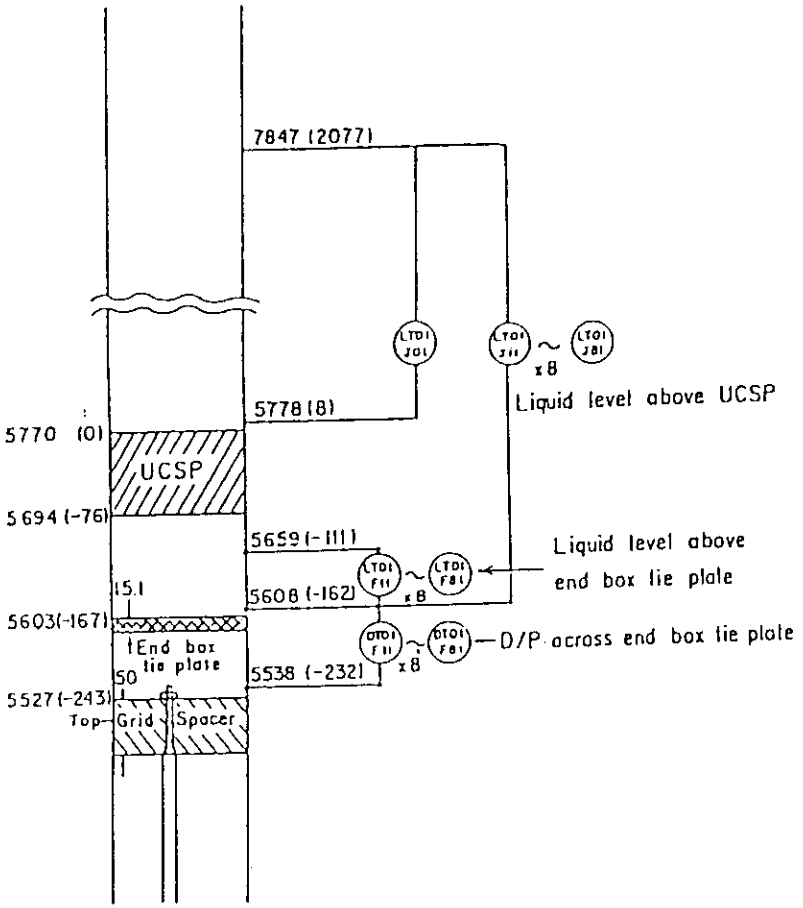

Fig. A-23 Locations of Differential Pressure Measurements across End Box Tie Plate and and Liquid Level Measurements above UCSP and End Box Tie Plate

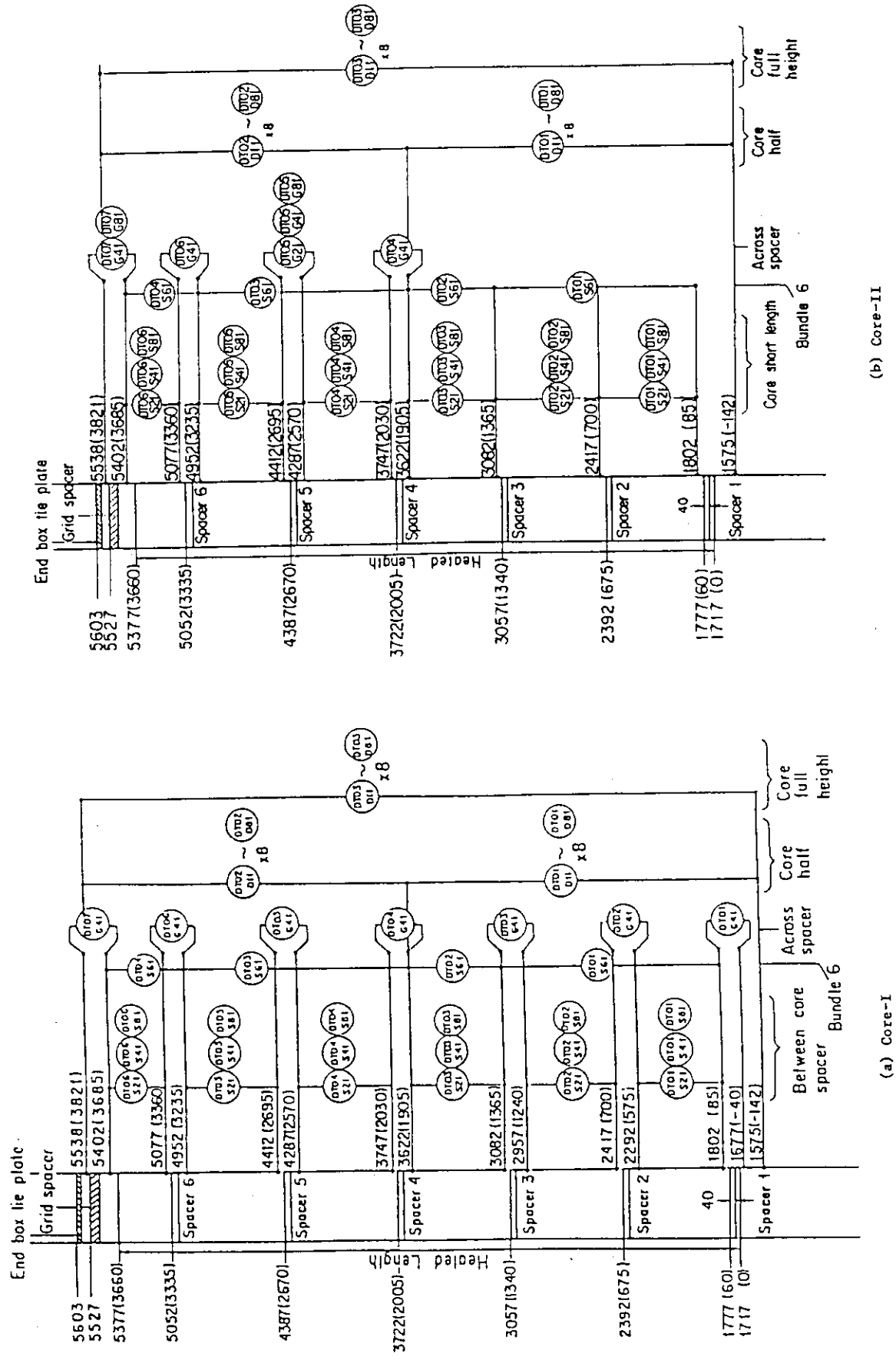

Fig. A-24 Locations of Vertical Differential Pressure Measurements in Core

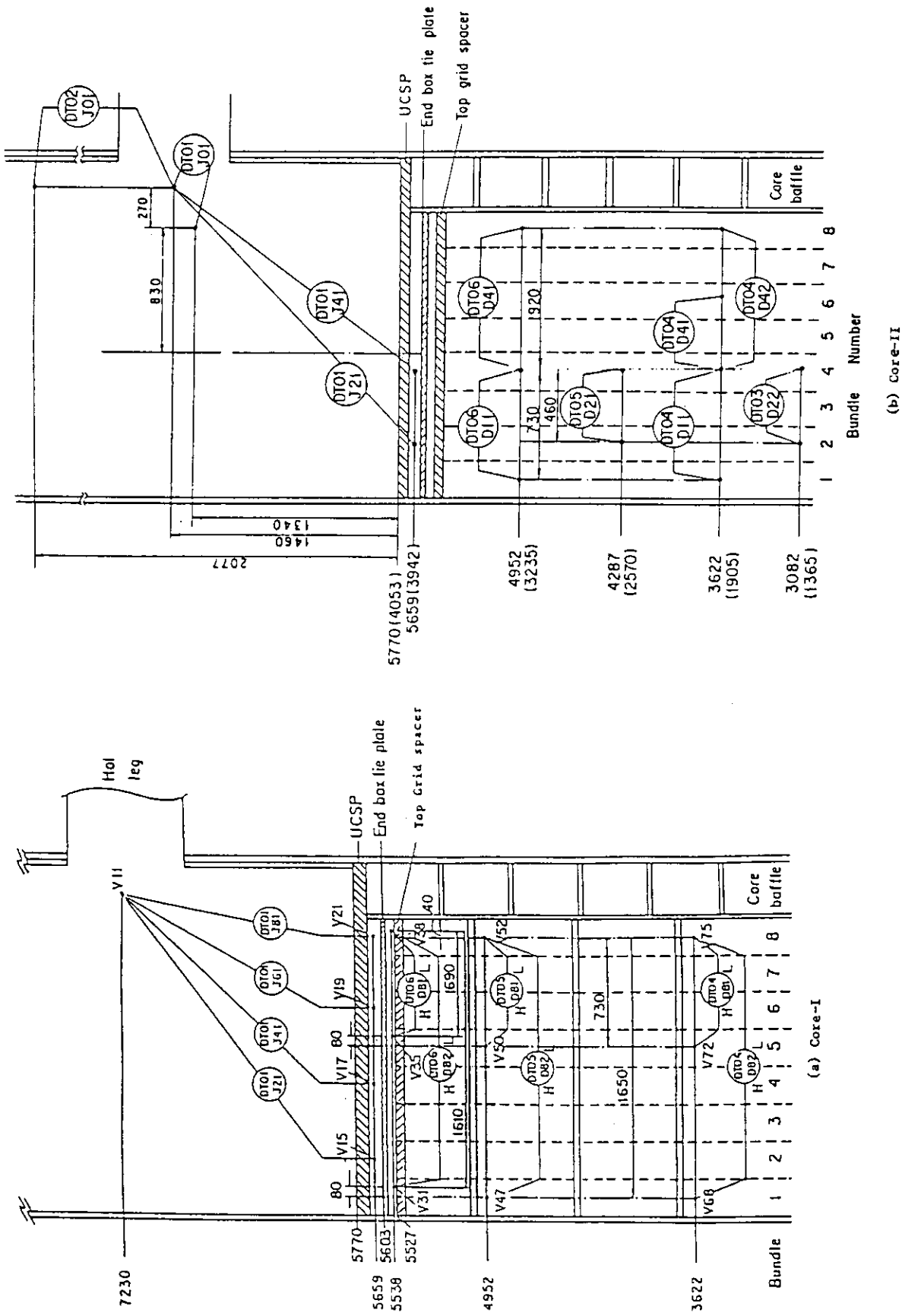

Fig. A-25 Locations of Horizontal Differential Pressure Measurements in Core and Differential Pressure Measurements between End Box and Inlet of Hot Leg

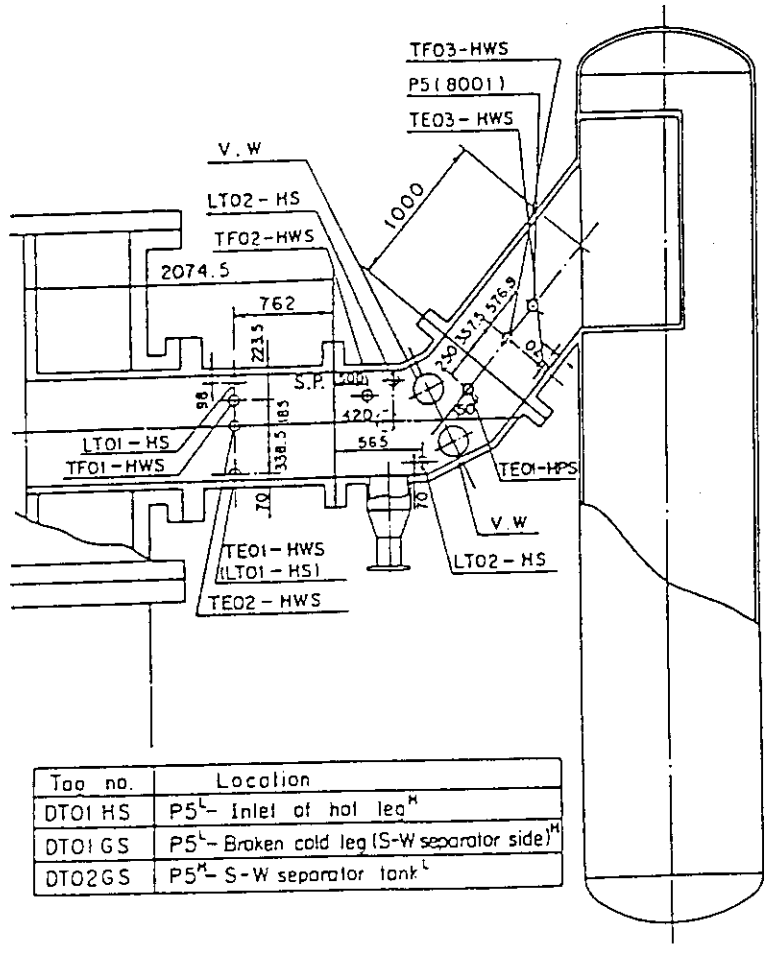

Tag no.	Location
DT01HS	$P5^{L}$- Inlet of hot leg^{M}
DT01GS	$P5^{L}$- Broken cold leg (S-W separator side)^{M}
DT02GS	$P5^{M}$- S-W separator tank^{L}

Fig. A-26 Locations of Hot Leg Instrumentation

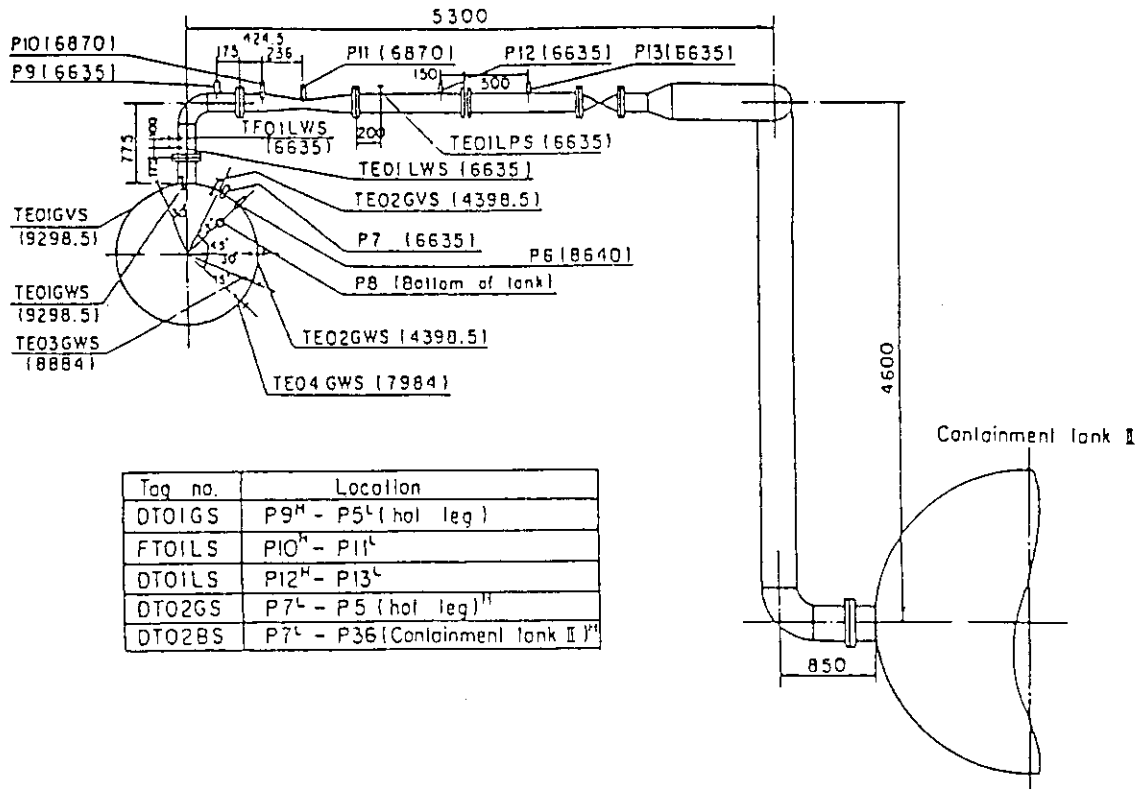

Tag no.	Location
DT01GS	$P9^{H}$ - $P5^{L}$ (hot leg)
FT01LS	$P10^{H}$ - $P11^{L}$
DT01LS	$P12^{H}$ - $P13^{L}$
DT02GS	$P7^{L}$ - P5 (hot leg)^{H}
DT02BS	$P7^{L}$ - P36(Containment tank II)^{H}

Fig. A-27 Locations of Steam-Water Separator Side Broken Cold Leg Instrumentation

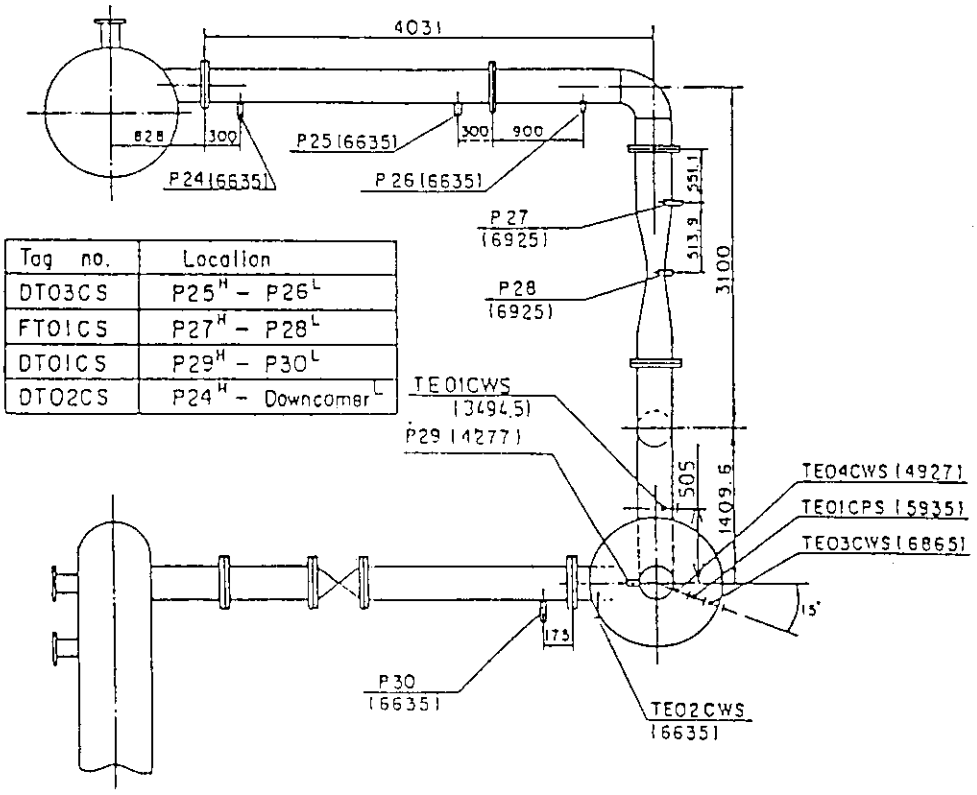

Tag no.	Location
DT03CS	$P25^{H}$ - $P26^{L}$
FT01CS	$P27^{H}$ - $P28^{L}$
DT01CS	$P29^{H}$ - $P30^{L}$
DT02CS	$P24^{H}$ - Downcomer^{L}

Fig. A-28 Locations of Intact Cold Leg Instrumentation

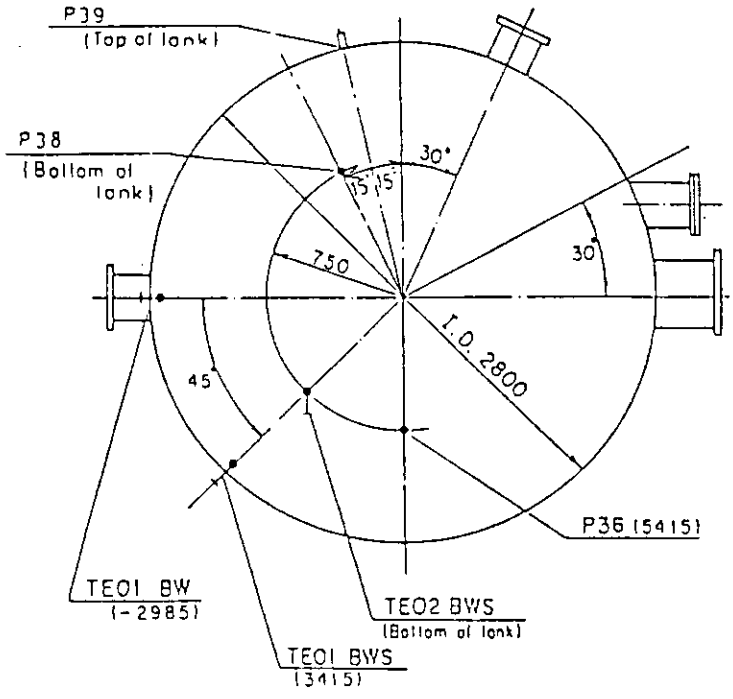

Tag no.	Location
DT01 BS	P36[H]－ Upper plenum[L]
DT02 BS	P36[H]－ S-W Separator[L]
DT01 E	P36[L]－ P35 (C.T.I)[H]
PT01 B	P36
LT01 1B	P38[H]－ P39[L]

Fig. A-29 Locations of Containment Tank-II Instrumentation

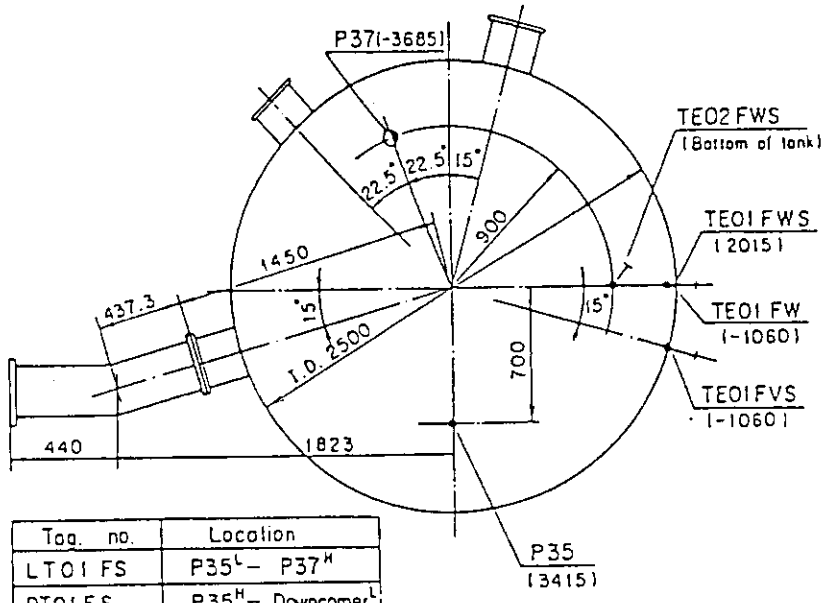

Tag. no.	Location
LT01 FS	P35[L]－ P37[H]
DT01 FS	P35[H]－ Downcomer[L]
DT01 E	P35[H]－ P36(C.T. II)[H]
PT01 F	P35

Fig. A-30 Locations of Containment Tank-I Instrumentation

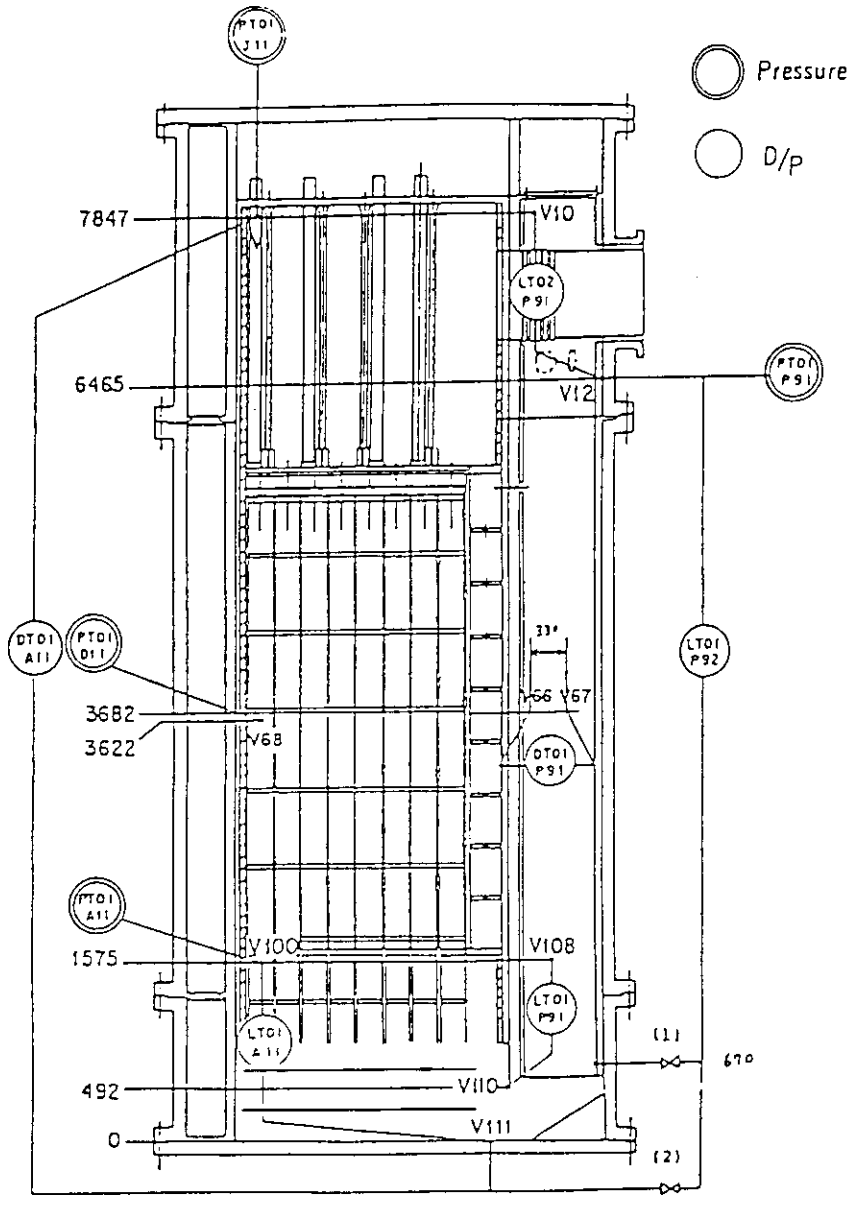

Fig. A-31 Location of Pressure Measurements in Pressure Vessel, Differential PressuredMeasurements between Upper and Lower Plenums and liquid Level Measurements in Downcomer and Lower Plenum

Appendix B

Selected Test Data from Test S2-13 (Run 618)

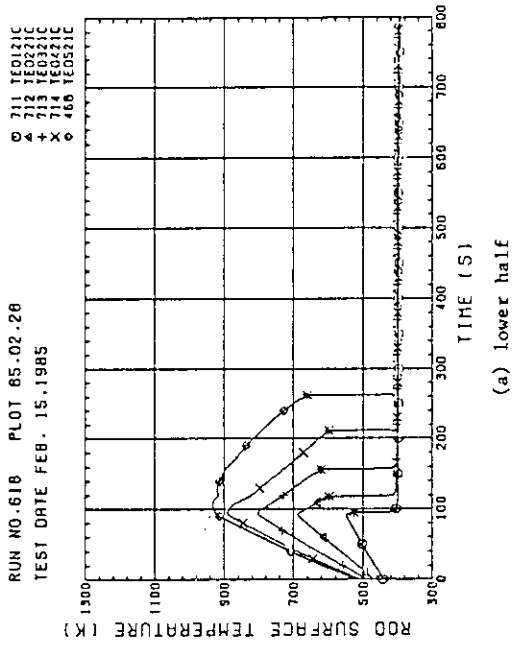

(a) lower half

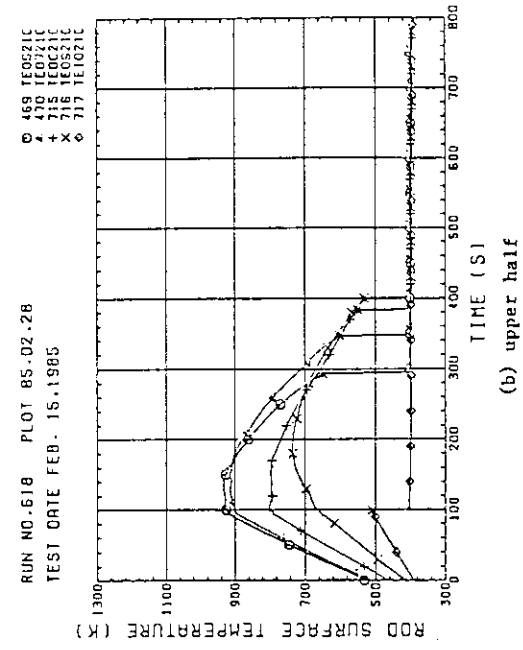

(b) upper half

Fig. B-2 Heater Rod Temperature at center of Bundle 2

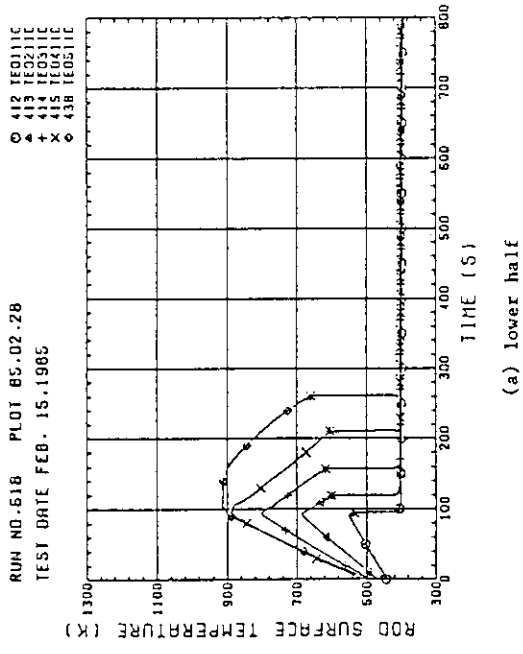

(a) lower half

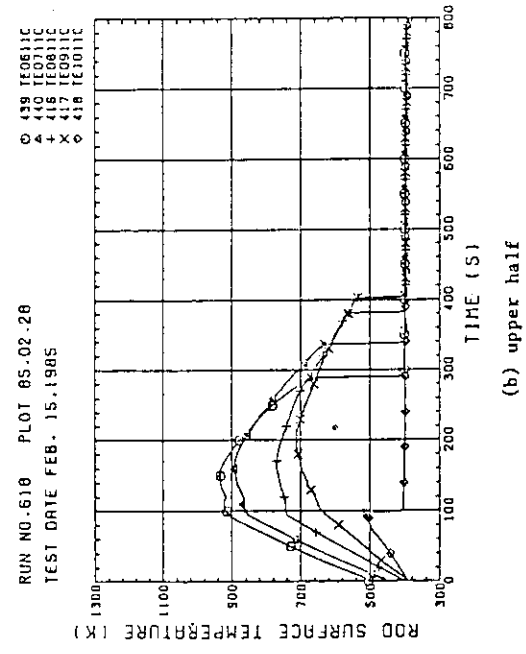

(b) upper half

Fig. B-1 Heater Rod Temperature at center of Bundle 1

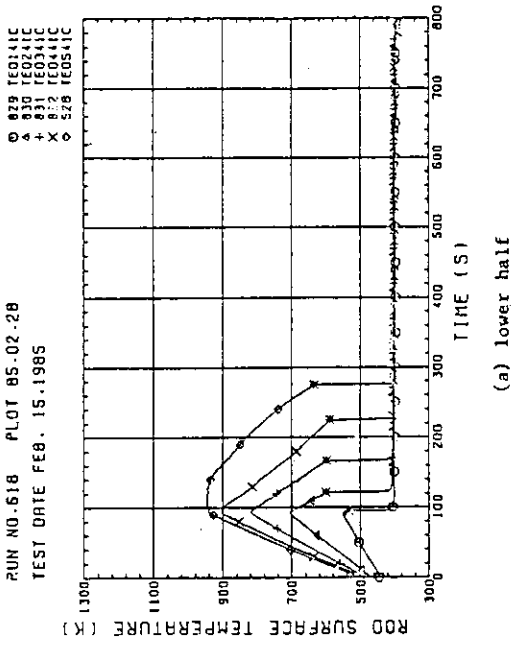

(a) lower half

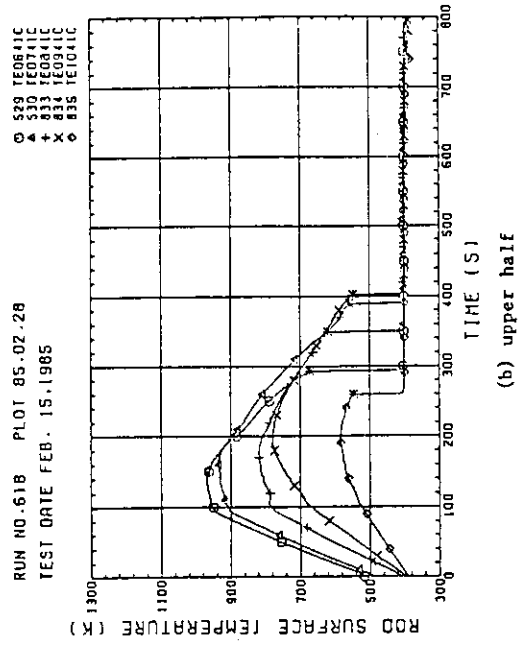

(b) upper half

Fig. B-4 Heater Rod Temperature at center of Bundle 4

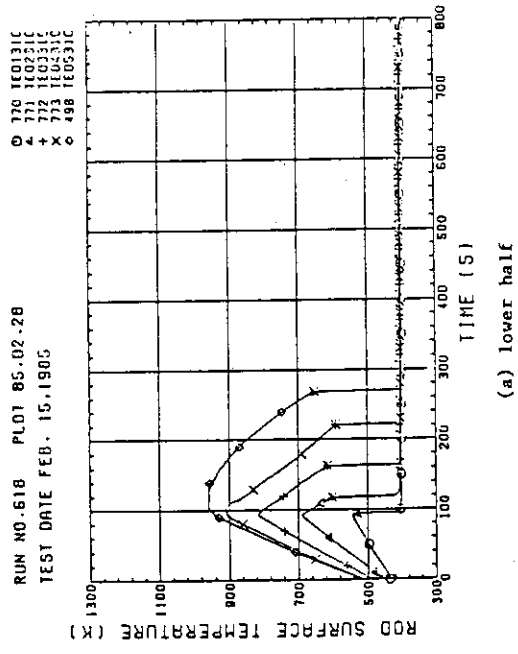

(a) lower half

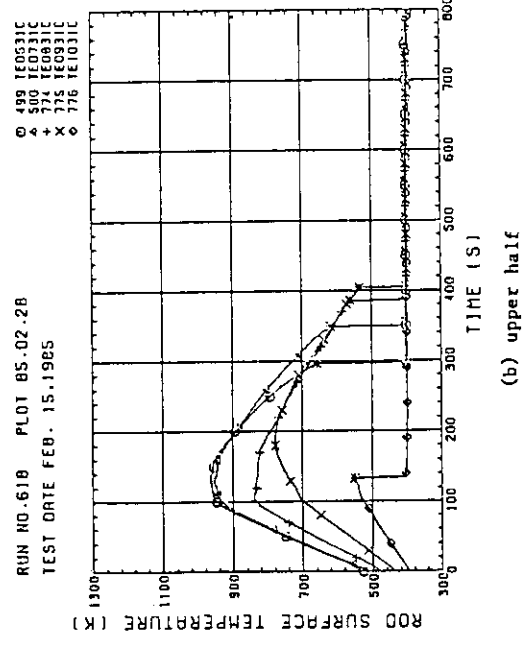

(b) upper half

Fig. B-3 Heater Rod Temperature at center of Bundle 3

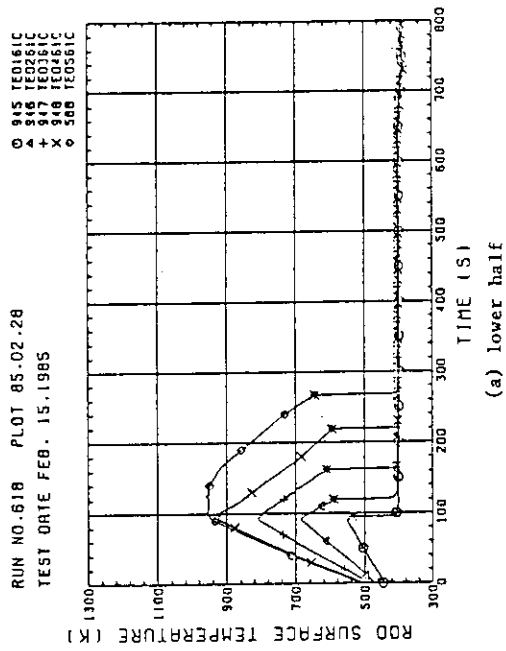

Fig. B-6 Heater Rod Temperature at center of Bundle 6

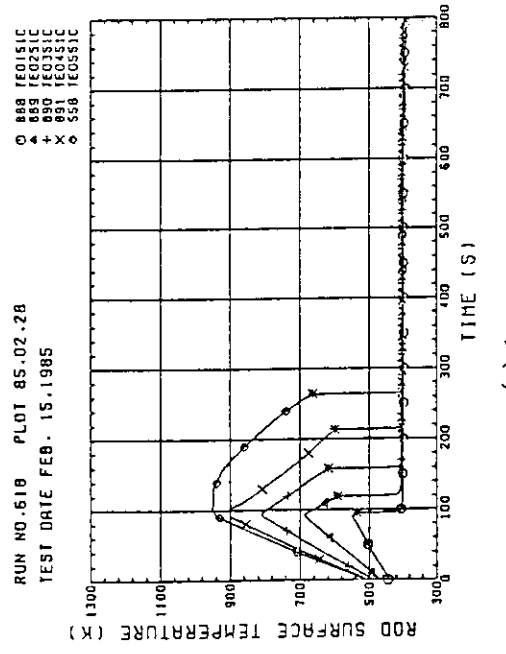

Fig. B-5 Heater Rod Temperature at center of Bundle 5

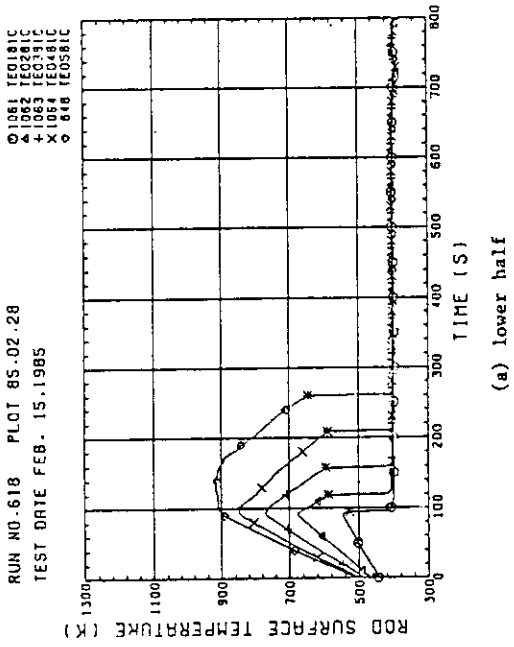

(a) lower half

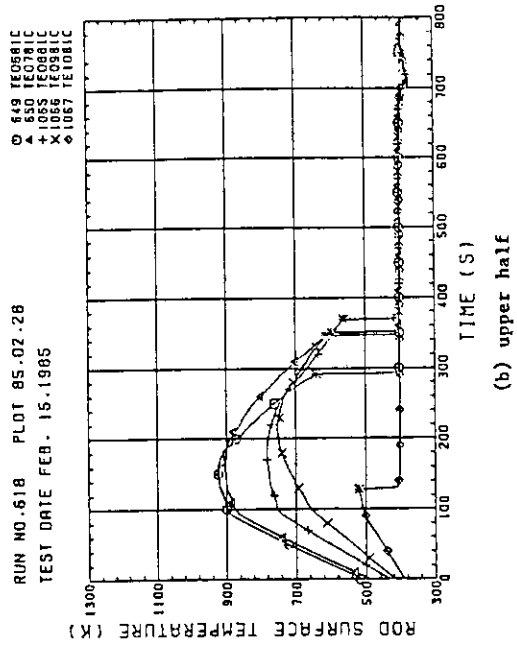

(b) upper half

Fig. B-7 Heater Rod Temperature at center of Bundle 7

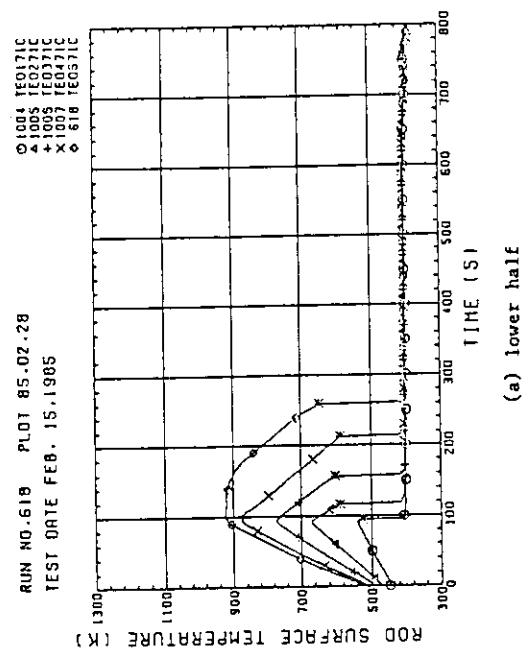

(a) lower half

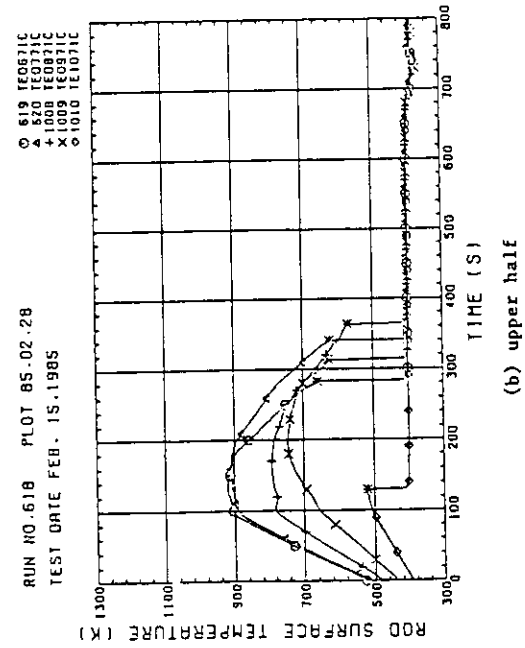

(b) upper half

Fig. B-8 Heater Rod Temperature at center of Bundle 8

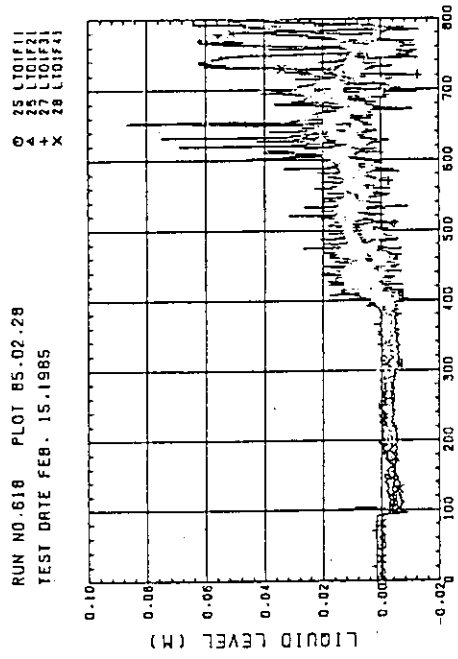

(a) Bundles 1～4

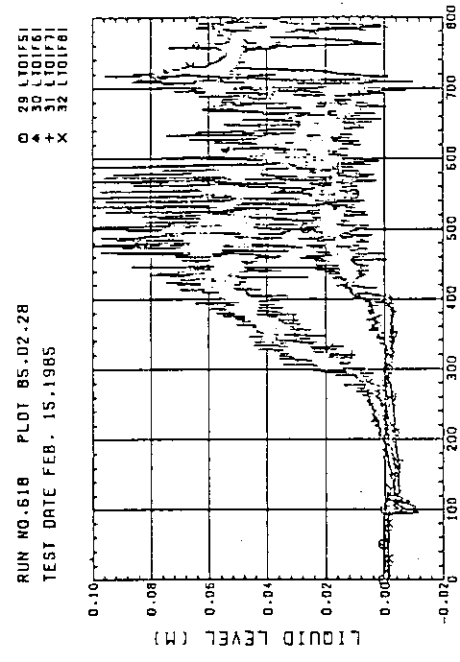

(b) Bundles 5～8

Fig. B-10 Liquid Level above End Box Tie Plate

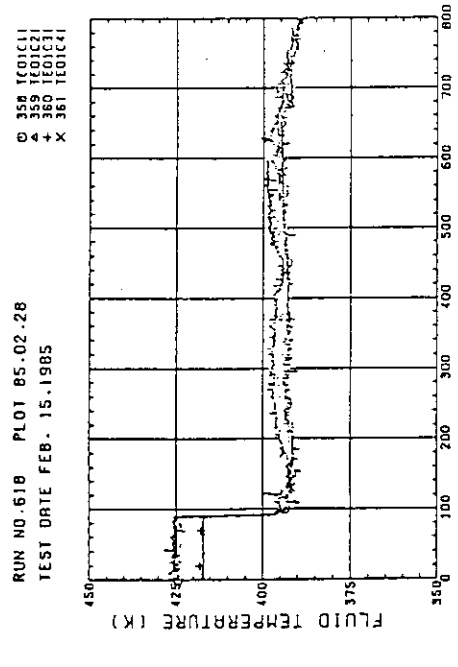

(a) Bundles 1～4

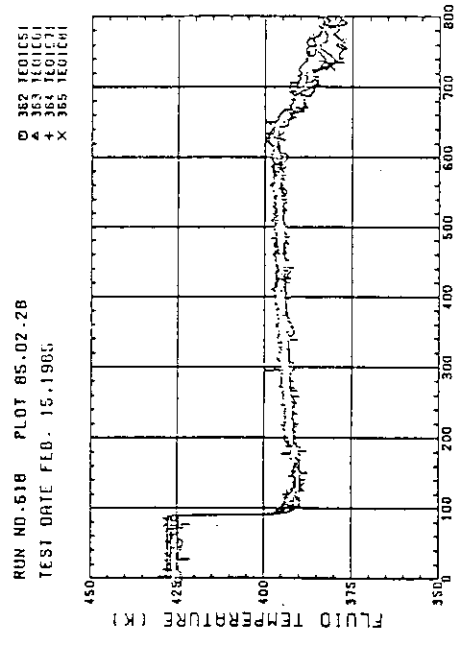

(b) Bundles 5～8

Fig. B-9 Fluid Temperature at Core Inlet

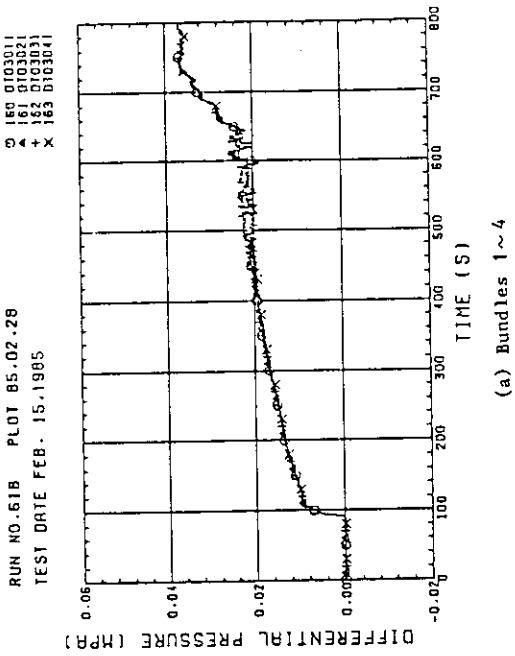

(a) Bundles 1～4

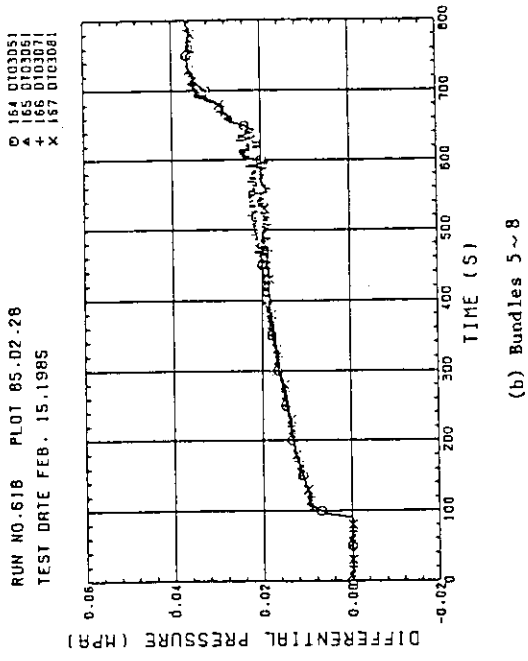

(b) Bundles 5～8

Fig. B-12 Differential Pressure across Core Full Height

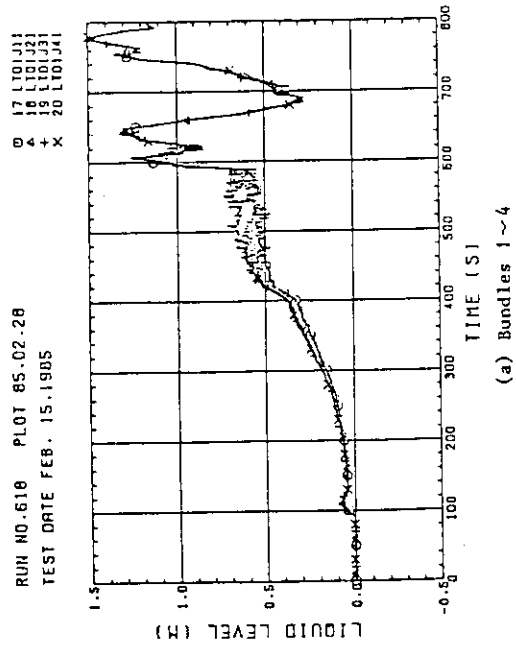

(a) Bundles 1～4

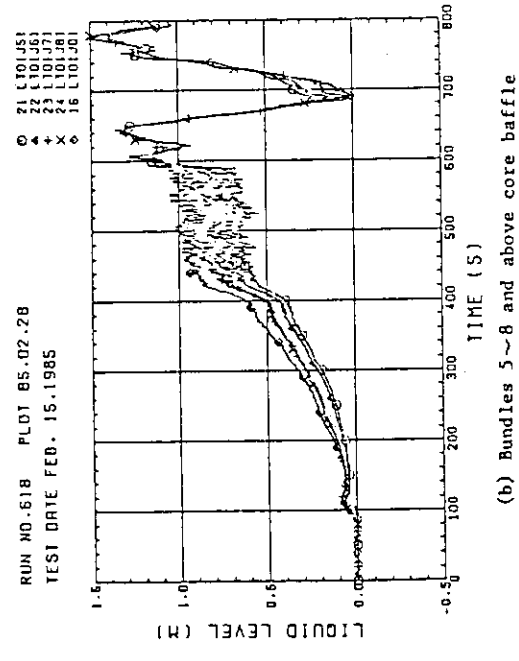

(b) Bundles 5～8 and above core baffle

Fig. B-11 Liquid Level above UCSP

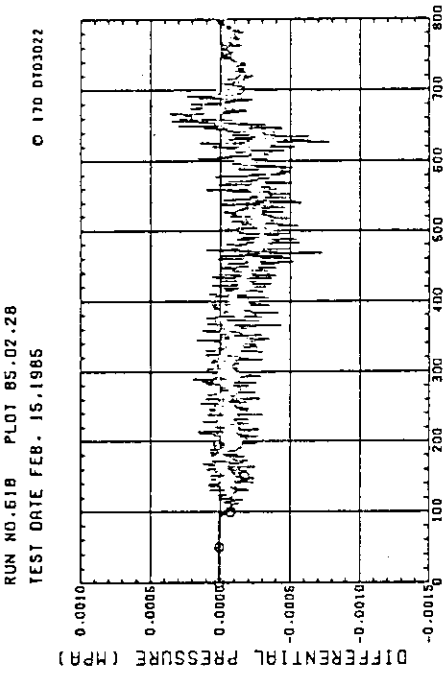

(a) at 1365 mm, Bundle 2 - 4

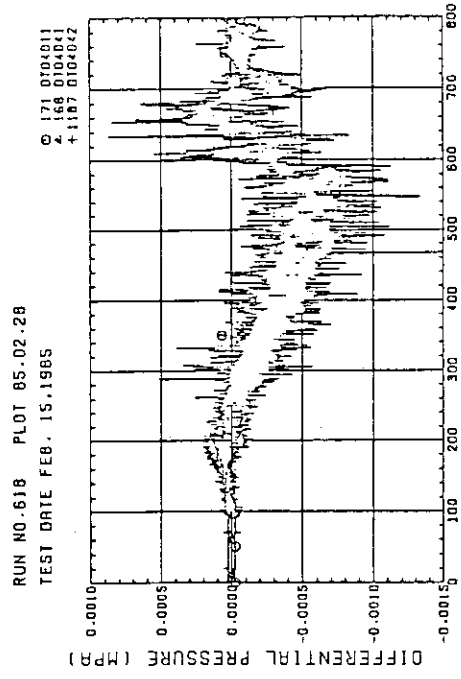

(b) at 1905 mm, Bundle 1 - 4, 4 - 8, 4 - 6

Fig. B-14 Differential Pressure, Horizontal

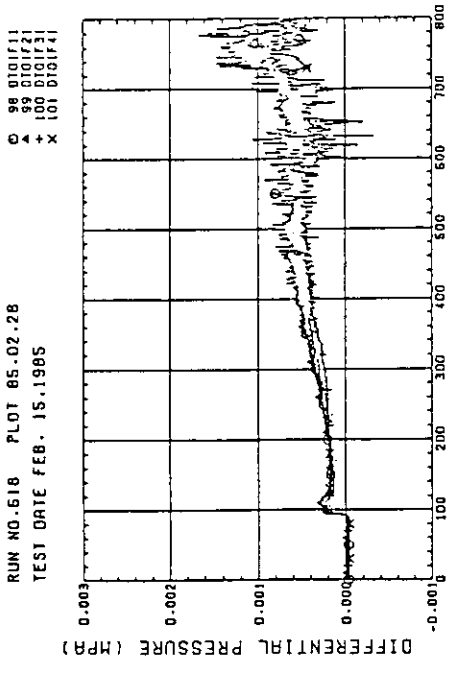

(a) Bundles 1 ~4

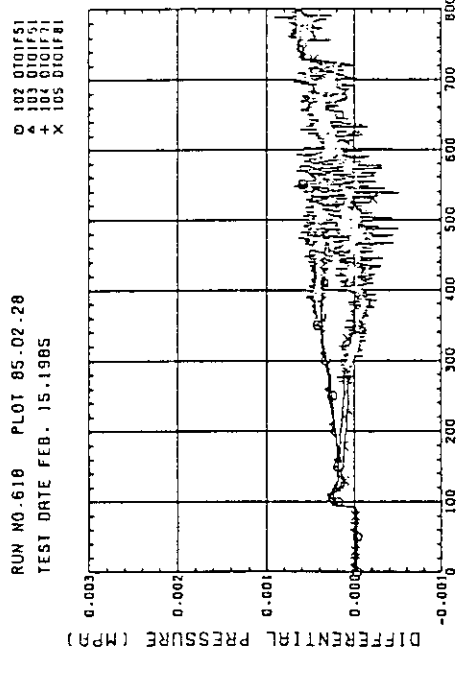

(b) Bundles 5~8

Fig. B-13 Differential Pressure across End Box Tie Plate

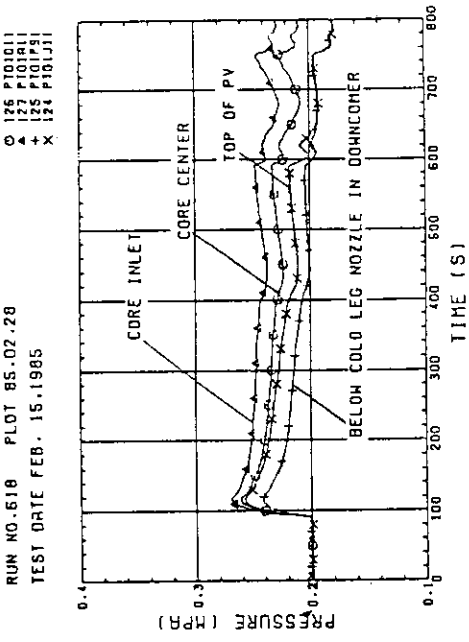

Fig. B-15 Pressure in PV

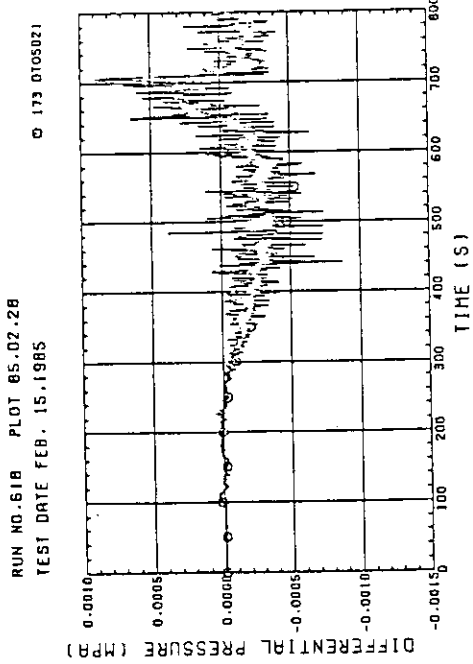

(c) at 2570 mm, Bundle 2 - 4

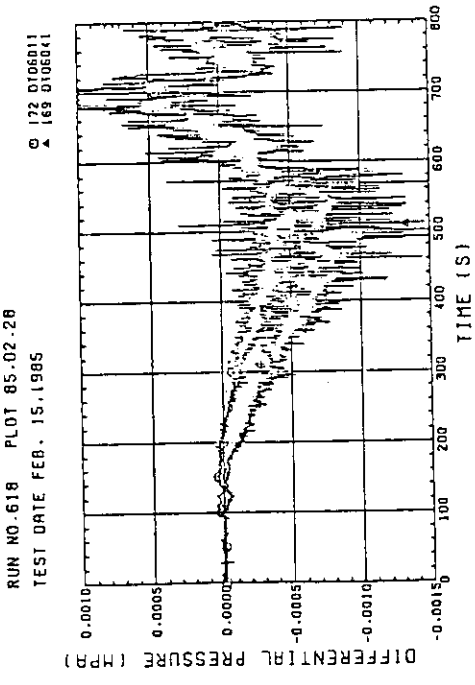

(d) at 3235 mm, Bundle 1 - 4, 4, 8

Fig. B-14(cont.)

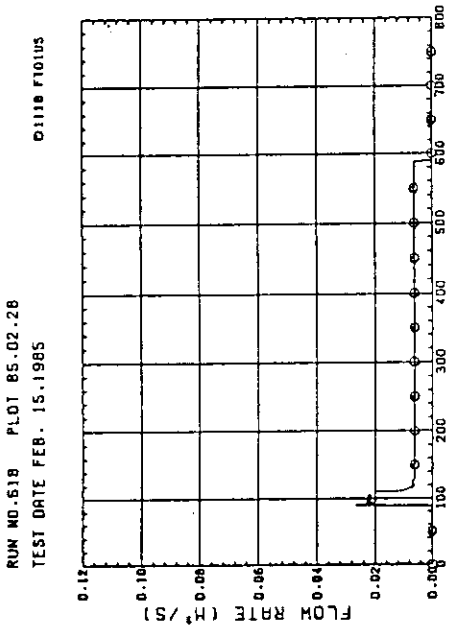

Fig. B-17 Flow Rate of ECC Water

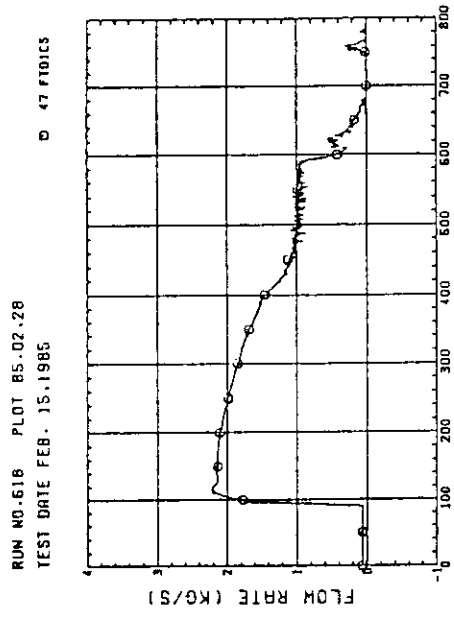

Fig. B-18(a) inlact cold leg

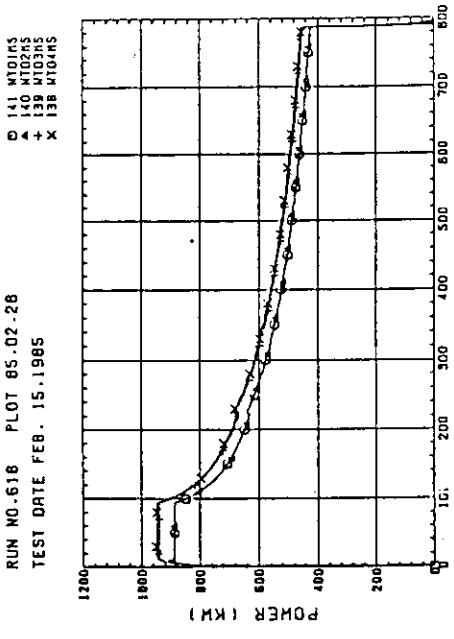

(a) Bundles 1～4

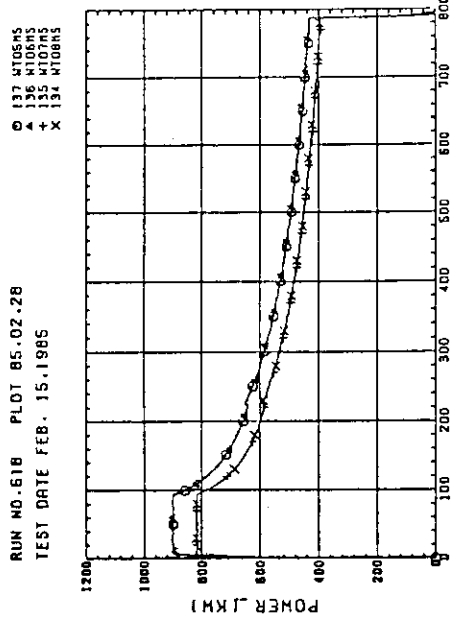

(b) Bundles 5～8

Fig. B-16 Bundle Power

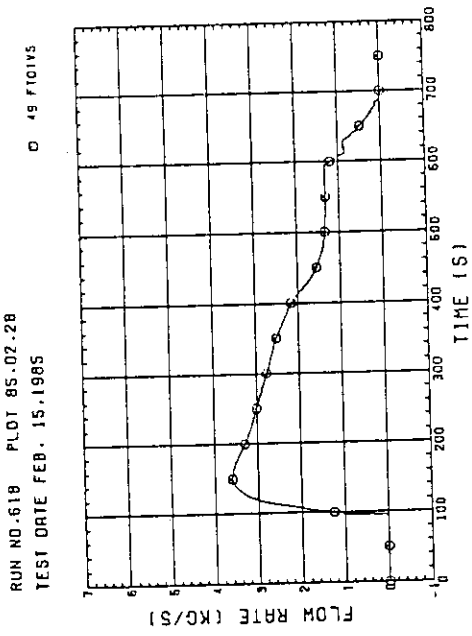

Fig. B-19 Steam Flow Rate of Discharge from Containment Tank-II

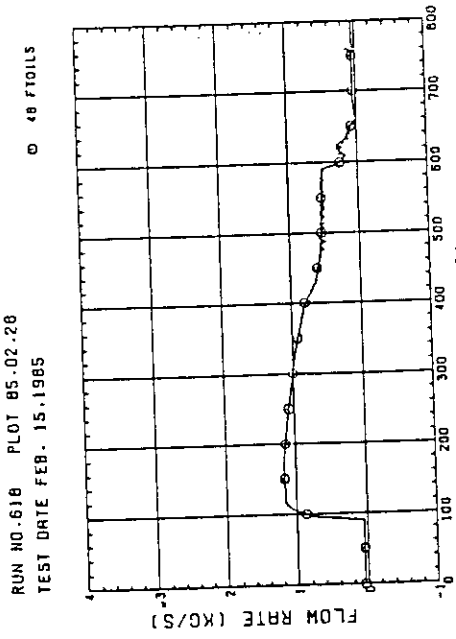

Fig. B-18(b) broken cold leg-steam/water separator side

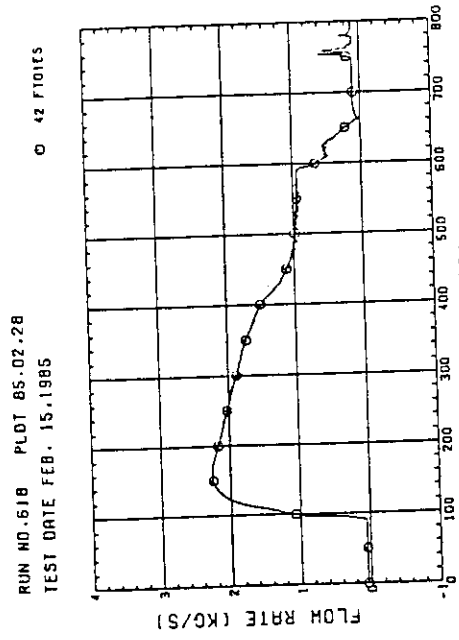

Fig. B-18(c) containment tank-I to -II